MODELING STREAM DISCHARGE IN FOREST CATCHMENTS ACROSS CANADA: HYDRAULIC CONDUCTIVITY CALIBRATIONS

by

Marie-France Jutras

BSc. Forestry, University of New Brunswick, 2009

A Thesis Submitted in Partial Fulfillment
of the Requirements for the Degree of

Masters of Science in Forestry

in the Graduate Academic Unit of
Forestry and Environmental Management

This thesis is accepted by the
Dean of Graduate Studies

THE UNIVERSITY OF NEW BRUNSWICK

September 2012

© Marie-France Jutras, 2012

ABSTRACT

This thesis informs about the process of (i) using soil texture, organic matter and soil depth to predict hydraulic conductivities at soil saturation (K_{sat}), and (ii) refining these predictions by way of catchment-level calibrations. The process also involves the application of the Forest Hydrology Model (ForHyM2). This model uses daily rain, snow, and mean air temperature, as well as basic soil (forest floor, rooted mineral soil, and subsoil) and catchment (slope, aspect, elevation) specifications as inputs. Model output refers to changes in soil moisture and temperature, snowpack (depth, water equivalents, density) and flow rates (run-off, percolation, interflow, baseflow) at the daily level, summer through winter, with and without forest canopies. The catchment calibrations focused on matching the model output snowpack depth and stream discharge with actual data at six well-calibrated forest catchments across Canada (Nova Scotia: Moosepit Brook, Pockwock Lake; New Brunswick: Hayward Brook; Quebec: Lac Laflamme; Ontario: Turkey Lakes, Basin 31; and British Columbia: Rithet Creek). The resulting multi-year calibrations yielded good agreements with R^2 values of about 0.65, 0.77, 0.86, and 0.98, at the daily, weekly, monthly, and annual level, respectively. The multiplier adjustments concerning the predetermined hydraulic conductivity for downward flow (infiltration) varied from 0.5 to 2, but were still in general agreement with actual field-determined values. For lateral flow (interflow), these adjustments were more variable, because terrain and soil conditions would not uniform as set within the ForHyM2 formulation. The soil texture, organic matter and slope mediated impacts on modelled K_{sat}, interflow, infiltration, baseflow and stream discharge were analyzed for

the Turkey Lakes and Moosepit Brook watersheds by way of a sensitivity analysis. As to be expected, increases in the sand content would increase infiltration and baseflow rates over interflow. Increasing the slope would favour interflow over baseflow. Changing the organic matter leads to non-linear responses, with optimal infiltration and interflow rates at an OM content of 15-25%, due to organic matter-induced soil granulation in mineral soil layers. For organic soils, K_{sat} as well as infiltration and interflow would be affected by the state of organic matter composition, being high within fibric layers, and orders of magnitude lower within sapric layers.

TABLE OF CONTENTS

Page

ABSTRACT II

LIST OF TABLES VII

LIST OF FIGURES VIII

CHAPTER 1 - INTRODUCTION 1

SPECIFIC RESEARCH OBJECTIVES 3

THESIS OUTLINE 4

LITERATURE CITED 5

CHAPTER 2 – HYDROLOGY & HYDRAULIC CONDUCTIVITY 7

THE WATER CYCLE 7

HYDRAULIC CONDUCTIVITY 8

METHODS OF DETERMINATION: EXPERIMENTAL APPROACH 11

Laboratory Measurements *11*

Field Measurements *12*

METHODS OF DETERMINATION: EMPIRICAL APPROACH 13

Early Empirical Formulas *13*

PedoTransfer Functions (PTF) *16*

Hydrology Models *24*

IMPORTANCE OF K_{SAT} 26

LITERATURE CITED 28

CHAPTER 3 - RESEARCH SITES 33

RITHET CREEK, BC 33

TURKEY LAKES, ONT 37

LAC LAFLAMME, QC 39

HAYWARD BROOK, NB 40

POCKWOCK, NS 42

MOOSEPIT BROOK, NS 44

LITERATURE CITED 46

CHAPTER 4 - THE FOREST HYDROLOGY MODEL (FORHYM2) 49
INTRODUCTION 49
MODEL INTERFACES 49
MODEL INPUTS 53
MODEL OUTPUTS 55
HYDROLOGY MODULE 55
Estimating soil moisture, modeling K_{sat} *59*
Deep Groundwater Percolation *61*
Hydrothermal Relationships *62*
MODEL LIMITATIONS 66
LITERATURE CITED 68

CHAPTER 5 – MODELING K_{SAT} 69
INTRODUCTION 69
OUTLINE OF METHODS 69
Data Collection *69*
Data Quality Control *71*
Model Calibration *71*
Calculating Results *74*
RESULTS 75
DISCUSSION 92
CONCLUSIONS 98
LITERATURE CITED 100

CHAPTER 6 – SENSITIVITY ANALYSIS 102
INTRODUCTION 102
METHODS 103
RESULTS 105
DISCUSSION 116
CONCLUDING REMARKS 118
LITERATURE CITED 120

CHAPTER 7 - CONCLUSIONS 122
THESIS SUMMARY 122
ORIGINAL CONTRIBUTIONS 123
SUGGESTIONS FOR FUTURE WORK 124
LITERATURE CITED 127

APPENDIX I – PRIMARY FORHYM2 MODELING INPUTS 128
1.1 INPUTS FOR RITHET CREEK 129
1.2 INPUTS FOR TURKEY LAKES 130
1.3 INPUTS FOR LAC LAFLAMME 131
1.4 INPUTS FOR HAYWARD BROOK 132
1.5 INPUTS FOR POCKWOCK 133
1.6 INPUTS FOR MOOSEPIT BROOK 134

APPENDIX II – FORHYM2 USER'S GUIDE 136

CURRICULUM VITAE

LIST OF TABLES

Table Page

1. Representative values of saturated hydraulic conductivity (Clapp and Hornberger 1978) 10

2. Best-fitted results for D_b, FC, PWP, and K_{sat} (cm hr-1) including their respective a, b, c, and d coefficients, R2, MAE, and RMSE for the NB and NS soils data (Balland, 2008). 22

3. Correlation coefficients between a, b, c, and d parameters of equations 1 to 4, New Brunswick and Nova Scotia soil data (Balland et al. 2008). 23

4. Watershed description by site. 35

5. List of weather stations and hydrometric stations used to collect primary input data to run ForHyM for each watershed. 70

6. Hydraulic conductivity and snowpack adjustments by site. 77

7. Hydrothermal soil profile, needed for the daily soil moisture, temperature and stream discharge calculations. 86

8. Max, min, and mean values for hydrothermal parameters across all six basins. 87

9. Stream discharge broken down by runoff, interflow, and baseflow for all six basins. 87

10. Comparing ForHyM-modeled with measured daily, weekly, monthly and annual cumulative discharge: actual mean discharge (Q, mm/time interval), coefficient of determination (R^2), linear regression coefficient (β; intercept = 0), root mean square error (RMSE, %), Standard Error (SE), T-Value, and P-Value 88

11. Status quo scenario soil input parameters for Moosepit Brook and Turkey Lakes. 104

12. Sensitivity results for various levels of sand and OM against K_{sat}, D_b and D_p for Moosepit Brook and Turkey Lakes. 107

13. Lateral flows and stream discharge for Scenarios 1-8 for Moosepit Brook and Turkey Lakes. 108

LIST OF FIGURES

Figure Page

1. The hydrological cycle (modified from Brassington 2007). 8

2. Left and middle: 3-D visualizations of how $\log_{10}K_{sat}$ varies with increasing soil bulk density (D_b), sand fraction and organic matter (OM) fraction. Right: best-fitted $\log_{10}K_{sat}$ versus actual data (Balland et al. 2008). 23

3. Location points for research sites across Canada. 34

4. Rithet Creek study area with watershed delineation and location map (see Table 4 for coordinates). 36

5. Turkey Lakes study area with watershed delineation and location map (see Table 4 for coordinates). 38

6. Lac Laflamme study area with watershed delineation and location map (see Table 4 for coordinates). 40

7. Hayward Brook study area with watershed delineation and location map (see Table 4 for coordinates). 42

8. Pockwock study area with watershed delineation and location map (see Table 4 for coordinates). 43

9. Moosepit Brook study area with watershed delineation and location map (see Table 4 for coordinates). 45

10. Specification overview for the Forest Hydrology Model related to catchment characteristic inputs (Balland 2002). 50

11. Sample of STELLA interface connections showing the various object types. 51

12. ForHyM2 model opened in STELLA showing input parameters. 52

13. ForHyM2 user interface in Excel showing watershed and soil input parameters. 54

14. Hydrology calculations for the ForHyM model in Stella. 56

15. Soil water flow hydrology sub-module, focused on the water capacity and flow slope for the A and B horizons. 58

16. Hydrology parameters module - specifically soil water capacity, K_{sat} and volume by horizon. Example inputs (blue squares), example output (red circle). 60

17. Flow into ground flow (blue flow parameter coming from Perc A B) addition with stream to ground calibration adjustor (red converter), outline in red dotted box, part of the main hydrology module. 62

18. Thermal parameters module, showing heat capacity and thermal conductivity. .. 64

19. Temperature module showing thermal conductivity and soil layer temperature. . 65

20. Heat capacity parameters for determining potential water freeze or potential ice melt, found in the snow and ice module. 66

21. Calibration panel for ForHyM in the Excel interface, used to calibrate catchment specific evopotranspiration, snow parameters and water flow. 72

22. Calibration parameters and connections for ForHyM in STELLA 73

23. ForHyM2 generated output for snowpack, frost depth, soil temperature, and stream discharge for Moosepit Brook, NS from 1999-2004. 78

24. ForHyM2 generated output for snowpack, frost depth, soil temperature, and stream discharge for Peggy Brook, NS from 1999-2004. 79

25. ForHyM2 generated output for snowpack, frost depth, soil temperature, and stream discharge for Hayward Brook, NB from 1993-1997. 80

26. ForHyM2 generated output for snowpack, frost depth, soil temperature, and stream discharge for Lac Laflamme, QC from 1990-1997. 81

27. ForHyM2 generated output for snowpack, frost depth, soil temperature, and stream discharge for Turkey Lakes, ONT from 1997-2004 82

28. ForHyM2 generated output for snowpack, frost depth, soil temperature, and stream discharge for Rithet Creek, BC from 1994-2003. 83

29. Overall cumulative water balance, including precipitation (P), discharge (D), evapotranspiration (ET), soil storage (SS), and deep water (DW) for Moosepit Brook, NS 84

30. Overall cumulative water balance, including precipitation (P), discharge (D), evapotranspiration (ET), soil storage (SS), and deep water (DW) for Hayward Brook, NB. 84

31. Overall cumulative water balance, including precipitation (P), discharge (D), evapotranspiration (ET), soil storage (SS), and deep water (DW) for Lac Laflamme, QC. 85

32. Actual and modelled correlation regression plots with R^2 values for (a) yearly (mm/year), (b) monthly (mm/month), (c) weekly (mm/week), and (d) daily (mm/day) cumulative stream discharge for Moosepit Brook, NS. 89

33. Actual and modelled correlation regression plots with R^2 values for (a) yearly (mm/year), (b) monthly (mm/month), (c) weekly (mm/week), and (d) daily (mm/day) cumulative stream discharge for Peggy Brook, NS. 89

34. Actual and modelled correlation regression plots with R^2 values for (a) yearly (mm/year), (b) monthly (mm/month), (c) weekly (mm/week), and (d) daily (mm/day) cumulative stream discharge for Hayward Brook, NB. 90

35. Actual and modelled correlation regression plots with R^2 values for (a) yearly (mm/year), (b) monthly (mm/month), (c) weekly (mm/week), and (d) daily (mm/day) cumulative stream discharge for Lac Laflamme, QC. 90

36. Actual and modelled correlation regression plots with R^2 values for (a) yearly (mm/year), (b) monthly (mm/month), (c) weekly (mm/week), and (d) daily (mm/day) cumulative stream discharge for Turkey Lakes, ON. 91

37. Actual and modelled correlation regression plots with R^2 values for (a) yearly (mm/year), (b) monthly (mm/month), (c) weekly (mm/week), and (d) daily (mm/day) cumulative stream discharge for Rithet Creek, BC. 91

38. Mineral texture class triangle for fine soil (CANSIS 2000), with textures from scenarios 1-4 highlighted. 105

39. Lateral stream flow broken down by horizon for texture sensitivity scenarios (Sand, Silt, Heavy clay) versus status quo, for Moosepit Brook, NS in 2003. ... 109

40. Lateral stream flow broken down by horizon for OM sensitivity scenarios (Double OM, Half OM, no OM, 100% OM) versus status quo, for Moosepit Brook, NS in 2003. 110

41. Soil water content on the surface, in the forest floor, in the mineral soil, and in the subsoil, as well as the cumulative discharge for, a) scenario with 100% OM, and b) status quo, for Moosepit Brook, NS in 2003. 111

42. Lateral stream flow broken down by horizon for texture sensitivity scenarios (Sand, Silt, Heavy clay) versus status quo, for Turkey Lakes, ON in 2000. 112

43. Lateral stream flow broken down by horizon for OM sensitivity scenarios (Double OM, Half OM, no OM, 100% OM) versus status quo, for Turkey Lakes, ON in 2000. 113

44. Soil water content on the surface, in the forest floor, in the mineral soil, and in the subsoil, as well as the cumulative discharge for, a) scenario with 100% OM, and b) status quo, for Turkey Lakes, ON in 2000. 114

45. K_{sat} of the A&B layers by cumulative stream discharge % for Moosepit Brook (top), and Turkey Lakes (bottom) across all 8 scenarios (vertical dashed line represents the status quo scenario). 115

46. Evapotranspiration (FF + A&B) at Moosepit Brook (A) during 2003 and Turkey Lakes (B) during 2000, for scenario 8 (100% OM), with status quo (100% vegetation), scenario 8^1 (50% vegetation), and scenario 8^2 (10% vegetation). 116

CHAPTER 1 - INTRODUCTION

Many applications in watershed management, forestry, agriculture, and horticulture require hydrologically feasible estimates for assessing the rate at which water infiltrates and percolates through the soil, and how much of that is either taken up by the vegetation, or passes through the ground until entering flow channels and streams further below in the landscape. In the literature, there are many approaches to do this, ranging from direct field measurements to theoretical constructs (Di Frederico and Tartakosky 2000; Sudicky et al. 2010). Field measurements focus, e.g., on (i) direct measurements regarding the rate of infiltration, (ii) hydraulic gradients and hydraulic conductivities along hill slopes and aquifers, and (iii) stream discharge. Theoretical means are used to infer soil and subsoil water retention and hydraulic conductivities from basic soil properties such as soil texture and density (Schaap 2006). In turn, these estimates are then used to determine changes in soil moisture and water flow from point locations within fields and along hill slopes and catchments using various time scales and means ranging from simple trickle-down models (e.g., Church 1997) to geographically distributed hydrology models (Kim et al. 2008). The most elaborate models generate atmosphere-vegetation-soil transference fluxes, based on empirical Eddy correlation techniques (Kuchment et al. 2006), while the simpler models use weather records involving precipitation and air temperature to assess daily changes in soil moisture and water flow (Balland et al. 2006).

This Thesis (i) presents a generalized methodology for deriving and calibrating the hydraulic conductivity at saturation, i.e., K_{sat}, from known texture and organic matter values in relation to soil depth and bulk density for a wide range of natural soil conditions (Balland et al. 2006), and (ii) applies this framework for modeling water retention and flow including stream discharge through well-studied forest catchments. The catchments studied were: Moosepit Brook and Pockwock in Nova Scotia, Hayward Brook near Peticodiac New Brunswick, Lac Laflamme in the Montmorency Experimental Forest in Quebec, Turkey Lakes near Sault St. Marie Ontario, and Rithet Creek on Vancouver Island, British Columbia. The modeling was done with the aspatial, deterministic, trickle-down Forest Hydrology Model (ForHyM2; Arp and Yin 1992; Meng 1995).

Special attention was given to ensure that constraints, such as field capacity (FC), is less than saturation point (SP) and greater than the permanent wilting point (PWP) (SP>FC>PWP), as well as the soil bulk density (D_b), always being less than the particle density (D_p), were strictly adhered to for each soil and subsoil layer. In doing this, focus was on estimating D_b, D_p, SP, FC, PWP and K_{sat} from soil survey data regarding soil texture (i.e., sand, silt and clay content), organic matter content (OM), coarse fragment content (CF), bulk density and depth. For example, higher soil OM would change soil structure through increased particle aggregation, thereby increasing the macro- and micro-pore space distribution within the soil. In turn, this would affect D_b and therefore K_{sat} as well (Nemes et al. 2003; Balland et al. 2006). Traffic-induced soil compaction would enforce the opposite (Vega-Nieva et al. 2008).

Equations for estimating D_b, D_p, FC, PWP, and K_{sat} from soil texture and organic matter content are known as "point pedotransfer functions", or point PTFs (Bouma 1989; Gijsman et al. 2003; Børgesen and Schaap 2005). These point estimates are then used to estimate, respectively: run-off, the amount soil water that is free to flow on account of gravity alone ("gravitational water", or soil moisture content above FC), and the amount of water that is potentially available for plant uptake, e.g. soil moisture between PWP and FC. The "scaling up" from the point to catchment scales is by adjusting these layer-specific K_{sat} values based on daily stream discharge from well-studied forest catchments across Canada from east to west. The resulting values are then compared with (i) available literature values for K_{sat} based on direct soil and/or subsoil measurements dealing with hydraulic gradients and water flow rates in wells, (ii) reports about K_{sat} versus increasing length of hydraulic gradient.

SPECIFIC RESEARCH OBJECTIVES

The specific research objectives of this thesis were to:

i. examine how K_{sat} is affected by permeability-affecting soil properties such as soil texture, organic matter content and density;

ii. use this information to improve and calibrate the K_{sat} formulation within ForHyM2 using stream discharge data within the context of modeling the hydrothermal fluxes through the forest soils of the six well-studied watershed locations;

iii. summarize all this for the purpose of guiding ForHyM2 users to generate realistic values for the daily variations in soil moisture, temperature, and flow rates (run-off, infiltration, interflow, baseflow, stream discharge) through forested catchments based on basin-representative soil profiles (depth of forest floor and mineral soil layers, texture, organic matter content) and slope.

THESIS OUTLINE

Based on the above objectives, the thesis is constructed as follows:

- Chapter 2: introduces the concept of hydrology and explains the importance of hydraulic conductivity, as well as introduces various hydrology models and equations used to estimate hydraulic conductivity.
- Chapter 3: provides an overview of the six research sites including a detailed background of the site location, vegetation, geology, and climate.
- Chapter 4: describes the ForHyM2, including the model inputs, outputs, and calculations for estimating soil moisture, K_{sat}, and hydrothermal conductivity.
- Chapter 5: elaborates on the methods used to model K_{sat} at each site, including data collection, model improvements, calibrations, and statistics. It also summarizes the results, including statistical work and result validation.
- Chapter 6: provides an overview of the sensitivity analysis of hydraulic conductivity by changing soil texture, organic matter, and bulk density.
- Chapter 7: summarizes the work done, statement of original contributions and includes suggestions for future work.

LITERATURE CITED

Balland, V, Bhatti, J. S., Errington, R., Castonguay, M., Arp, P. A. 2006. Modeling soil temperature and moisture regimes in a jack pine, black spruce and aspen forest stand in central Saskatchewan (BOREAS SSA). *Canadian Journal of Soil Science*. 86:203–217.

Børgesen, C.D., Schaap, M.G. 2005. Point and parameter pedotransfer functions for water retention predictions for Danish soils. *Geoderma* 127:154–167.

Bouma, J. 1989. Using soil survey data for quantitative land evaluation. *Advanced Soil Science.* 9:177–213.

Church, M.R. 1997. Hydrochemistry of forested catchments. *Annual Reviews Earth Planet Science.* 25:23–59.

Di Frederico, V., Tartakosky, D.M. 2000. Effective hydraulic conductivity in multiscale random fields with truncated power variograms. *Geological Society of America*. 348:80-89.

Gijsman, A., Jagtap, S.S., Jones, J.W. 2003. Wading through a swamp of complete confusion: how to choose a method for estimating soil water retention parameters for crop models. *European Journal of Agronomy.* 18:75-105.

Kim, K.W., Chung, I.M., Won, Y.S., Arnold, J.G. 2008. Development and application of the integrated SWAT-MODFLOW model. *Journal of Hydrology*. 356:1-16.

Kuchment, L.S., Demidov, V.N., Startseva, Z.P. 2006. Coupled modeling of the hydrological and carbon cycles in the soil–vegetation–atmosphere system. *Journal of Hydrology*. 323:4-21.

Meng, F.-R., Bourque, P. A., Jewett, K., Daugharty, D., and Arp, P. A. 1995. The Nashwaak experimental watershed project: analysing effects of clearcutting on soil temperature, soil moisture, snowpack, snowmelt and streamflow. *Water, Air and Soil Pollution*. 82:363-374.

Nemes, A., Schaap, M. Wösten, H. 2003. Functional evaluation of pedotransfer functions derived from different scales of data collection. *Soil Science Society of America Journal*. 67:1093-1102.

Schaap, M.G. 2006. Models for indirect estimation of soil hydraulic properties. Encyclopedia of Hydrological Sciences. DOI: 10.1002/0470848944.hsa078

Sudicky, E.A., Illman, W.A. Goltz, I.K., Adams, J.J., McLaren, R.G. 2010. Heterogeneity in hydraulic conductivity and its role on the macroscale transport of a solute plume: From measurements to a practical application of stochastic flow and transport theory. *Water Resources Research*. 46:1-16.

Vega-Nieva, D.J., Castonguay, M., Ogilvie, J., Arp, P.A. 2009. Development of a modular terrain model to estimate daily variations in machine-specific forest soil trafficability, year-round. *Canadian Journal of Soil Science*. 89:93-109.

CHAPTER 2 – HYDROLOGY & HYDRAULIC CONDUCTIVITY

The purpose of this chapter is to outline hydrological principles and related thesis background with special emphasis on hydraulic conductivity at saturation (K_{sat}) and past and present methods used to determine K_{sat}.

THE WATER CYCLE

All life on earth depends on water and as such, depends on the hydrological cycle. Over 70% of the earth's surface is covered in water, which equals nearly 1400 million km^3 (Brady and Weil 2001). Of this water, only a minute fraction is active in the hydrological cycle. Water found on ocean surfaces, in lakes and rivers, in the atmosphere, groundwater, and in the soil make up this crucial cycle.

Over open water sources, water evaporates into the atmosphere via direct vapourization. Over land however, water evaporates due to plant transpiration and is referred to as evopotranspiration. The resulting atmospheric moisture is carried by wind over land. Water then precipitates (via rain, snow, condensation, etc...) over land and completes the full cycle back to open water by either runoff or percolating through the soil and moving laterally as groundwater (Figure 1). Each process in this cycle is important to the hydrological balance of any given landscape.

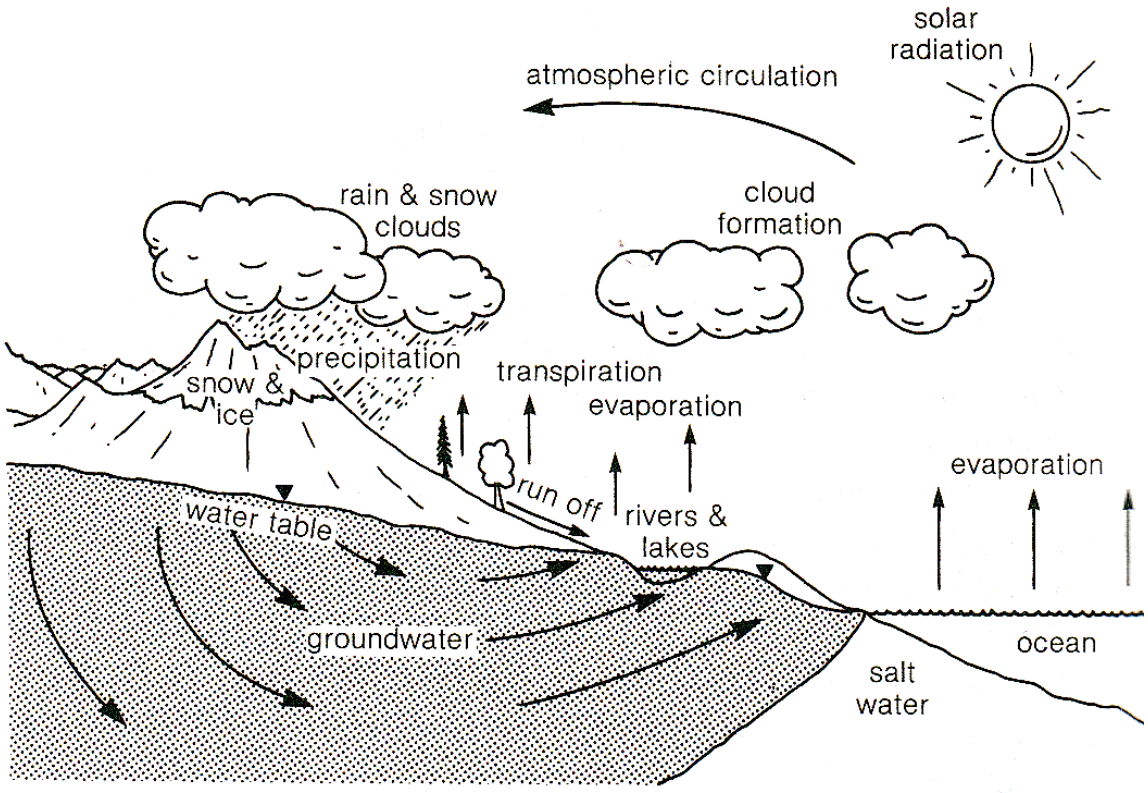


Figure 1. The hydrological cycle (modified from Brassington 2007).

HYDRAULIC CONDUCTIVITY

Groundwater is made up of water that is beneath the ground surface in soil pores and in rock fractures. Water moves through the soil to its natural discharge point by infiltrating and percolating along the soil's hydraulic gradient, flowing from high to low water potential. The ease at which water can flow through a soil medium given the potential gradient is called *hydraulic conductivity* (K) (Brady and Weil 2001). In some instances it is also called water permeability. It is expressed in Darcy's Law, which describes the flow of a liquid through a porous medium over time.

$$Q = -AK\left(\frac{\Delta h}{L}\right) \quad (1)$$

where,

Q - volumetric flow rate per unit area (m^3/s)

A - unit of area (m^2)

K - hydraulic conductivity (m/s)

Δh - change in water potential

L - flow path length

minus sign - direction of flow towards decreasing water potential

Darcy's Law is the basis for understanding the flow of water through a watershed. It looks at a proportional relationship between the permeability of a medium, the area of the flow, and the difference in pressure or water potential. Saturated hydraulic conductivity (K_{sat}), the ease of the flow of water through a medium with pores saturated with water, is a very important process in groundwater flow (Brady and Weil 2001). Understanding K_{sat} can help determine how well a soil will perform under various scenarios, which is valuable when modeling hydrological flows of watersheds. Knowing the discharge rate of a watershed, Darcy's Law can be rearranged to calculate K_{sat}:

$$K_{sat} = -\frac{Q}{A} * \frac{L}{\Delta h} \quad (2)$$

The rate of K_{sat} depends on the properties of the watershed, as well as the water itself. The soil pores, and anything that affects them will influence K_{sat} most. Porosity, the amount of void spaces in the soil, is determined by the shape and size of soil particles, as well as its structural strength. The larger the pores, the faster K_{sat} will be. Sandy soils generally have larger macropores than fine-textured soils, such as clay, and will thus usually have a high K_{sat} (Brady and Weil 2001). Soils that are poorly sorted, or have mixed grain sizes will have decreased permeability due to smaller grains filling the empty

voids. Table 1 shows findings from a study by Clapp and Hornberger (1978) that generally summarizes hydraulic conductivity by variations of soil texture. It clearly shows a trend of decreasing permeability with decreasing texture size. Soils that are rich in biota will have a tendency to have macropores channels created by burrowing animals and insects. These burrows act like tunnels for groundwater and help increase the permeability of the soil. Temperature is major factor that can affect the viscosity of ground water. Brassington (2007) states that with increasing temperature viscosity decreases and permeability increases. Ground temperature varies only slightly in deep soils therefore temperature generally only affects watersheds that have shallow soils and/or extreme climate changes. Some saturated soils have pockets of air trapped in the soil column. Entrapped air can act as a barrier for water, which will slow down the soil's permeability.

Table 1. Representative values of saturated hydraulic conductivity (Clapp and Hornberger 1978)

Soil Texture	K_{sat} cm/min
Sand	1.056
Loamy sand	0.938
Sandy loam	0.208
Silt loam	0.043
Loamy sand	0.042
Sandy clay loam	0.038
Silty clay loam	0.010
Clay loam	0.015
Sandy clay	0.013
Silty clay	0.006
Clay	0.007

METHODS OF DETERMINATION: EXPERIMENTAL APPROACH

Laboratory Measurements

In the laboratory, several methods are used to determine K_{sat}. One of these methods is the *constant-head method*. This method works well with medium- to coarse-textured soils, but is generally too slow for fine-textured soils. The purpose of the constant head method is to allow water to move through a sample of soil under a steady pressure head and to measure the volume of water that flows through the soil over a period of time (Eq. 3). The resulting flow rates are generally quantified using Darcy's Law given by Equation 3:

$$K_{sat} = \left[\frac{VL}{Ath}\right] \tag{3}$$

where,

V - amount of water after time (t) in (cm^3)

L - flow path length

A - cross sectional area perpendicular to flow (cm^2)

t - time interval (mins)

h - constant pressure difference

The *falling head method* uses the same principles as the constant-head method, but can be used for both fine- and coarse-grained soils. This method tests how long water will move through a sample of soil without a constant pressure head on the soil. This method utilizes the following equation to determine K_{sat} given by Equation 4:

$$K_{sat} = \frac{L}{t} log\left[\frac{h_1}{h_2}\right] \tag{4}$$

where h_1 and h_2 - upper and lower water level from time 0 to time "t".

Field Measurements

There are different methods that can be used to measure hydraulic conductivity *in situ*. They are generally broken into two different categories; 1) those for sites near or below the water table, on fully saturated soils (K_{sat}), and, 2) those for sites well above the water tables measuring field saturated hydraulic conductivity (K_{fsat}). Field saturated hydraulic conductivity is the permeability of a soil that is not fully saturated. When testing for K_{fsat} the soil needs to be saturated with water first to initialize the test for permeability, since these soils are generally dry.

Some tests for K_{sat} measurement include the auger-hole test, piezometer test, slug test and well pumping test. Each of these tests follows the general procedure of digging a hole in the soil, waiting for the water in the hole to equalize with the water table, removing the water and finally calculating how fast it takes for the hole to refill to equilibrium (Bouwer and Rice 1976; Beers 1983). Each test has its benefits and downfalls but can be picked based on the results needed. For example, the auger-hole method is probably the simplest and is used for soils with high homogeneity, whereas the piezometer method uses a solid pipe in the well, which can be used to test specific horizons.

To test K_{fsat} in non-saturated soil different tests include the Guelph permeameter, double-tube test, and infiltrometer. The general principle behind these tests is to calculate how fast the water will filter into the soil using either a constant or falling head pressure. For example, the Guelph permeameter measures the steady state liquid recharge of a well

utilizing the constant head method (Reynolds and Elrick 1986). The permeameter is placed in a hole that is then filled to a calibrated line with water. The permeameter then keeps a constant flow of water into the hole, which keeps the water with a constant pressure head. The rate at which water infiltrates into the soil is calculated by finding the difference in water loss from the permeameter over time.

METHODS OF DETERMINATION: EMPIRICAL APPROACH

In some cases, direct field measurements of K_{sat} can be impractical and quite expensive, depending on the size and range of the study area. Because of this, hydrological modeling via empirical formulas becomes invaluable to estimating K_{sat}, as well as other hydrological and hydrothermal outputs.

Early Empirical Formulas

Process-specific equations were developed to estimate overall watershed hydrology functions. Many of these equations estimating K_{sat} were based on the fundamental basics of Darcy's law (Eq. 1). The early stages of hydrology modeling required a connection between K_{sat}, and soil's grain size and granular distribution. An early example of this is the Hazen Method (Hazen 1892; Hazen 1911; Bear 1972). Developed for clean filter sands, it looks at an empirical correlation between K_{sat} and sand particle size (Eq. 5):

$$k = C_H(D_{10})^2 \tag{5}$$

where,

C_H - single dimensionless coefficient

D_{10} - particle size diameter (cm) with soil made up of 10% fine and 90% coarse particles

This method was originally designed for coarse sandy soils, but has proved acceptable within the fine sand to gravel range (Freeze and Cherry 1979). Many studies used the Hazen Method and a large range of C_H coefficients was developed, from 1 to 1,000 (Carrier 2003). Bradbury and Muldoon (1990) noted that when testing Hazen's method against other field and lab test samples, the equation underestimated the former by a magnitude of 2 and overestimated the latter by a magnitude of 1. They deduced that formula could still be used due to the approximate close agreement between lab test samples and the formula produced K_{sat}.

Half a century after Hazen, the Kozeny-Carmen equation was developed to estimate the permeability of porous media via a semi-empirical, semi-theoretical formula. The Hazen's method formula does not account for textural variation, while the Kozeny-Carmen formula looks more specifically at the correlation of fluid dynamics grain size and porosity (Eq. 6):

$$k = \left(\frac{pg}{\mu}\right)\left[\frac{n^3}{(1-n)^2}\right]\left(\frac{{d_m}^2}{180}\right) \quad (6)$$

where,

p - fluid density

g - gravitational constant

μ - dynamic viscosity of water

n - porosity

d_m - representative grain size

The Kozeny-Carmen formula is limited to sandy soil or, more specifically, non-plastic soils. Carrier (2003) noted that the formula doesn't take into consideration the electrochemical reaction between the soil and water and therefore isn't viable for clay soils.

The Fair and Hatch equation further refined the Kozeny-Carmen equation to include grain-size variation (Todd 1959; Freeze and Cherry 1979). It replaces the $\left(\frac{{d_m}^2}{180}\right)$ grain size parameter within the Kozeny-Carmen equation with one that uses a soil packing factor to account for the grain size distribution variability:

$$k = \left(\frac{pg}{\mu}\right)\left[\frac{n^3}{(1-n)^2}\right]\left[\frac{1}{m\left(\frac{\emptyset}{100}\sum\frac{P}{d_m}\right)^2}\right] \quad (7)$$

where,

m - packing factor (usually ~5)

Ø - the shape factor (ranging from 6 for spherical grains to 7.7 for angular gains)

P - % of material held between adjacent sieves, and d_m is the geometric mean of the rates sizes of adjacent sieves

Sperry and Peirce (1995) noted that even though this formula attempts to account for grain shape, it is limited to regular sand particles, unlike the more angular and irregular particles that naturally occur in soil.

PedoTransfer Functions (PTF)

The early formulas for estimating K_{sat} are still used in modern studies but the more prominent method of estimating soil hydraulic relationships within the last three decades is through the use of pedotransfer functions. In 1986, Johan Bouma coined the term *pedotransfer function* (PTF) to mean "translating data we have into something we need". This refers to relating soil parameter data, generally measurable data from soil surveys (such as texture, depth, OM, etc…), to soil hydraulic functions (Bouma 1989). The previous formulas could be viewed as 'early PTFs' since they do use known variables to predict K_{sat}. Modern PTFs are developed through statistical correlation, by utilizing a database of soil parameters (e.g., Universal Soil Database (UNSODA), Hydraulic Properties of European Soils (HYPRES) or any database created from local soil survey reports), and producing an equation through regression analysis that best produces the function in question. The PTFs are also calibrated against actual function parameters to produce the most accurate formulas. The importance of the creation of PTFs was recognized almost immediately due to the multiple uses of soil hydraulic functions (Pachepsky et al. 2006). Unlike the earlier formulas, which were more a function specific, PTFs provide a generalized blueprint on estimating a variety of different hydraulic functions based on input factors.

PTF analysis can be broken down into 3 categories, Class PTFs, Continuous PTFs, and neural networks. Class PTFs focus on a specific class type (e.g., sand, or topsoil). It assumes any soil within a related class will share similar hydraulic properties (Rasoulzadeh 2011). The limitation with class PTFs is large differences in estimated

outputs between classes. These differences create unrealistic flow of hydraulic properties over a large landscape, which represents a large number of class types. Continuous PTFs estimate hydraulic properties as a function of many variables (generally measured percentages of texture and OM). These PTFs include, simple to multiple linear regression (MLR), which express the direct linear relationships between function and input parameter (Wosten et al. 1999; Pandey et al. 2006; Balland et al. 2008). Finally, artificial neural network (ANN) PTFs is a relatively recent approach to estimating hydraulic properties. It was created as an adaptive system that uses many small functions which adjust to find patterns in data to estimate complex relationships (Pachepsky et al. 1996; Schaap and Leij 1998; Minasny et al. 1999).

Many studies have utilized PTFs to determine K_{sat}. A study by Pandey et al. (2006) compared estimated K_{sat} from alluvial soils in Patna, Bihar India. A multi-linear regression equation was developed from these soil using textural percentages and bulk density as the input parameters (Eq. 8).

$$K_s = -2.961 + 0.064 * S + 0.009 * Si + 1.012 * D_b \quad [R^2 = 0.51] \tag{8}$$

where,

S - sand (%)

Si - silt (%)

D_b - bulk density (g cm^{-3})

Pandey et al. (2006) also looked at K_{sat} produced via neural networks, and two empirical formulas and compared all four methods to lab-produced K_{sat}. Of the four

methods, the formula for relative effective porosity (REP) (Eq. 9) produced the best correlation to lab-produced outputs with an R^2 of 0.721.

$$K_s = 75(\emptyset_{er})^2 \quad [R^2 = 0.721] \tag{9}$$

wh

$\emptyset_{er}$ - relative effective porosity, which is defined as effective porosity divided by field capacity (FC)

In another study, Wösten et al. (1999) looked at class PTFs based on the closed-form analytical expression for K from van Genuchten's (1980) model using Mualem's predictive conductivity model. Van Genuchten's is a well-established model which is used to estimate unsaturated hydraulic conductivity and utilizes water retention parameters. In addition to the class PTFs, Wösten et al. (1999) also used the HYPRES database of European soils to determine a continuous function of K_{sat} via linear regression analysis of D_b, OM, and texture percentages. The calculated geometric means and fitted curves used for the class PTFs using Van Genuchten's model showed very good agreement, but unfortunately, the R^2 obtained when predicting K_{sat} under continuous PTFs was not good (0.19).

$$K_s = 1.15741 * 10^{-7} \exp(x) \quad [R^2 = 0.19] \tag{10}$$

where x is:

$$x = 7.755 + 0.0352(Si) + 0.93(TS) - 0.967\left(D_b{}^2\right) - 0.000322(Si^2) + \frac{0.001}{S} - \frac{0.0748}{OM} - 0.643 * \ln(Si) - 0.01398 * (D_b) * (C) - 0.1673 * (D_b) * (OM) + 0.02986 * (TS) * (C) - 0.03305 * (TS) * (Si)$$

and where,

Si - silt (%)

C - clay (%)

TS - topsoil, a quantitative parameter which represents 1 for topsoils and 0 for subsoils

D_b - bulk density (g cm^{-3})

OM - organic matter (%)

A study by Tietke and Hennings (1996) compared the findings of six different PTFs, four of which focused on regression equations based on soil texture (Cosby et al. 1984; Brakensiek et al. 1984; Saxton et al. 1986; Vereecken et al. 1990), and two which looke at grain size distribution (Campbell 1974; Bloemen 1980). Tietkey and Hennings (1996) applied each PTF in the study to field and laboratory soil data from Lower Saxony in Northern Germany. They found that K_{sat} estimations using PTFs is site specific and dependent on specific dataset. For example, poor results were found using Vereecken et al.'s (1990) PTF due to the equation being based on a larger scale of texture classes. Not all PTFs are created in the same way and should therefore be tested for accuracy on the soils in question.

More recently, a study by Balland et al. (2008) developed PTFs for the following hydraulically important soil properties:

- *saturation point* (SP) - the point at which no more water can be absorbed into the soil. All of the pores are filled with water;
- *field capacity* (FC) - the amount of water that is held the soil after the water has drained due to gravity;

- *permanent wilting point* (PWP) - the limit when there is not enough water left in the soil for productive plant growth;
- *bulk density* (D_b) - the weight of oven-dried soil divided by the total soil volume;
- *particle density* (D_p) - the density of the solid fraction of the soil;
- *saturated hydraulic conductivity* (K_{sat}) - the ease of the flow of water through a medium with pores saturated with water.

As a general rule, the soil moisture content at FC is always smaller than soil moisture content at the SP, and PWP is always smaller than FC (SP>FC>PWP). Also, the D_b is always smaller than the mean D_p of the soil. The PTF of each of these primary soil moisture parameters was calculated in order for the model to estimate the soil water capacity and flow by soil horizons. The estimates for D_b, D_p, SP, FC, PWP and K_{sat} are functionally related to soil depth, texture (i.e. sand, silt, and clay content, %), and organic matter content (OM, %). By predicting the relationship between hydraulic function and these soil properties, Balland et al. (2008) developed linear regression PTF equations that generated layer-specific estimates for the soil moisture parameters. The following equations were used to this effect:

$$D_b = \frac{a_{Db}+(D_p-a_{Db}-b_{Db}\,SAND)(1-\exp(c_{Db}\,x\,DEPTH)}{1+d_{Db}\,OM} \quad (11)$$

$$FC = SP\left(1-\exp\left(\frac{-a_{FC}(1-SAND)-b_{FC}\,OM}{SP}\right)\right) \quad (12)$$

$$PWP = FC\left(1-\exp\left(\frac{-a_{PWP}\,CLAY-b_{PWP}\,OM}{FC}\right)\right) \quad (13)$$

$$\log_{10}K_{sat} = -a_{Ksat} + b_{ksat}\log_{10}(D_b - D_p) + c_{Ksat}\,SAND \quad (14)$$

$$\frac{1}{\mathrm{Dp}} = \frac{\mathrm{OM}}{\mathrm{Dp_{om}}} + \frac{1-\mathrm{OM}}{\mathrm{Dp_{min}}} \quad (15)$$

where,

a, b, c, and d - D_b, FC, PWP and K_{sat}-specific calibration coefficients.
Dp_{OM} - particle density of OM (1.3 gcm^{-3})
Dp_{min} - particle density of mineral soils (2.65 gcm^{-3})
SAND, CLAY, OM, FC, PWP, and FC - fine dry soil weight fractions (fine earth fraction only)
DEPTH - the mid depth of each soil layer (cm)

Balland et al. (2008) used data taken from New Brunswick (NB) and Nova Scotia (NS) soil survey reports (CANSIS 2000) to produce the following results by way of regression analysis:

$$D_b = \frac{1.23+(\mathrm{D_p}-1.23-0.75\ \mathrm{SAND})(1-\exp(10.0106\ \mathrm{x\ DEPTH})}{1+6.83\ \mathrm{OM}} \quad (16)$$

$$\mathrm{FC} = \mathrm{SP}\left(1-\exp\left(\frac{-0.588(1-\mathrm{SAND})-1.73\ \mathrm{OM}}{\mathrm{SP}}\right)\right) \quad (17)$$

$$\mathrm{PWP} = \mathrm{FC}\left(1-\exp\left(\frac{-0.511\ \mathrm{CLAY}-0.865\ \mathrm{OM}}{\mathrm{FC}}\right)\right) \quad (18)$$

$$\log_{10}K_{sat} = -0.98 + 7.94\log_{10}(\mathrm{D_p}-\mathrm{D_b}) + 1.96\ \mathrm{SAND} \quad (19)$$

The best-fitted values for coefficient of determination (R^2), mean absolute error (MAE), root mean square error (RMSE) and the corresponding a, b, c and d regression coefficients are listed in Table 2. These results show that the precision so achieved varied in the following order: FC > PWP > D_b > K_{sat}. This order likely reflects the extent by

which changes in soil structure (or state of soil aggregation) affect the measurement of these variables. It appears that such changes have (i) only small if any effects on the pressure-plate determinations for FC and PWP, (ii) moderate effect on the in-situ D_b determinations, but (iii) large effects on K_{sat} on account of disproportionate flow rates through fine to large pores, root channels and cracks. With organic soils, varying degrees of humification also matter, with well-humified matter being more compactable and less permeable than fibrous matter (Pepin et al., 1992; Paquet et al., 1993; Balland et al. 2008). The modelled variations of K_{sat} with changing OM, sand content, and D_b are shown in Figure 2, together with plots of actual versus best-fitted NB and NS K_{sat} data.

Table 2. Best-fitted results for D_b, FC, PWP, and K_{sat} (cm hr-1) including their respective a, b, c, and d coefficients, R_2, MAE, and RMSE for the NB and NS soils data (Balland, 2008).

Property	ax	bx	cx	dx	R2	MAE	RMSE
D_b, g cm^{-3}	1.17 ±0.05	0.83 ±0.08	0.022 ±0.004	6.12 ±0.8	0.83	0.14	0.18
FC, g g^{-1}	0.588 ±0.016	1.734 ±0.049			0.96	0.03	0.05
PWP, g g^{-1}	0.511 ±0.025	0.865 ±0.057			0.65	0.03	0.04
$Log_{10}K_{sat}$	-0.98 ±0.11	7.94 ±0.48	1.96 ±0.21		0.80	0.38	0.49

Subscript x for a, b, c d mean D_b, FC, PWP, or Ksat, as pertinent by row

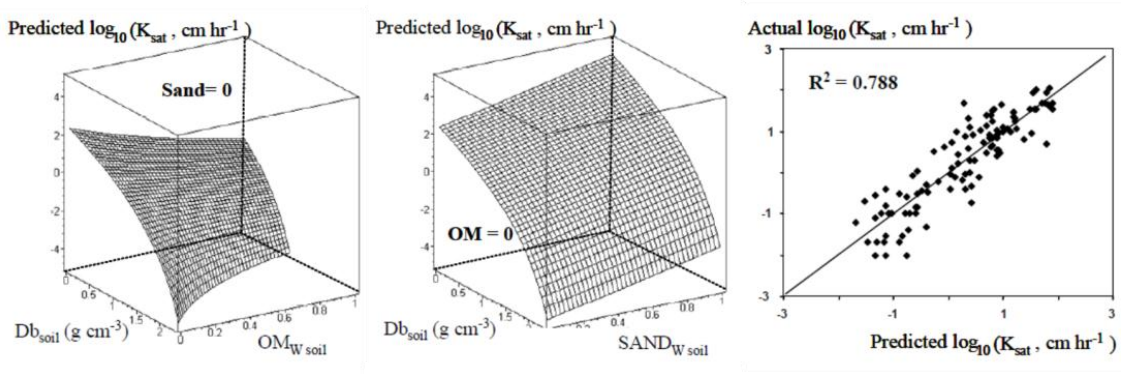


Figure 2. Left and middle: 3-D visualizations of how $\log_{10}K_{sat}$ varies with increasing soil bulk density (D_b), sand fraction and organic matter (OM) fraction. Right: best-fitted $\log_{10}K_{sat}$ versus actual data (Balland et al. 2008).

The extent of inter-parametric correlations among the regression coefficients is shown in Table 3. These correlations should, ideally, be as close to zero as possible to narrow the equifinal solution space for the best-fitted a, b, c and d coefficients. For example, the -0.89 correlation between aK_{sat} and cK_{sat} implies that an increase in cK_{sat} will produce a corresponding decrease in aK_{sat}. Hence, large non-zero inter-coefficient correlations numbers imply large uncertainties about the best-fitted coefficients for the parameter pair so identified.

Table 3. Correlation coefficients between a, b, c, and d parameters of equations 1 to 4, New Brunswick and Nova Scotia soil data (Balland et al. 2008).

$D_b$soil	**ax**	**bx**	**cx**	**dx**	**Log10(K_{sat}soil)**	**ax**	**bx**	**cx**
ax	1				ax	1		
bx	-0.0067	1			bx	-0.043	1	
cx	-0.45	-0.75	1		cx	-0.89	-0.15	1
dx	0.77	0.062	-0.16	1				
FCwsoil	**ax**	**bx**			**PWPwsoil**	**ax**	**bx**	
ax	1				ax	1		
bx	-58	1			bx	-0.34	1	

Applying the K_{sat} formulation to the Universal Soil Database (UNSODA, Leij 1996), instead of NB and NS data yielded,

$$log_{10}k_{sat} = (-1.05 \pm 0.08) + (6.1 \pm 0.4)log_{10}(D_p - D_b) + (2.2 \pm 0.1)SAND \quad (20)$$

(n = 481; R^2 = 0.52; RMSE = 0.68; MAE = 0.54)

Hence, the $\log_{10}K_{sat}$ formulation based on the NS and NB data alone remained valid in its general form, but the coefficient values changed slightly, with the largest change associated with the $\log_{10}(D_p - D_b)$ coefficient, i.e., dropping from 7.9 to 6.1. This change may relate to procedural differences, e.g., using estimated D_p values from known SP and D_b values (NB and NS data) versus direct D_p measurements (UNSODA). The plot of actual versus best fitted values in Figure 2 suggests a general agreement between the above K_{sat} formulation and the data from both sources.

Hydrology Models

Hydrology models can be either spatial or aspatial. Spatial models, or distributed models, view a watershed as many smaller units by way of changes in slope and aspect of each unit, and analyze the geospatial variations in soil, water, topography and other parameters. These models are generally based on high resolution parameters, requiring considerable input data and make use of Geographical Information System (GIS) tools, as well as Remote Sensing technology, such as aerial photography and satellite imagery (Lastoria 2008). For example, Topmodel is a deterministic distributed model that simulates overland flow, as well as infiltration, evapotranspiration and subsoil flow for a water basin (Beven and Kirby 1979; Beven and Freer 2001). It uses high quality digital

elevations maps (DEM) to account for variability in hydrological response due to changes in topography via slope. Similar distributed models include the Soil and Water Assessment Tool (SWAT) (Srinivasan and Arnold 1994; Neitsch et al. 2002), the Snowmelt Runoff Model (SRM) (Martinec et al. 2008), and the Semi-distributed Land Use-based Runoff Processes (SLURP) model (Kite 1991; Kite and Haberlandt 1999). Aspatial models, or lumped models, view the whole watershed catchment as a single entity with the variables and outputs averaged over the entire area (Lastoria 2008; Refsgaard 1996). These models use more easily acquired data, generally climate, soil and site parameters. For example, PROSPER is a one dimensional model that looks to emulate the exchange between plants, soil and the atmosphere (Swift et al. 1975; Vose and Maass 1999). It uses physical and biological parameters to create connections between watershed functions, and uses daily temperature, solar radiation, water vapour pressure, and wind speed to estimate local energy balances and evapotranspiration rates. Other lumped models include EDP-RIV1 (USACE 1995; Martin and Woll 2002), MIKE11 RR (Rainfall Runoff) (DHI 2008; Shamsudin and Hashim 2002), and the Forest Hydrology Model (ForHyM2) (Meng et al. 1995).

Hydrology models attempt to quantify the flow of heat and water through a system using empirical formulas for each modeled process referring to (e.g.) interception, evaporation, transpiration, freezing, thawing, infiltration, interflow, baseflow, and heat conduction as well as insulation, by soil and subsoil layer at regular time steps (e.g., hourly, daily, weekly, monthly). Impacts of varying weather and climate conditions, substrate permeability, local topography and extent of vegetation cover are also

addressed. Typical model formulations range from deterministic and stochastic. Deterministic models use algebraic expressions to quantify cause-effect relationships. Stochastic models may use the same expressions, but modify the associated parameters across their known uncertainty range through probabilistic random number selections (Nick and Harp 1980). Deterministic models are generally preferred due to their simplified input and output requirements. Stochastic models allow for scoping the effects of error propagation on the overall model outcome and related uncertainties (Yevjevich 1987; Vogel 1999). This thesis deals with deterministic modeling only. The issue of error propagation is in part addressed calibrating the model parameters including K_{sat} to match modeled output for snowpack depth and stream discharge with actual data at daily input and output steps for several years.

IMPORTANCE OF K_{SAT}

Many aspects of surface and ground water flow are affected by local soil drainage and permeability conditions. For example, rural communities rely heavily on groundwater for clean drinking water, and the soil's ability to filter contaminants from septic tanks, agriculture and industrial operations. In terms of agriculture, knowing K_{sat} can help (i) to minimize soil erosion and reduce the amount of nutrient pollution runoff from fertilizers downstream (Jadczyszyn and Niedzwiecki 2005) and (ii) to determine the type of method used for soil pollution remediation (Mulligan et al. 2001). Typically, soils with higher K_{sat} drain water and pollutants quicker, while soil materials with low K_{sat} can be valuable to redirect contaminated water (Starr and Cherry 2005). Soil compaction and changes to its K_{sat} in agriculture and forestry lead to decreased infiltration and increased

surface runoff (Gilmour et al. 1987; Zimmerman et al. 2006; Zimmerman et al. 2010; Scheffler et al. 2011; Alaoui et al. 2011). Remediation of deforestation through tree planting has been shown to partially restore the hydraulic capacity of ‘damaged’ soils (Zimmerman et al. 2006; Bonell et al. 2010). A study by Román et al. (2003) looked at soil remediation by organic amendment by means of incorporating urban waste into degraded semiarid soils. The study showed an improvement of hydraulic conductivity between 72-245% throughout the soil profile, leading to reduced site erosion (Román et al. 2003).

LITERATURE CITED

Arp, P.A., Yin, X. 1992. Predicting water fluxes through forests from monthly precipitation and mean monthly air temperature records. *Canadian Journal of Forest Research*. 22:864-877.

Alaoui, A., Lipiec, J., Gerke, H.H. 2011. A review of the changes in the soil pore system due to soil deformation: a hydrodynamic perspective. *Soil & Tillage Research*. 115-166:1-15.

Balland, V., Pollacco, J.A.P., Arp, P.A. 2008. Modeling soil hydraulic properties for a wide range of soil conditions. *Ecological Modeling*. 219:300-316.

Bear, J. 1972. *Dynamics of fluids in porous media*. New York, New York: American Elsevier Publishing Company, Inc.

Beers, W.F.J. 1983. *The auger hole method: A field measurement of the hydraulic conductivity of soil below the water table*. 6th ed. Wageningen, Netherlands: International Institute for Land Reclamation and Improvement.

Beven, K. and Freer, J. 2001. A dynamic TOPMODEL. *Hydrological Processes*. 15:1993-2011.

Beven, K. J., Kirby, M. J. 1979. A physically based, variable contributing area model of basin hydrology. *Hydrological Sciences Bulletin*. 24(1):43-69.

Bloemen, W. 1980. Calculation of hydraulic conductivities of soils from texture and organix matter content. *Z. Pflanzenernahr Bodenkd.* 43:581-605.

Bonell, M., Purandara, B.K., Venkatesh, B., Krishnashwamy, J., Acharya, H.A.K., Singh, U.V., Jayakumar, R., Chappell, N. 2010. The impact of forest use and reforestration on soil hydraulic conductivity in the Western Ghats of India: Implications for surface and sub-surface hydrology. *Journal of Hydrology*. 391:47-62.

Bouwer, H. and Rice, R.C. 1976. A slug test for determining hydraulic conductivity of unconfided aquafers with completely or partially penetrating wells. *Water Resource Research*. 123:423-428.

Brady, N.C., Weil, R.R. 2001. *The Nature and Poperties of Soils*. 13th ed. Upper Saddle River, New Jersey: Prentice Hall.

Brassington, R. 2007. *Field Hydrogeology*. 3rd ed. Chichester, West Sussex: John Wiley & Sons Ltd.

Brakensiek, D.L., Rawls, W.J., and Stephenson, G. R. 1984. "Modifying SCS hydrologic soil groups and curve numbers for rangeland soils." ASAE Paper No. PNR-84-203, St. Joseph, Mich.

Campbell, G.S. 1974. A simple method for determining unsaturated conductivity from moisture retention data. *Soil Science*. 117:311-314.

CANSIS. 2000. "Canadian Soil Information System." (http://sis.agr.gc.ca/cansis/).

Chi, X. 2008. "Hydrogeological assessment of stream water in forested watershed: temperature, dissolved oxygen, pH, and electrical conductivity." MSc. Thesis., Forestry, University of New Brunswick, Fredericton.

Clapp, R.B., Hornberger, G.M. 1978. Empirical equations for some soil hydraulic properties. *Water Resource Research*. 144:601-604.

Cosby, B.J., Hornberger, G.M., Clapp, R.B., Gunn, T.R. 1984. A statistical exploration of relationships of soil moisture characteristics to the physical properties of soils. *Water Resource Research*. 20:682-690.

DHI. 2008. "MIKE 11 - A modeling system for rivers and channels." Short Introduction Tutorial, DHI.

Freeze, R.A., Cherry, J.A. 1979. *Groundwater*. Englewood Cliffs, N.J.: Prentice-Hall, Inc.

Gilmour, D.A., Bonell, M., Cassells, D.S. 1987. The effects of forestation on soil hydraulic properties in the middle hills of Nepal: a preliminary assessment. *Mountain Research and Development*. 7(3):239-249.

Hazen, A. 1892. "Some physical properties of sand and gravel, with special reference to their use in infiltration." 24th Annual Report, Massachusetts State Board of Health.

Hazen, A. 1911. Discussions of 'Dams on sand foundations' by A. C. Koenig. *Transactions of the American Society of Civil Engineers*. 73:199-203.

Jadczyszyn, J., Niedzwiecki, J. 2005. Relation of saturated hydraulic conductivity to soil losses. *Polish Journal of Environmental Studies*. 145:431-435.

Jutras, M.-F., Arp, P.A. 2011. "Determination of hydraulic conductivity from soil characteristics and its application for modeling stream discharge in forest catchments." in *Hydraulic Conductivity - Issues, Determination and Applications*, edited by Lakshmanan Elango (Ed.). InTech. Pp. 189-202

Kite, G.W. 1991. A watershed model using satellite data applied to a mountain basin in Canada. *Journal of Hydrology*. 128:157-169.

Kite, G.W., Haberlandt, W. 1999. Atmospheric model data for macroscale hydrology. *Journal of Hydrology*. 30:303-313.

Lastoria, B. 2008. "Hydrological processes on the land surface: a survey of modeling approaches." Technical Report, Dipartimento di Ingegneria Civile e Ambientale, Università degli Studi di Trento, Trento.

Leji, F.J., Alves, W.J., van Genuchten, M.T., Williams, J.R. 1996. "The UNSODA unsaturated soil hydraulic database." User's Manual, Version 1.0, National Risk Management Laboratory, U.S. Environmental Protection Agency, Cincinnati, OH.

Martin, J. L. Woll, T. 2002. "A dynamic one dimensional model of hydrodynamics and water quality EPD-RIV1, Version 1.0." User's Manual., AScI Cooperation, Athens, Georgia.

Martinec, J., Rango, A., Roberts, R. 2008. "Snowmelt Runoff Model (SRM) User's Manual." Special Report 100, Agricultureal Experiment Station, College of Agriculture and Home Economics, Las Cruces, New Mexico.

McBratney, A.B., Minasny, B., Cattle, S.R., Vervoort, R. W. 2002. From pedotransfer function to soil inference systems. *Geoderma*. 109:41-73.

Meng, F.-R., Bourque, P. A., Jewett, K., Daugharty, D., and Arp, P. A. 1995. The Nashwaak experimental watershed project: analysing effects of clearcutting on soil temperature, soil moisture, snowpack, snowmelt and streamflow. *Water, Air and Soil Pollution*. 82:363-374.

Minasny, B., McBratney, A.B., Bristow, K. 1999. Comparison of different approaches to the development of pedotransfer functions for water-retention curves. *Geoderma*. 93:225-253.

Mulligan, C.N., Yong, R.N., Gibbs, B.F. 2001. Surfactant-enhanced remediation of contaminated soil: a review. *Engineering Geology*. 60:371-380.

Neitsch, S.L., Arnold, J.G., Kiniry, J.R., Williams, J.R., King, K.W. 2002. "Soil and Water Assesstment Tool Theoretical Documentation." User Manual, Grassland, Soil and Water Research Laboratory, Agricultural Research Service, Temple, Texas.

Nick, A.D., Harp, J.F. 1980. Stochastic generation of temperature and solar radiation data. *Journal of Hydrology*. 48:1-17.

Pachepsky, Y.A., Rawls, W.J., Lin, H.S. 2006. Hydropedology and pedotransfer functions. *Geoderma*. 131:308-316.

Pachepsky, Y.A., Timlin, D., Yarallyay, G. 1996. Artificial neural networks to estimate soil water retention from easily measurable data. *Soil Science Society of America Journal*. 60(3):727-733.

Pandey, N.G., Chakravorty, B., Kumar, S., and Mani, P. 2006. Comparison of estimated saturated hydraulic conductivity for alluvial soils. *Hydrology Journal*. 28(3-4):59-72.

Paquet, J.M., Caron, J., Banton, O. 1993. In-situ determination of the water desorption characteristics of peat substrates. Canadian Journal of Soil Science. 73:329–339.

Pepin, S., Plamondon, A., Stein, J. 1992. Peat water content measurement using time domain reflectometry. Canadian Journal of Forest Research. 22:534–540.

Rasoulzadeh, A. 2011. "Estimating hydraulic conductivity using pedotransfer functions." in *Hydraulic Conductivity - Issues, Determination and Applications*, edited by Lakshmanan Elango. InTech. Pp. 145-164

Refsgaard, J.C. 1996. "Terminology, modeling protocol and classification of hydrological model codes." in *Distributed hydrological modeling*. Dordrecht, The Netherlands: Kluwer Academic Publishers. P. 238

Reynolds, W.D. and Elrick, D.E. 1986. A Method for Simultaneous In Situ Measurement in the Vadose Zone of Field-Saturated Hydraulic Conductivity, Sorptivity and the Conductivity-Pressure Head Relationship. *Ground Water Monitoring & Remediation*. 6:84-95.

Richardson, C.W. 1981. Stochastic simulation of daily precipitation, temperature and solar radiation. *Water Resource Research*. 17(1):182-190.

Román, R., Fortùn, C., García López de Sá, M.E., Almendros, G. 2003. Successful soil remediation and reforestation of a calcis regosol amended with composted urban waste. *Arid Land Research and Management*. 17:297-311.

Saxton, K.E., Rawls, W.J., Romberger, J.S., Papendick, R.I. 1986. Estimating generalized soil-water characteristics from texture. *Soil Science Society of America*. 50:1031-1036.

Schaap, M.G., Leij, F.J. 1998. Using neural networks to predict soil water retention and soil hydraulic conductivity. *Soil & Tillage Research*. 47:37-42.

Scheffler, R., Neill, C., Krusche, A., Elsenbeer, H. 2011. Soil hydraulic response to land-use change associated with recent soybean expansion at the Amazon agricultural frontier. *Agriculture, Ecosystems and Environment*. 144:218-289.

Shamsudin, S., Hashim, N. 2002. Rainfall runoff simulation using MIKE11 NAM. *Jurnal Kejuruteraan Awam*. 15(2):1-13.

Sperry, J.M., Peirce, J. J. 1995. A model for estimating the hydraulic conductivity of granular material based on grain shape, grain size, and porosity. *Ground Water*. 33(6):892-898.

Srinivasan, R., Arnold, J. G. 1994. Integration of a basin-scale water quality model with GIS. *Water Resource Bulletin*. 30(3):453-462.

Starr, R.C., Cherry, J. A. 2005. In situ remediation of contaminated ground water: the funnel-and-gate system. *Ground Water*. 323:465-476.

Swift, L.W., Swank, W.T., Mankin, J.B., Luxmoore, R.J., Goldstein, R.A. 1975. Simulation of evapotranspiration and drainage from mature and clear-cut deciduous forests and young pine plantations. *Water Resources Research*. 11(5):667-673.

Tietje, O., Hennings, V. 1996. Accuracy of the saturated hydraulic conductivity prediction by pedo-transfer functions compared to the variability within FAO textural classes. *Geoderma*. 69:71-84.

Todd, D.K. 1959. *Groundwater Hydrology*. New York , NY: J. Willey and Sons.

USACE. 1995. "CE-QUAL-RIV1: A dynamic, one-dimensional (longitudinal) water quality model for streams." User's Manual.

van Genuchten, M.T. 1980. A closed-form equation for predicting the hydraulic conductivity of unsaturated soils. *Soil Science Society of America*. 44:892-898.

Vereecken, H., Maes, J., Feyen, J. 1990. Estimating unsaturated hydraulic conductivity from easily measured soil properties. *Soil Science*. 149:1-12.

Vogel, R.M. 1999. Editorial - Stochastic and deterministic world views. *Journal of Water Resources Planning and Management*. 125(6):311-313

Vose, J.M., Maass, J.M. 1999. "A comparative analysis of hydrologic responses of tropical deciduous and temperate deciduous watershed ecosystems to climatic changes." RMRS-P-12, USDA Forest Services Proceedings.

Wösten, J.H.M., Lilly, A., Nemes, A., and Bas, C.L. 1999. Development and use of a database of hydraulic properties of European soil. *Geoderma*. 90:169-185.

Yevjevich, V. 1987. Stochastic models in hydrology. Stochastic Hydrology and Hydraulics. 1:17-36.

Zimmerman, B., Elsenbeer, H., Moraes, J.M. 2006. The influence of land-use changes on soil hydraulic properties: implications for runoff generation. *Forest Ecology and Management*. 222:29-38.

Zimmerman, B., Papritz, A., Elsenbeer, H. 2010. Asymmetric response to disturbance and recovery: Changes of soil permeability under forest-pasture-forest transitions. *Geoderma*. 159:209-215.

CHAPTER 3 - RESEARCH SITES

The six catchments selected for this research are Moosepit Brook, Nova Scotia on metamorphic slate; Pockwock, Nova Scotia on igneous granodiorite (Peggy Brook catchment within Pockwock); Hayward Brook, New Brunswick on sedimentary sandstones/shale; Lac Laflamme, Quebec on metamorphic gneiss; Turkey Lakes, Ontario on igneous mafic, metavolcanic basalt; and Rithet Creek, on Vancouver Island in British Columbia on igneous volcanic, undivided intrusive rock (Figure 3; Table 4). These watersheds were chosen, because each of these provide records of sufficient detail regarding daily weather, stream discharge and snow accumulations. They were also chosen, because they differ in terms of terrain type and bedrock formations, which are the basis for comparison in this project.

RITHET CREEK, BC

Rithet Creek is located on the southeastern tip of Vancouver Island, British Columbia, approximately 30 km northwest of Victoria (Figure 4). The watershed is 1630 ha large and drains into Sooke Lake. It is primarily composed of 150 year old mature Douglas-fir (*Pseudotsuga menziesii*) stands alongside young 40 year old plantations of Douglas-fir and western red cedar (*Thuja plicata*) (Wulder et al. 2000). The average annual rainfall and snowfall amount to 1720 mm and 70 cm, respectively, and mean monthly temperatures range from 3.0 °C in January to 22.7 °C in July.



Figure 3. Location points for research sites across Canada.

Table 4. Watershed description by site.

Site Parameters	Moosepit Brook Nova Scotia (NS)	Pockwock Nova Scotia (NS)	Hayward Brook New Brunswick (NB)	Lac Laflamme Quebec (QB)	Turkey Lakes Ontario (ON)	Rithet Creek Vancouver Island, British Columbia (BC)
References	Bobba et al. (1986) Jutras et al. (2011)	Jutras et al. (2011)	Pomeroy (2003) Chi (2008)	Barry et al. (1990)	Murphy et al. (2009) Murray and Buttle (2005)	Zhu and Mazumder (2008)
Abbreviation	MP	PB	HB	LL	TL	GB
Latitude (N)	44°28'	44°49'	45°52'	47°17'	47°03'	48°32'
Longitude (W)	65°03'	63°51'	65°11'	71°14'	84°25'	123°42'
Area (ha)	1670	196	508	69	1050	1630
Elevation (m)	100-150	172-227	96-162	777-884	350-400	375
Slope (%)	1	7	8	11	8	17
Deciduous:coniferous	50:50	75:25	50:50	10:90	100:0	0:100
Rooting habit	Medium	Shallow	Medium	Medium	Deep	Deep
Forest floor depth (cm)	5	5	5	8	7	15
Mineral soil: depth (cm); texture	50; SL	70; SL	40; S-LS	31; S	60; SilL	70; SL
Subsoil: depth (cm); texture	70; LS	100; SL	100; SL	100; LS	100; LS	100; SL
Bedrock	Metamorphic greenschist slate	Granite	Sedimentary shale, lithic-feldspathic sandstone	Metamorphic charnockite gneiss	Metavolcanic basalt	Volcaniclastic rock, undivided intrusive rock
Land Formation	Glacial till	Ablation till	Ablation till	Sandy till	Ablation till on basal till	Colluvium
Topography	Rolling	Flat to rolling	Undulating to rolling	Rolling to hummocky	Undulating to rolling	Hummocky
Mean yearly temperature (°C)	7.02	6.35	6.01	1.49	4.52	8.97
Mean yearly snow depth (cm)	5	7	16	50	23	1
Mean yearly rainfall (mm)	1140	1180	970	1005	790	1700
Model Run Years	1999-2004	1999-2004	1993-1998	1990-1997	1997-2004	1994-2003

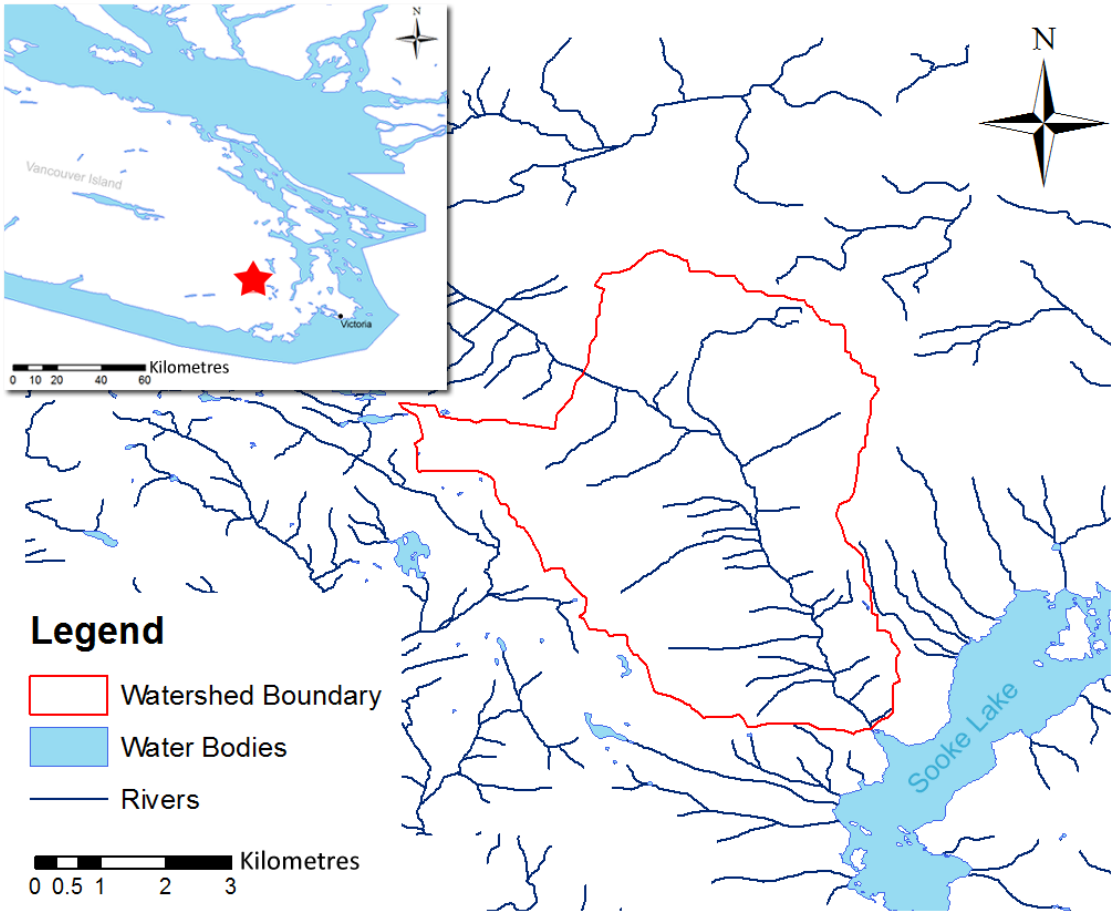


Figure 4. Rithet Creek study area with watershed delineation and location map (see Table 4 for coordinates).

The bedrock geology at Rithet creek consists of igneous volcanic, undivided intrusive rock, which means that the bedrock was formed by magma cooling slowly under the earth's surface (Monroe et al. 2007). Slow cooling of the intrusive bedrock allows for larger minerals to form, which in turn predisposes the area to have coarser textured soils. As a result, the soils at this site are primarily gravelly loam sand to sandy loam with higher large coarse fragment content (between 30-65%). The land formation associated with this site is primarily sandy colluvium, as well as fluvial soils, which follows the creek bed (Jungen and Ag 1985). Colluvium soil is defined by Brady and

Weil (2001) as deposits of rock fragments and soil material accumulated at the base of steep slopes as a result of gravitational action. Given the location of the study area, nestled in the outskirts of the Rocky Mountains, coupled with the steep slopes associated with the area, it is logical to see a large portion of the watershed covered in colluvium. These soils at this study area are defined as Orthic Humo-Ferric Podzols and Duric Dystric Humo-Ferric Podzols (Zhu and Mazumder 2008; Jungen and Ag 1985).

TURKEY LAKES, ONT

The Turkey Lakes study area is located approximately 60 km north of Sault St. Marie, Ontario, near Lake Superior (Figure 5). The watershed is approximately 1050 ha large and encompasses four lakes, which are interconnected by Norberg Creek and subsequently drains into Lake Superior to the west (Beall et al. 2001). The woody vegetation is made up of mostly over mature hardwoods, mainly sugar maple (*Acer saccharum*). Average annual rainfall and snowfall amount to 790 mm and 330 cm, respectively and mean monthly temperatures range from -12.8 °C in January to 16.12 °C in July.

Bedrock geology at Turkey Lakes is predominately Precambrian silicate greenstone (metavolcanic basalt) with small granite intrusions (Murray and Buttle 2005; Hazlett and Foster 2002). The surficial geology consists of well drained silt loam ablation till underlain by compacted, poorly drained, sandy loam basal till (Arp and Yin 1992; Hazlett et al. 2001). Ablation and basal till are classified as glacial deposits, which is unstratified material deposited by a glacier as it moves over the surface (basal till) and as

it recedes (ablation till) (Brady and Weil 2001). Due to the dense basal till, perched water tables can form along the ablation/basal till interface causing lateral flow during high periods of saturation (e.g., snowmelt and storm events) (Hazlett et al. 2001). The soil at Turkey Lake is primarily Humo-Ferric Podzol.

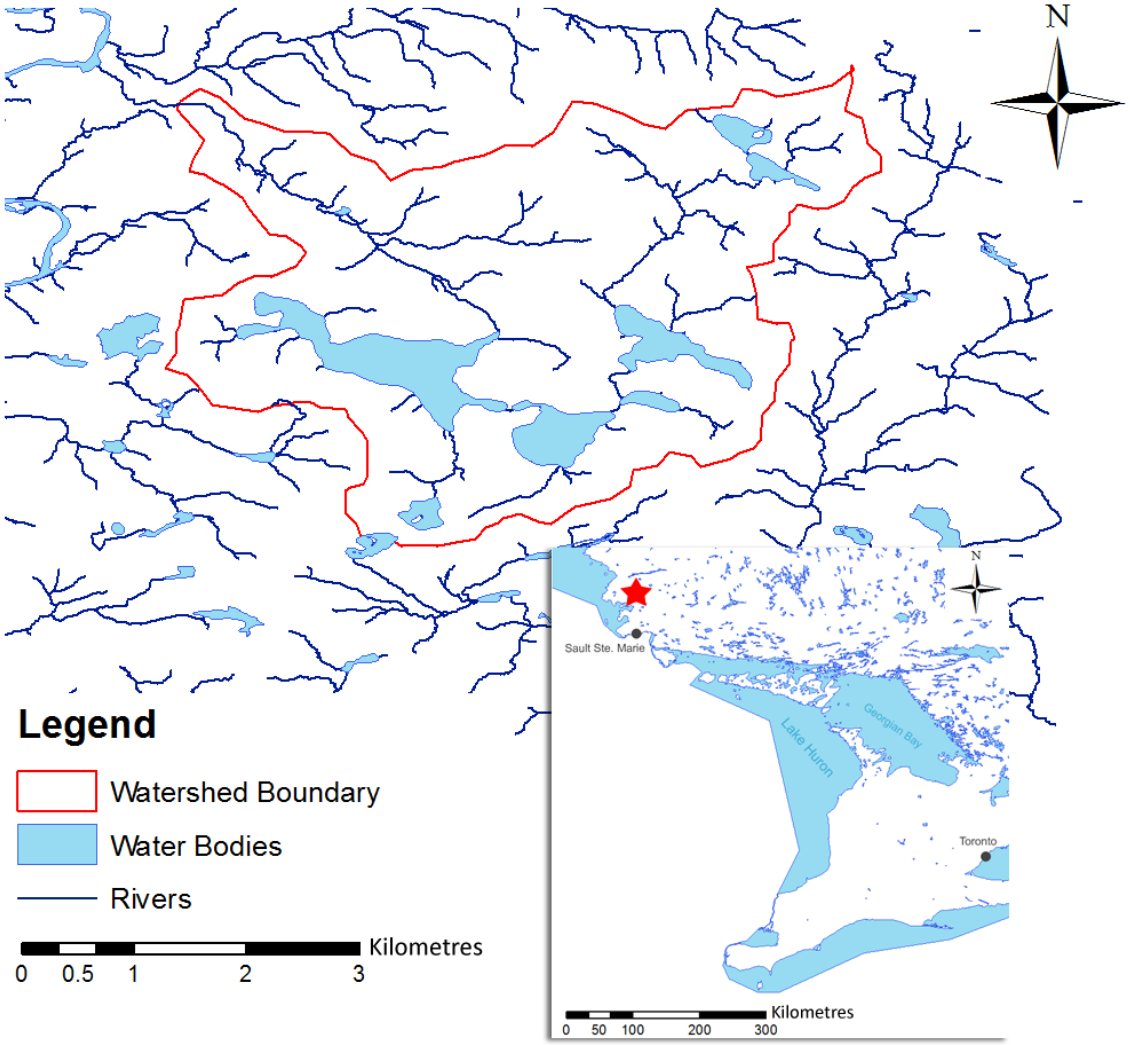


Figure 5. Turkey Lakes study area with watershed delineation and location map (see Table 4 for coordinates).

LAC LAFLAMME, QC

The Lac Laflamme watershed is located within the Montmorency Experimental Forest, 80 km north of Quebec City, on the Laurentian Shield (Figure 6). The watershed covers 68 ha and drains from Lac Laflamme into the Montmorency River. It consists of mainly balsam fir (*Abies balsamea*) with a small percentage of white spruce (*Picea glauca*) and white birch (*Betula papyrifera*) (Barry et al. 1988; Arp and Yin 1992). The average annual rainfall and snowfall amount to 1005 mm and 680 cm, respectively, and mean monthly temperatures range from -14.8 °C in January to 14.6 °C in July.

The bedrock morphology at Lac Laflamme is composed of Precambrian charnockitic gneiss (Barry et al. 1990). The soil is an Orthic Ferro-Humic Podzol which was developed from well drained, sandy loam till, rich in coarse fragments. The till depth can ranges from 0.5 to 5 m in some areas and has a compacted c horizon (Arp and Yin 1992).

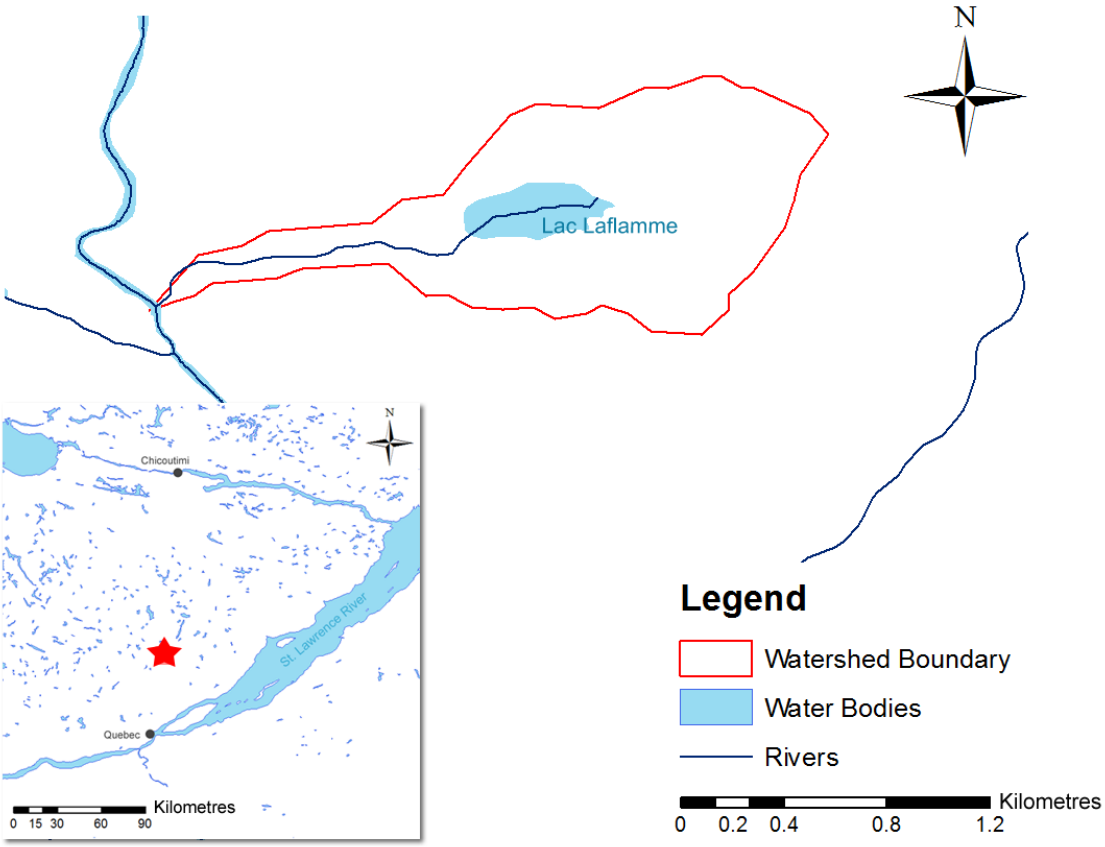


Figure 6. Lac Laflamme study area with watershed delineation and location map (see Table 4 for coordinates).

HAYWARD BROOK, NB

Hayward Brook is located within the Fundy Model Forest roughly 5 km south of Petitcodiac and 40 km southwest of Moncton, New Brunswick (Figure 7). With its association to the Fundy Model Forest, Hayward Brook has been well studied in the past decade in an effort to describe ecosystem responses to forest disturbances, as well as characterizing the biodiversity and landscape for management and educational purposes. The watershed covers 508 ha and drains into the Peticodiac River to the north. It is predominately 80-year old mixed Acadian forest, composed of red maple (*Acer rubrum*), red spruce (*Picea rubens*), aspen (*Populus* sp.), white birch (*Betula papyrifera*) and white

pine (*Pinus strobus*). The intolerant hardwoods dominate the south and the conifers are predominately in the north. Average annual rainfall and snowfall amount to 970 mm and 265 cm, respectively. Mean monthly temperatures range from -7.9 ℃ in January to 19.1 ℃ in July.

The Hayward Brook watershed lies within the Caledonia Highlands geomorphic region. It is made up of various bedrock formations such as Pennsylvanian grey sandstone, shale and conglomerate (Holmstrom 1986; Fahmy and Colpitts 1995). Due to the variable bedrock the surficial geology found at Hayward Brook is made up 3 different soil units, Salisbury, Parry and Sunbury. The Salisbury and Parry soils are well to imperfectly drained sandy loam till and the Sunbury soil is well drained loam to loamy sand till rich in coarse fragments (Pomeroy 2003; Stanley 2003; Chi 2008). The soil is predominantly Humo-Ferric Podzol.

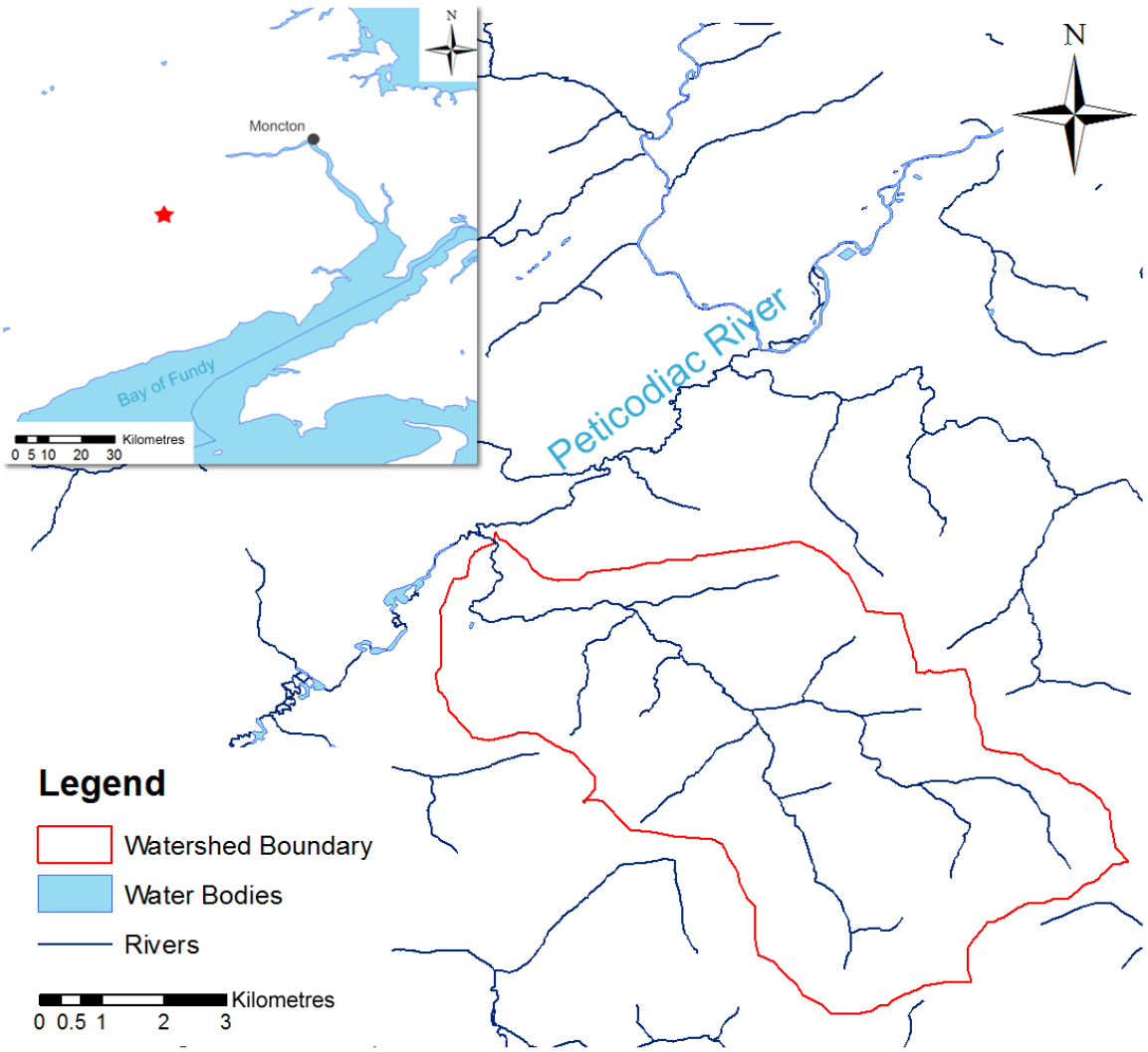


Figure 7. Hayward Brook study area with watershed delineation and location map (see Table 4 for coordinates).

POCKWOCK, NS

The study area for Pockwock is located approximately 30 km northwest of Halifax, Nova Scotia, in the southern portion of Hants County bordering Halifax County (Figure 8). The Pockwock study area consists of four basins, Long Pond, Walsh Brook, Sandy Brook West, and Peggy Brook. For the purposes of this study, the Peggy Brook basin is used. The Peggy Brook watershed covers 196 ha and drains into Pockwock Lake to the south. The woody vegetation in the area consists of mainly coniferous,

predominantly red spruce (*Picea rubens*), with small clumps of hardwood and mixed forest (Vaidya et al. 2008). The average annual rainfall and snowfall amount to 1180 mm and 215 cm, respectively, and mean monthly temperatures range from -5.5 °C in January to 18.7 °C in July.

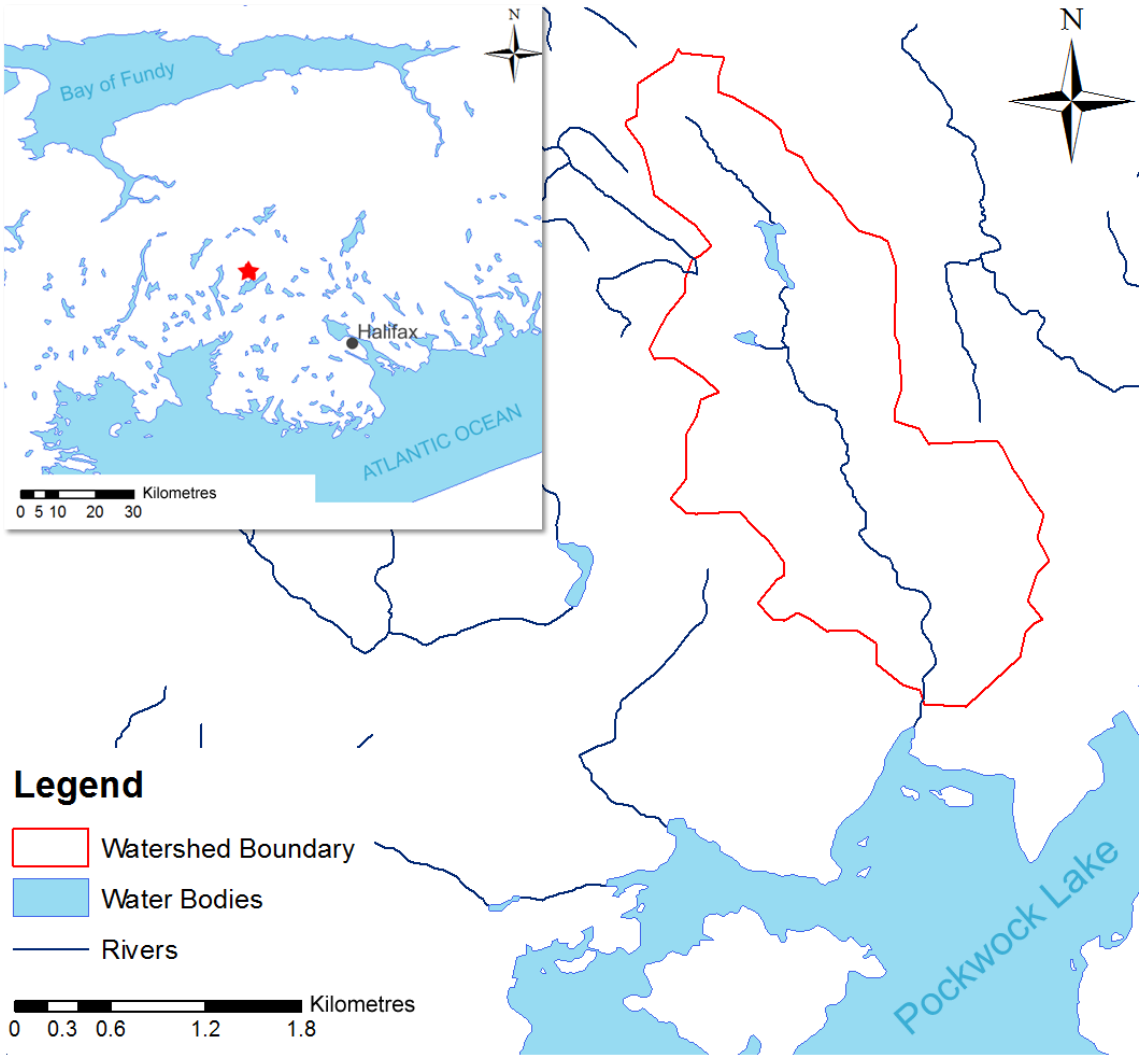


Figure 8. Pockwock study area with watershed delineation and location map (see Table 4 for coordinates).

The bedrock geology of the area is impervious Middle Devonian granodiorite. The granite bedrock produces a coarse-textured, shallow, and stony till with a sandy loam texture, of the Gibraltar soil type (Cann et al. 1954). Loamy Humo-Ferric Podzol is the dominant soil type in the ecoregion. The area is generally well to imperfectly drained but it also has innumerable poorly drained, sphagnum bog depressions (Chi 2008).

MOOSEPIT BROOK, NS

Moosepit Brook is located near the Kejimkujik National Park, which is roughly 100 km northeast of Yarmouth, Nova Scotia (Figure 9). The watershed covers 1670 ha and consists of a mixture of white spruce (*Picea glauce),* black spruce (*Picea mariana*), balsam fir (*Abies balsamea*) and mixed wood. Average annual rainfall and snowfall of 1140 mm and 250 cm, respectively and monthly mean temperatures range from -5.2 °C in January to 19.1 °C in July.

The bedrock found at Moosepit Brook contains Devonian granite and Cambro-Ordorician slate (Bobba and Lam 1989). According to MacDougall et al. (1969) Moosepit Brook borders both Queens County and Annapolis County and contains mostly the Bridgewater sandy loam soil type. A further breakdown of the surface geology consists of coarse textured sandy loan to loamy sand ablation till on top of compacted basal till (Yanni et al. 2000a). Due to the composition of the parent material, the subsoils of the region weather very slowly and produce shallow soil profiles (~<50cm), which are also generally impermeable (Bobba and Lam 1989; Yanni et al. 2000a). The study area for Moosepit Brook is considered to be moderate to poorly drained and over one-quarter

of the surface area is covered by sphagnum bogs (Christophersen et al. 1997). The soil classification for the area ranges from orthic humo-ferric podzol to orthic sombric brunisol, depending on the site morphology and drainage (Yanni et al. 2000b).

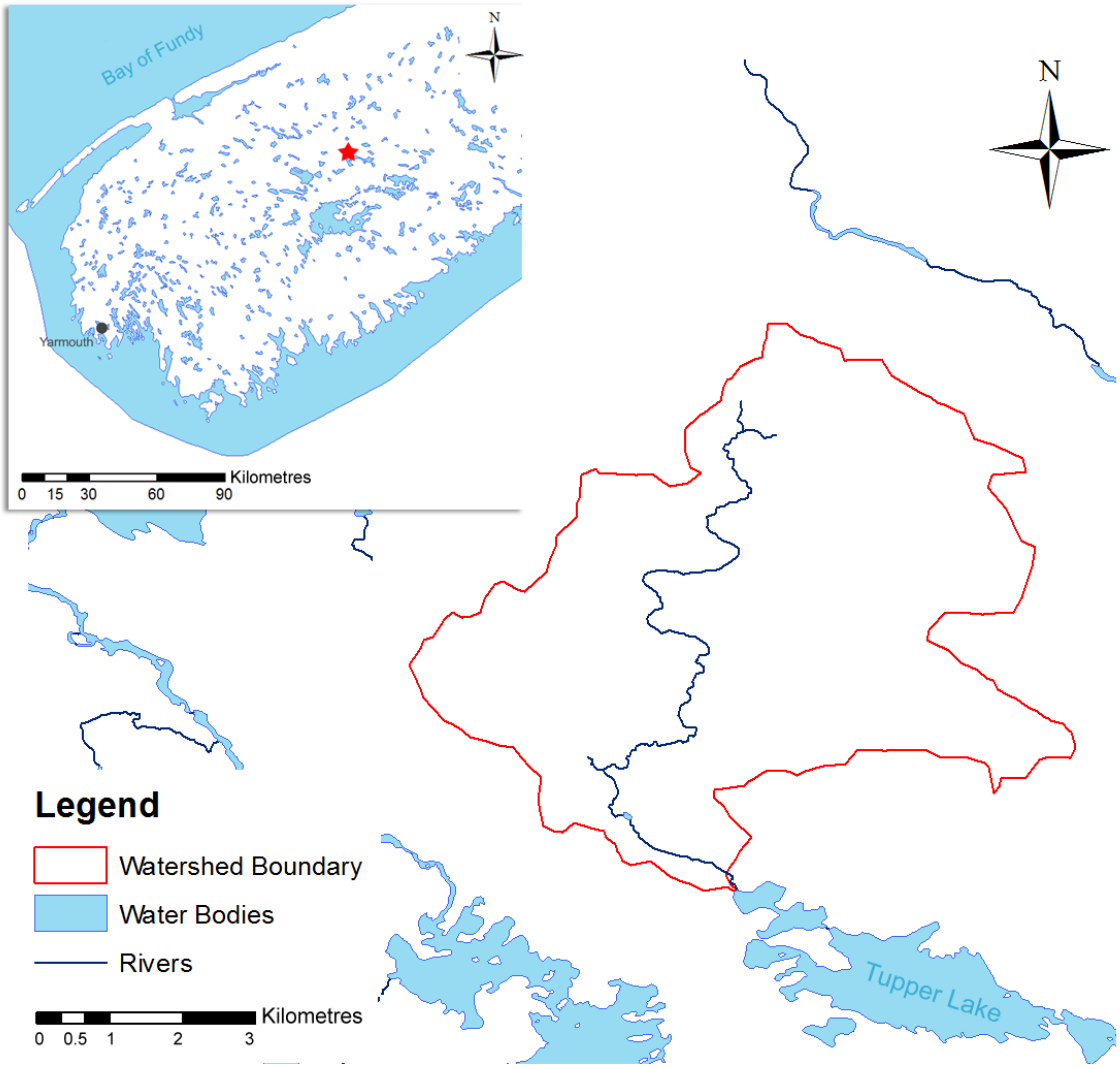


Figure 9. Moosepit Brook study area with watershed delineation and location map (see Table 4 for coordinates).

LITERATURE CITED

Arp, P.A., Yin, X. 1992. Predicting water fluxes through forests from monthly precipitation and mean monthly air temperature records. *Canadian Journal of Forest Research*. 22:864-877.

Barry, R., Plamondon, A. P., Stein, J. 1988. Hydrologic soil properties and application of a soil moisture model in a balsam fir forest. *Canadian Journal of Forest Research*. 18:427-234.

Barry, R., Prevost, M., Stein, J., Plamondon, A.P. 1990. Simulation of snowmelt runoff pathways on the Lac Laflamme watershed. *Journal of Hydrology*. 113:103-121.

Beall, F.D., Semkin, R.G., Jeffries, D. 2001. Trends in the Output of First-order Basins at the Turkey Lakes Watershed, 1982-96. *Ecosystems*. 4:514-526.

Bobba, A.G., Lam, D.C.L. 1989. Applications of hydrological model to acidified watersheds: a study on Mersey River and Moosepit Brook, Nova Scotia. *Water, Air, and Soil Pollution*. 46:261-275.

Brady, N.C., Weil, R.R. 2001. *The Nature and Poperties of Soils*. 13th ed. Upper Saddle River, New Jersey: Prentice Hall.

Cann, D.B., Hilchey, J.D., Smith, G.R. 1954. "Soil Survey of Hants County Nova Scotia." Nova Scotia Soil Survey No. 5, Department of Agriculture, Agriculture Canada, Truro.

Chi, X. 2008. Hydrogeological assessment of stream water in forested watershed: temperature, dissolved oxygen, pH, and electrical conductivity. Unpublished. MSc. Thesis., University of New Brunswick, Fredericton, NB.

Fahmy, S.H., Colpitts, M. C. 1995. "Soils of the Fundy Model Forest." Agriculture and Agri-Food Canada, Fundy Model Forest, Fredericton.

Hazlett, P.W., Semkin, R.G., Beall, F.D. 2001. Hydrologic pathways during snowmelt in first-order stream basins at the Turkey Lakes Watershed. *Ecosystems*. 4:527-535.

Hazlett, P.W., Foster, N.W. 2002. Topographic controls of nitrogen, sulfur, and carbon transport from a tolerant hardwood hillslope. *Water, Air, and Soil Pollution: Focus*. 2:63-80.

Holmstrom, D.A. 1986. "Soils of the Sussex Area of New Brunswick." New Brunswick Soil Survey, Research Branch, Agriculture Canada, Fredericton.

Jungen, J.R., Ag, P. 1985. Soils of Southern Vancouver Island. British Columbia Soil Survey, Ministry of Environment, Government of British Columbia, Victoria, B.C.

Jutras, M.-F., Nasr, M., Castonguay, M., Pit, C., Pomeroy, J., Smith, T. P., Zhang, C.-F., Ritchie, C.D., Meng, F.-R., Clair, T.A., Arp, P.A. 2011. Dissolved organic cardon concentrations and fluxes in forest catchments and streams: DOC-3 model. *Ecological Modeling*. doi:10.1016/j.ecolmodel.2001.03.035.

MacDougall, J.L., Nowland, J.L., Hilchey, J.D. 1969. "Soil Survey of Annapolis County Nova Scotia." Nova Scotia Soil Report No. 16, Nova Scotia Department of Agriculture, Agriculture Canada, Truro, Canada.

Monroe, J., Wicander, R., Hazlett, R. 2007. *Physical Geology - Exploring the Earth*. 6th ed. Belmont, CA: Thomsom Brooks/Cole.

Murphy, P.N.C., Castonguay, M., Ogilvie, J., Nasr, M., Hazlett, P., Bhatti, J., Arp, P.A. 2009. A geosptial and temporal framework for modeling gaseous N and other N losses from forest soils and basins, with application to the Turkey Lakes Watershed Project, in Ontario, Canada. *Forest Ecology and Management*. 258:2304-2317.

Murray, C. D., Buttle, J. M. 2005. Infiltration and soil water mixing on forested and harvested slopes during spring snowmelt, Turkey Lakes Watershed, central Ontario. *Journal of Hydrology*. 306:1-20.

Pomeroy, J.H. 2003. Stream turbidity signatures within the Hayward Brook watershed study. Unpublished. MSc. Thesis. University of New Brunswick, Fredericton, NB.

Stanley, B. 2003. The Hayward Brook Waterhsed Study: Hydrogeochemistry and responses to forest operations. Unpublished. MSc. Thesis. University of New Brunswick, Fredericton, NB.

Vaidya, O.C., Smith, T.P., Fernand, H. 2008. Forestry best management practices: evaluation of alternate streamside management zones on stream water quality in Pockwock Lake and Five Mile Lake watersheds in central Nova Scotia, Canada. *Environmental Monitoring and Assessment*. 137:1-14.

Wulder, M., Neimann, K.O., Goodenough, D. 2000. Local maximum filtering for the extraction of tree locations and basal area from high spatial resolution imagery. *Remote Sensing Environment*. 73:103-114.

Yanni, S., Keys, K., Clair, T., Arp, P.A. 2000a. Fog and acidification impacts on ion budgets of basins in Nova Scotia, Canada. *Journal of the American Water Resource Association*. 336:619-631.

Yanni, S., Keys, K., Meng, F.-R., Yin, X., Clair, T., Arp, P.A. 2000b. Modeling hydrological conditions in the maritime forest region of south-west Nova Scotia. *Hydrological Processes*. 14:195-214.

Zhu, J. Z., Mazumder, A. 2008. Estimating nitrogen exports in response to forest vegetation, age and soil types in two coastal-forested watershed in British Columbia. *Forest Ecology and Management*. 255:1945-1959.

CHAPTER 4 - THE FOREST HYDROLOGY MODEL (FORHYM2)

INTRODUCTION

The forest hydrology model (ForHyM2) is an amalgamation of ForHyM (forest hydrology model; Arp and Yin 1992) and ForSTEM (forest soil temperature model; Yin and Arp 1994). It was designed to calculate thermal and hydrological flows in a forest on a monthly scale (Meng et al. 1995). It was later adapted to produce daily results (Bhatti et al. 2000). In essence, it is a one-dimensional, lumped, deterministic model that utilizes empirical relationships in the forest to forecast hydrological and thermal fluxes. The primary functions in the model focus on hydrological processes such as canopy interception, evapo-transpiration, snowmelt, snowpack accumulation, and stream discharge by forest floor, mineral and subsoil (Figure 10). It also includes specific modules, like heat flow and energy balances, thermal properties and temperature variables, as well as a recently added dissolved organic carbon and mercury module (Jutras et al. 2011).

MODEL INTERFACES

ForHyM2 uses STELLA, a computer modeling software that enables users to create dynamical, graphical, object-based interfaces which simulate complex systems. Instead of employing intricate line-written programming code, STELLA users can model relationships using block icons (Figure 11). Each block has a specific function, an action or process, which defines how it interacts with other blocks in the model.

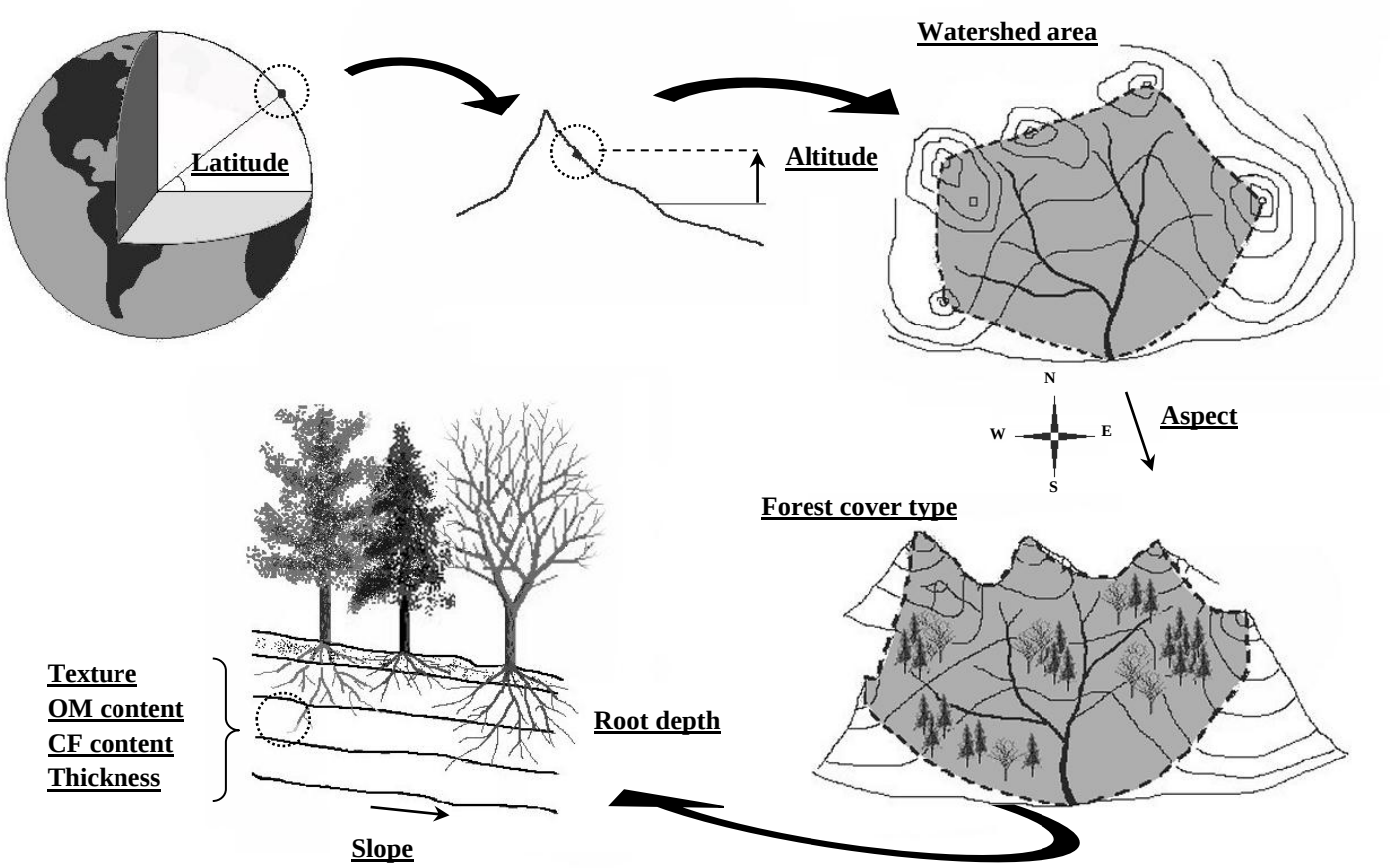


Figure 10. Specification overview for the Forest Hydrology Model related to catchment characteristic inputs (Balland 2002).

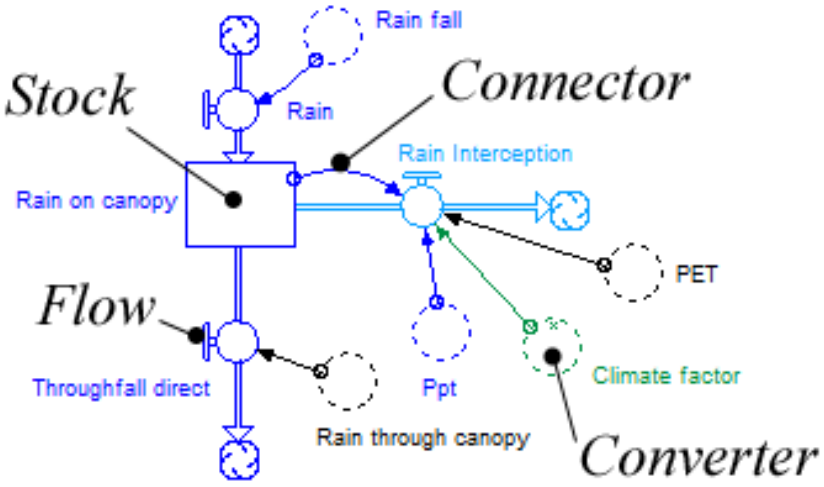


Figure 11. Sample of STELLA interface connections showing the various object types.

Using known equations about the various functional relationships built in the model, connections can be made for each block. From these connections the model can then produce outputs, which mimic the desired natural processes being modeled. ForHyM2 utilizes the STELLA interface to empirically formulate dynamic connections to forecast temperature and hydrological flows in a watershed (Figure 12). STELLA makes use of 4 basic building blocks:

- *Converters*: function that creates an output value during each time interval, e.g., temperature, stream flow. It can also be a constant variable, e.g., watershed area or texture by soil horizon.
- *Flows*: function representing activities that lead to input and outputs to stocks, e.g. thaw and freeze of forest floor.
- *Stock*: function used to represent things that accumulate, e.g., reservoirs, water in forest floor.
- *Connectors*: transmit information to adjust flows and converters

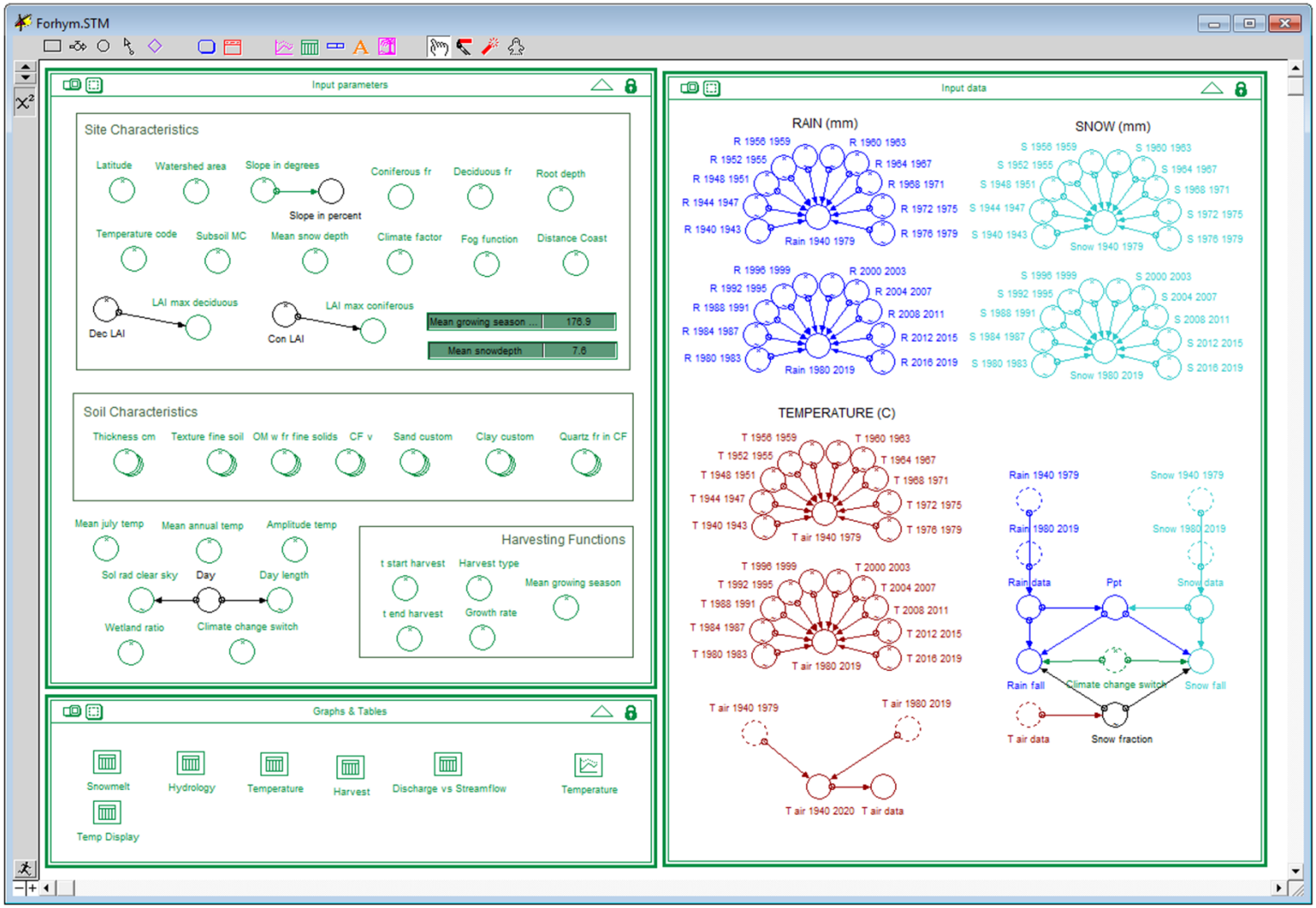


Figure 12. ForHyM2 model opened in STELLA showing input parameters.

ForHyM2 is connected to a secondary “user-friendly” interface in Excel (Figure 13). This interface is used to enable ease of model functionality, because the STELLA interface can be quite large and daunting for new users. It organizes all of the watershed information into easy to navigate tabs. Two tabs are for data inputs (Input Parameters and Data) and one for calibration purposes. The rest of the tabs in the interface use built-in Excel Macros to convert the input data into a STELLA-ready format. The data in these tabs is fed to the STELLA interface via a dynamic link. Having both the Excel and STELLA interface open enables users to easily alter input data and calibrate model results.

MODEL INPUTS

In order to run the model, a number of inputs are required. For each catchment, local weather data and catchment characteristics are used as primary inputs (Figure 13). The weather inputs are daily air temperature (°C), daily snow depth (cm), and daily precipitation (rainfall and snowfall in mm). The catchment characteristics are: latitude (°), altitude (m), watershed area (ha), fog function (takes into account the impact of the presence of fog on evapotranspiration from the forest; 0=False, 1=True), distance to the coast (km, used because of variation in wind patterns near coastlines), aspect (°), slope (°), tree species (expressed as a fraction for each, deciduous and coniferous), mean yearly snow depth (cm), tree root depth (coded 1-6 to describe roots that are from shallow to very deep), and soil inputs: horizon thickness (cm), sandy, silt and clay percentages, organic matter content (fraction by weight), coarse fragment percentage, fraction of quartz (present in coarse fragment).

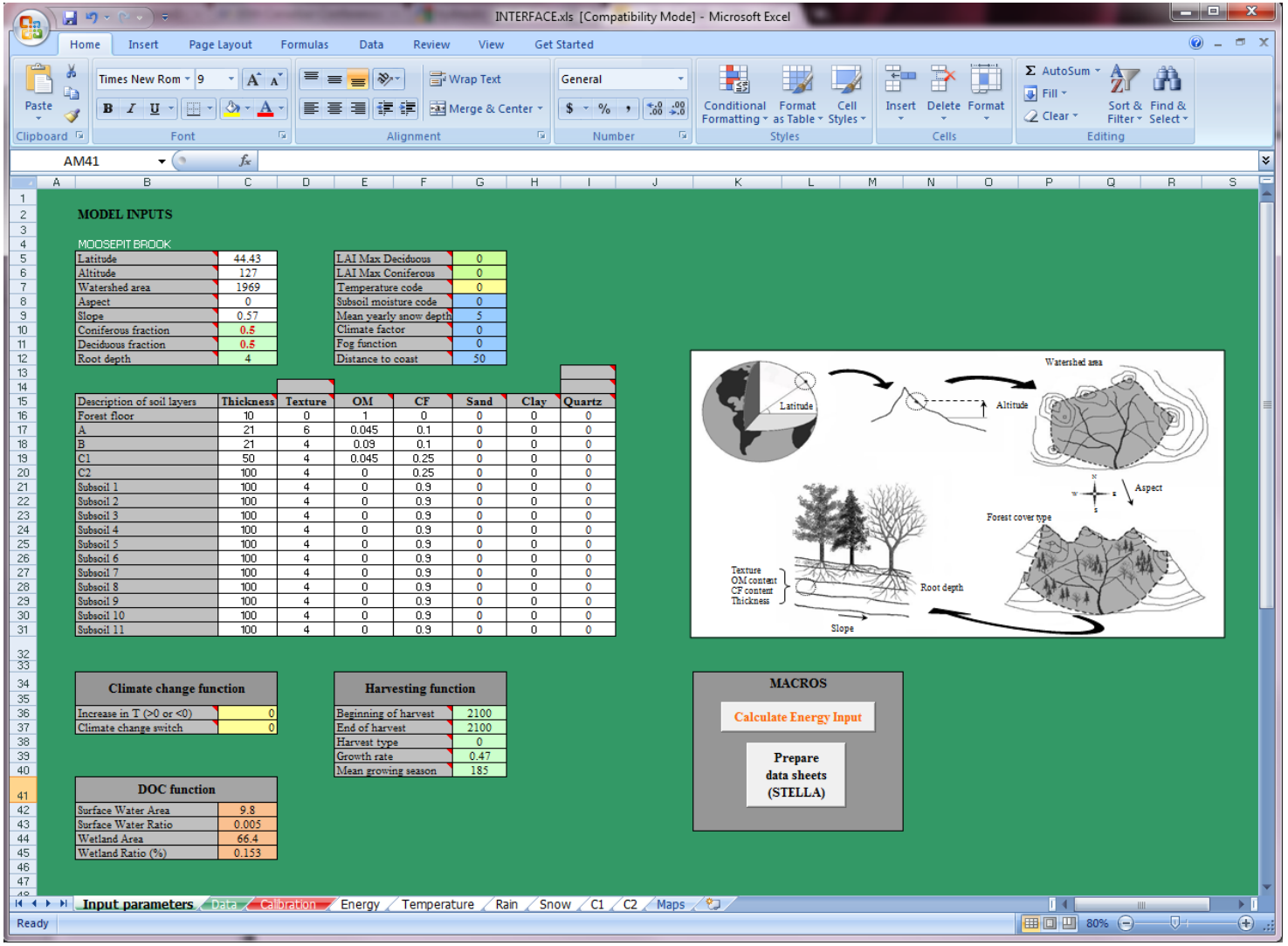


Figure 13. ForHyM2 user interface in Excel showing watershed and soil input parameters.

MODEL OUTPUTS

The primary outputs for the ForHyM2 model are (i) water content of the forest floor, mineral soil and subsoil via water fluxes, runoff, interflow and total discharge, (ii) soil frost (depth and duration), (iii) snowpack variables (including density, depth and amount of snowmelt), (iv) heat and water flow parameters, based on the soil characteristics, (v) net energy that is exchanged between the soil or snowpack, and atmosphere, (vi) daily variations of moisture and temperature in the forest floor, mineral soil and subsoil, and (vii) daily solar radiation.

HYDROLOGY MODULE

The hydrology module in ForHyM2 focuses on the flow and retention of water in a watershed (Figure 14). It uses daily precipitation, in the form of either rain or snow, as the primary input. Precipitation is first intercepted by the forest canopy. The amount of water the forest canopy intercepts is dependent on the leaf area index (LAI). For example, a thick forest canopy with a large LAI will intercept more water, and therefore less water will reach the forest floor. Precipitation can also be intercepted by snow on the canopy and snowpack, which is an accumulation of snow on the ground. Depending on the ambient temperature, as well as the snowpack temperature, water will either accumulated on the snowpack as ice or water, or reach the forest floor as snowmelt. The field capacity of the snowpack determines the maximum amount of liquid the snowpack can retain. The potential snowmelt is based on the energy input into the snowpack.

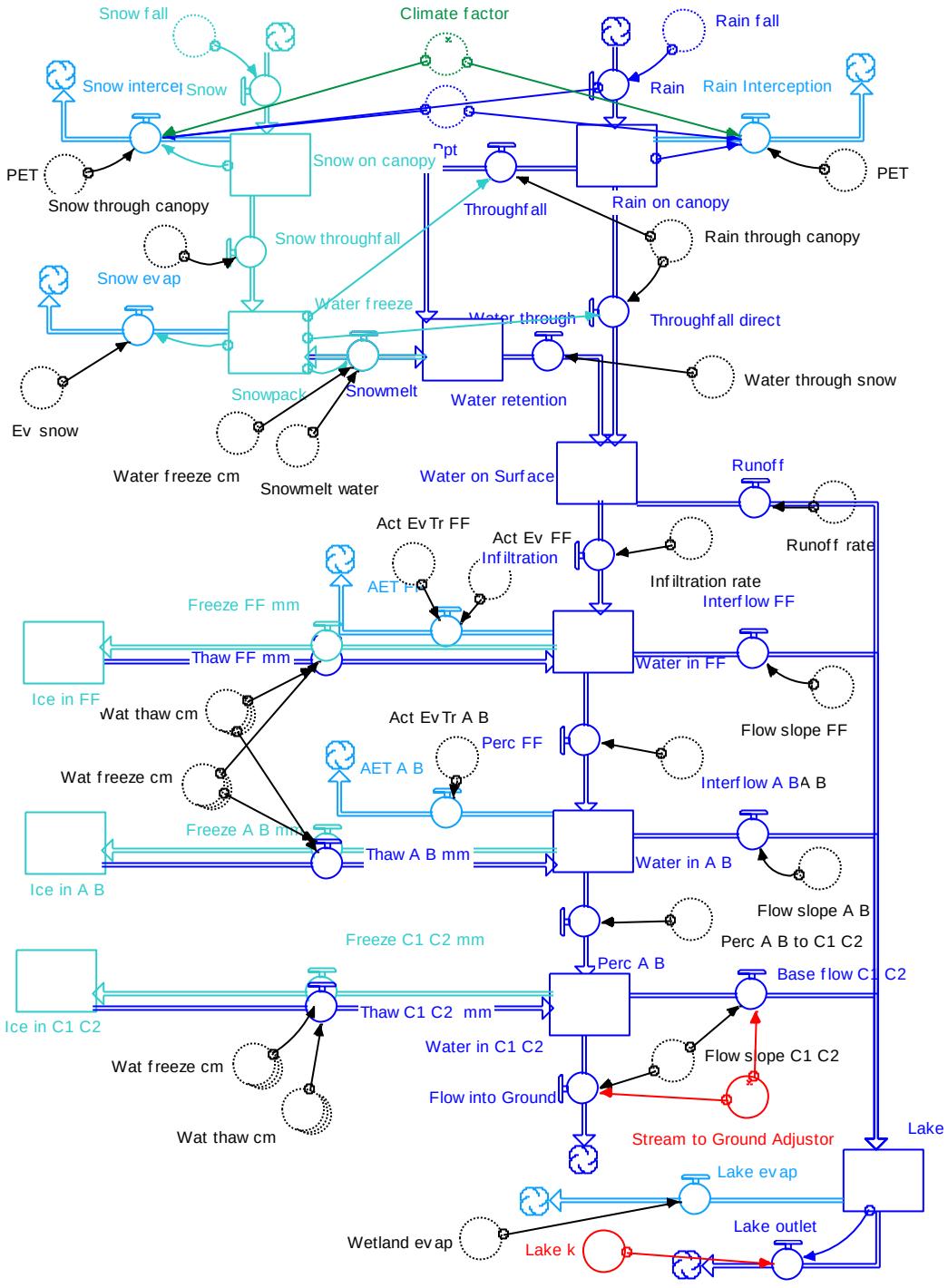


Figure 14. Hydrology calculations for the ForHyM model in Stella.

With interception via forest canopy, snow on the canopy, and snowpack, some of the water can evaporate into the atmosphere via evapotranspiration. The water that reaches the forest floor from throughfall and/or snowmelt can either infiltrate into the soil or become surface runoff. Infiltration is limited by the soil's capacity to take up water. In this model, only gravitational water is allowed to flow, i.e., the amount of soil moisture above field capacity (FC). The rate of this flow is set to be proportional to pore % of gravitational water multiplied by K_{sat} to estimate downward flow ("percolation", or "infiltration"), and adjusted for % slope of the basin to estimate "lateral flow" or "interflow". If the underlying layer is saturated, or constricts the movement of water, it will then flow laterally as interflow. Therefore, the deeper layer flow is calculated prior to the subsoil layer to determine the empty pores available for percolation, or if it will become interflow. Infiltration into unsaturated soils is determined; (i) by directly filling the partially available pore space up to SP, and (ii) by accommodating downward as well as lateral flow as long as the soil moisture content would remain above FC. The lateral flow of water in deep subsoil is referred to as baseflow. Water flows laterally until it finds either unsaturated subsoil or it reaches a natural discharge point (i.e. lake or river). The surface runoff, interflow and baseflow are calculated using Darcy's Law (Eq. 1) and rely on watershed slope as well as the K_{sat} of each soil layer in the mineral and subsoil to determine the flow rate for each soil horizon (Figure 15). The combination of surface runoff, interflow, and baseflow make up total stream discharge. The model produces flow rates per soil layer in mm/year but then, in keeping with Darcy's Law, utilizes the watershed area to calculate overall stream discharge in m^3/s.

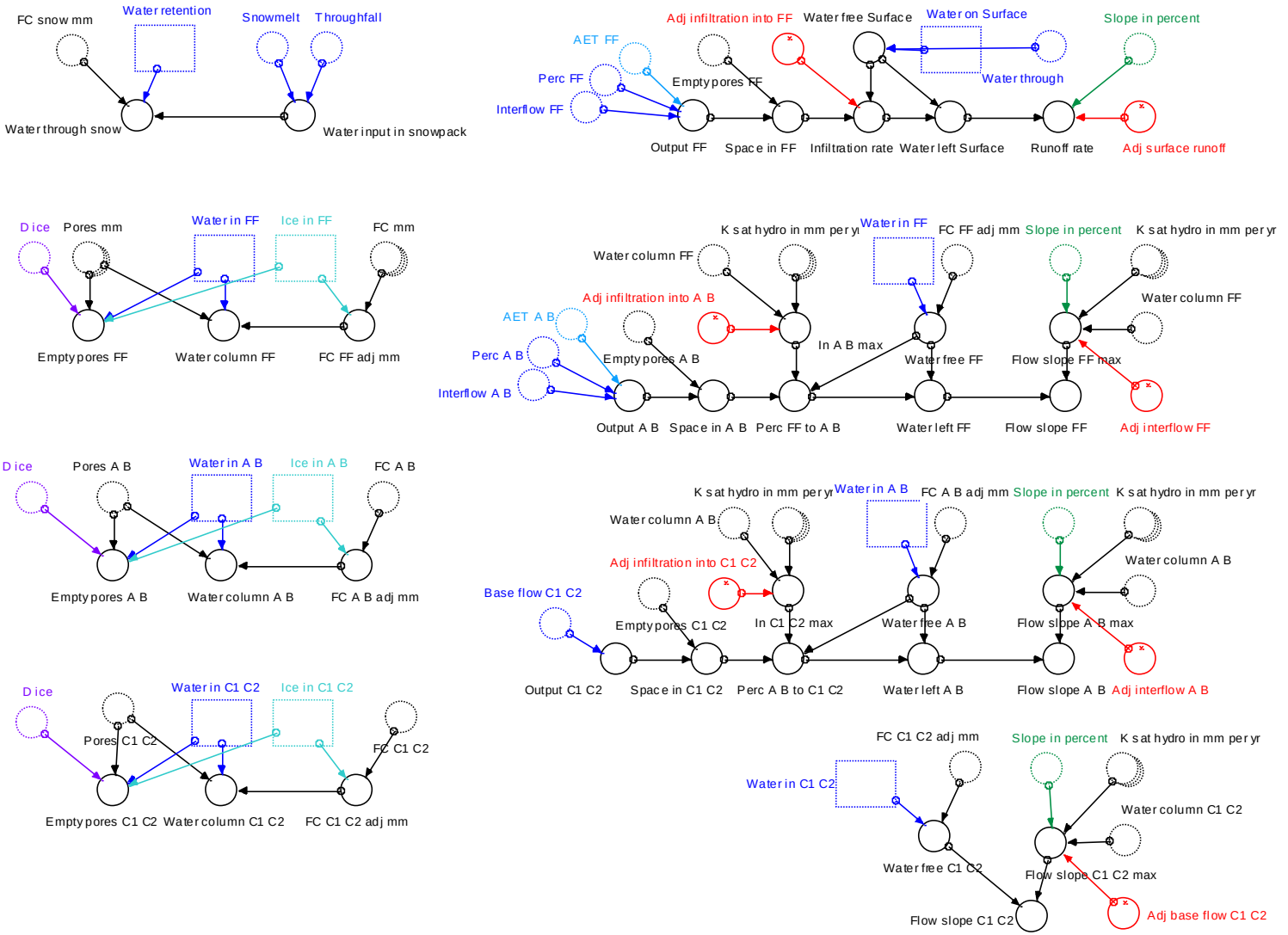


Figure 15. Soil water flow hydrology sub-module, focused on the water capacity and flow slope for the A and B horizons.

A minor adjustment was made to the hydrology sub-module. Flow slope, which is the maximum amount of water (in mm/yr) that can flow laterally inside a horizon, uses slope (%), K_{sat} (mm/yr), and the water column ratio (showing how the pore space, above field capacity, is saturated with gravitational water) (Figure 15). In the old model, flow slope was also multiplied by horizon depth, but was removed due to being accounted for in K_{sat} through D_b. In essence it was doubling the thickness used in Darcy's Law (Eq. 1).

Estimating soil moisture, modeling K_{sat}

Each soil moisture parameter equation (Eq. 15-19) was integrated into ForHyM2 using the input soil properties from the user interface that are required to run the model (soil texture, profile depth, and OM). Figure 16 illustrates connections made using these equations, as well as the outputs that are used in further calculations within the hydrology module and sub-modules (Figures 14 and 15). For example, "K_{sat} hydro fine soil", the output parameter created using the K_{sat} equation, uses sand %, D_p and D_b as input variables (Figure 16; red circle and blue squares). It is converted from cm/hr to mm/day and used to calculate flow slope and subsequently stream discharge.

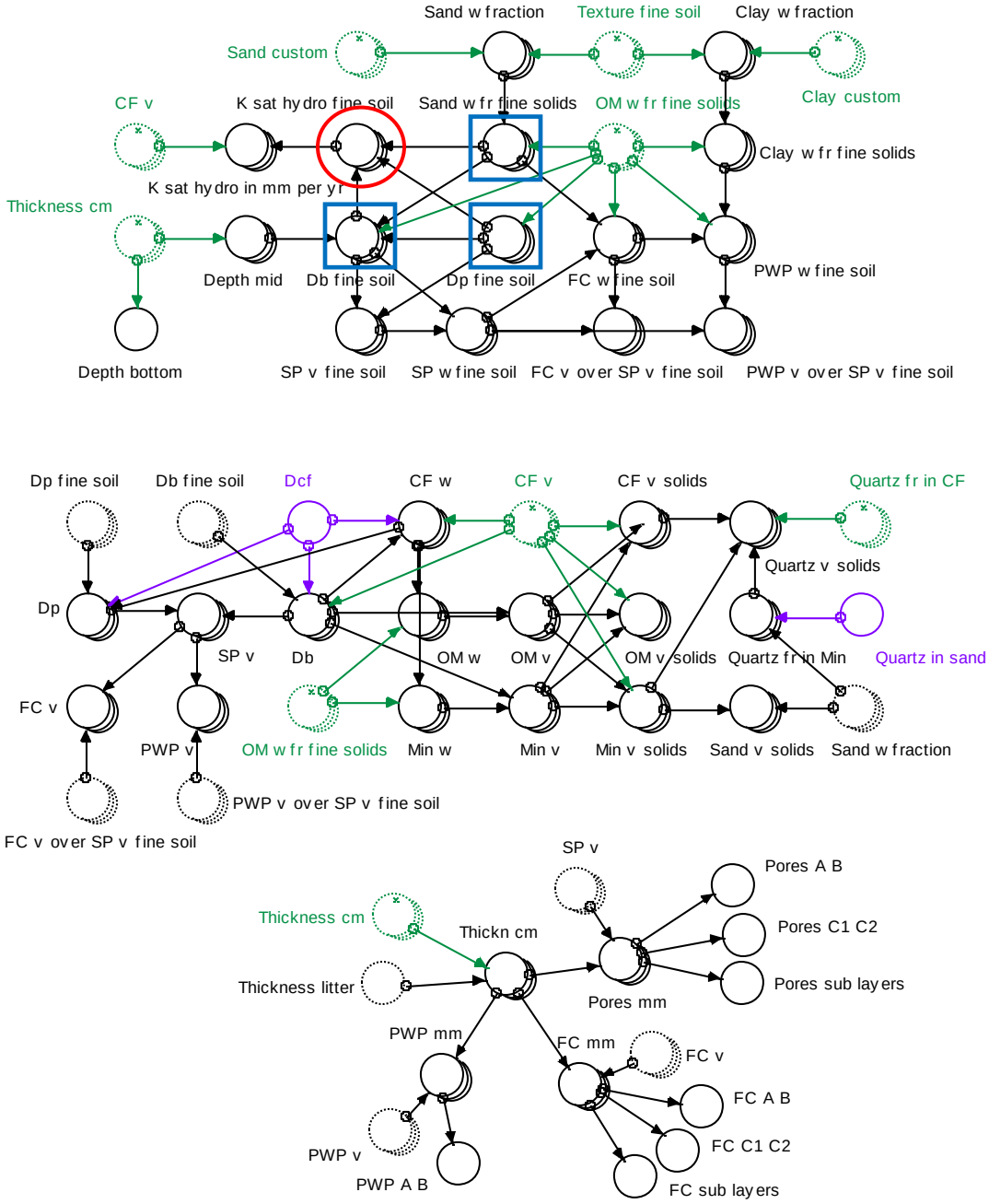


Figure 16. Hydrology parameters module - specifically soil water capacity, K_{sat} and volume by horizon. Example inputs (blue squares), example output (red circle).

Deep Groundwater Percolation

All of the water that flows through ForHyM2 is accounted for and keeps the model in proper water balance. Water balance equals total precipitation (P; rain and snow) minus total discharge (D), evapotranspiration (ET), and soil storage (SS) (Brady and Weil 2001). A minor adjustment was made to the total discharge in the ForHyM2 model. Due to the nature of some bedrock formations and soil composition at some of the sites (for example Hayward Brook sits on a heterogeneous mixture of calcareous shales, sandstones and conglomerate), an addition was made to the main hydrology module to add a deep ground water percolation flow. Prior to this, ForHyM2 assumed that all of the groundwater in the C horizon would flow laterally as baseflow into the reservoir (i.e. lake). Stream discharge monitoring stations in the watersheds only take into account water that ends up flowing laterally. Any water that is "leaked" out of the watershed by flowing into deep bedrock is not accounted for. By adding a new flow channel from the reservoir of water in the C horizon down through the bedrock as deep ground water percolation, ForHyM2 now accounts for basins with fragmented bedrocks or drainage tiles, which would instigate greater downwards flow. A stream to ground adjustor was added to the calibration process in order to direct the flow to either deep ground percolation or laterally towards the lake reservoir (Figure 17). Since total discharge only equals lateral flow, this 'leaky' deep water percolation makes up for the missing water in the water balance of the watershed. See Chapter 5 for examples of how the deep water percolation function affects different watersheds.

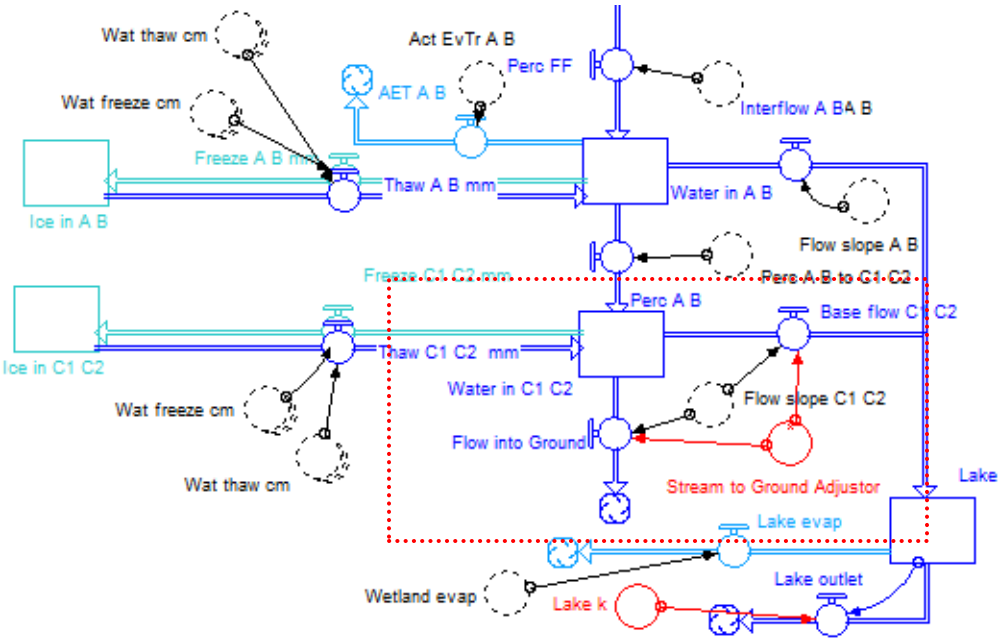


Figure 17. Flow into ground flow (blue flow parameter coming from Perc A B) addition with stream to ground calibration adjustor (red converter), outline in red dotted box, part of the main hydrology module.

Hydrothermal Relationships

Temperature and the storage of energy have important roles in the water flow of a watershed. ForHyM2 utilizes many connections of hydrothermal properties between the hydrology module and the temperature parameters modules (Figure 18). The PTFs developed by Balland et al. (2008) are complemented by equations dealing with estimating the rate of heat transfer through snow and soil, by relating heat capacity and conductivity to soil or snow density, texture, OM, coarse fragment content, and soil moisture content for the frozen and unfrozen state. The important parameters to look at specifically are: thermal conductivity (*k*, W m^{-1} $^{\circ}C^{-1}$), the soil's ability to conduct heat, and volumetric heat capacity (C, cal cm^{-3} $^{\circ}C^{-1}$), and the soil's ability to store energy during a temperature change (Eq. 20-21). The volumetric heat capacity parameter is significant because it is directly related to the energy that is required to either potentially

freeze water or thaw ice in the soil. If the volumetric heat capacity of the soil is low, then the potential water could be tied up as ice in the soil instead of liquid water, which in turn affects the flow (K_{sat}) through that soil. Figure 17 shows the connections from the heat capacity parameter to the energy used to melt or thaw, down to the actual quantity of water in either ice or liquid water form for each soil layer (which is used in the hydrology module to determine K_{sat} from available water).

Thermal conductivity looks at the transfer of heat through the soil and snowpack. In ForHyM2, *k* is used to create the temperature parameters for each soil layer which in turn helps to determine the potential freeze or thaw of the soil in the snow and ice module (Figure 19). In general, as soil moisture, ice and quartz content increase, *k* increases (Balland and Arp 2005), therefore knowing *k* can be useful when comparing different soils and the movement of water through a watershed.

$$k = \left(K_{wet} - K_{dry}\right) * K_e + K_{dry} \quad (21)$$

where,

K_{wet} = thermal conductivity of the soil if it is totally saturated (W m^{-1} $^{\circ}C^{-1}$)

K_{dry} = thermal conductivity of the soil if it is totally dry (W m^{-1} $^{\circ}C^{-1}$)

Ke = Kersten coefficient for all soils (frozen and unfrozen)

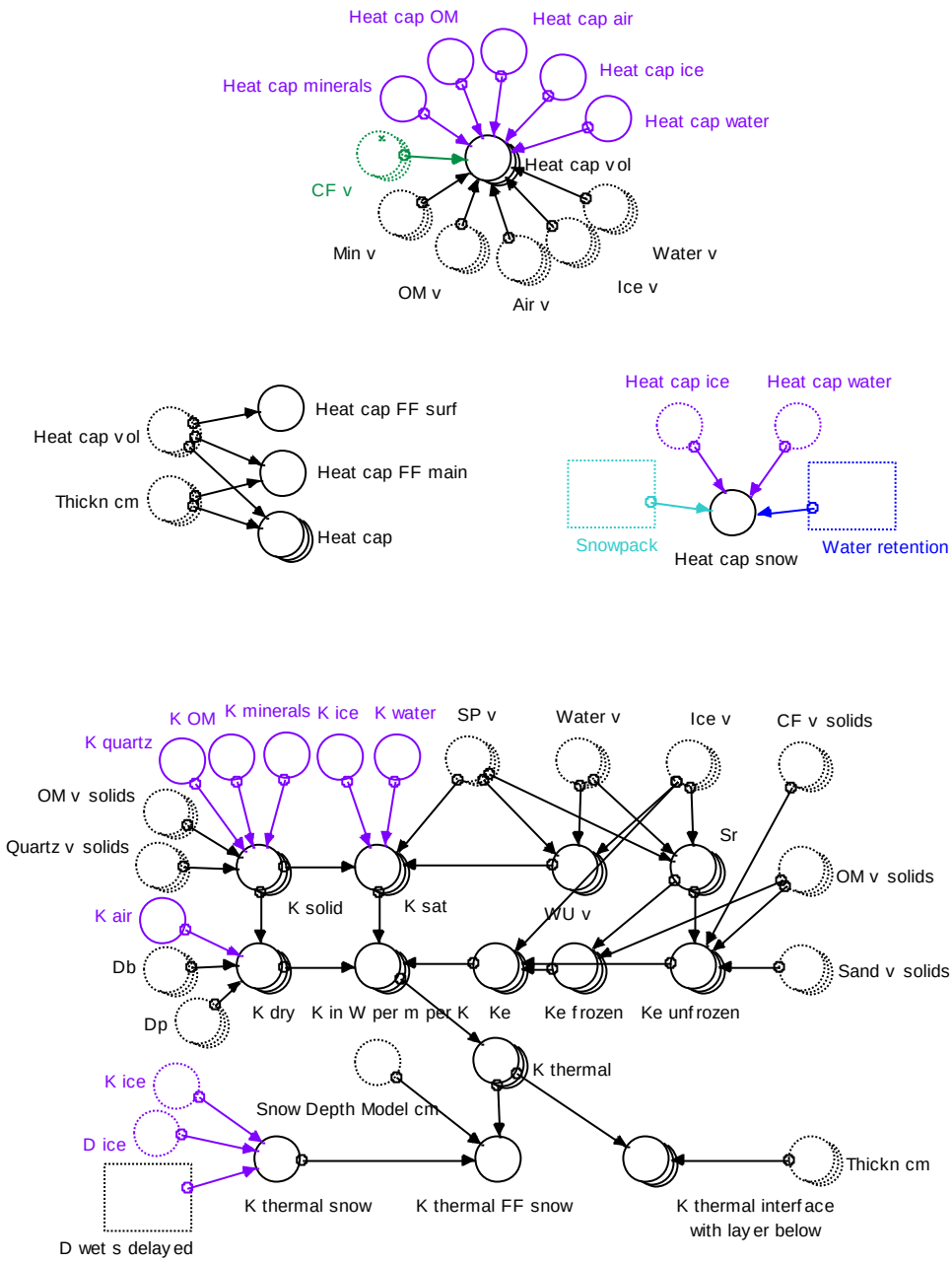


Figure 18. Thermal parameters module, showing heat capacity and thermal conductivity.

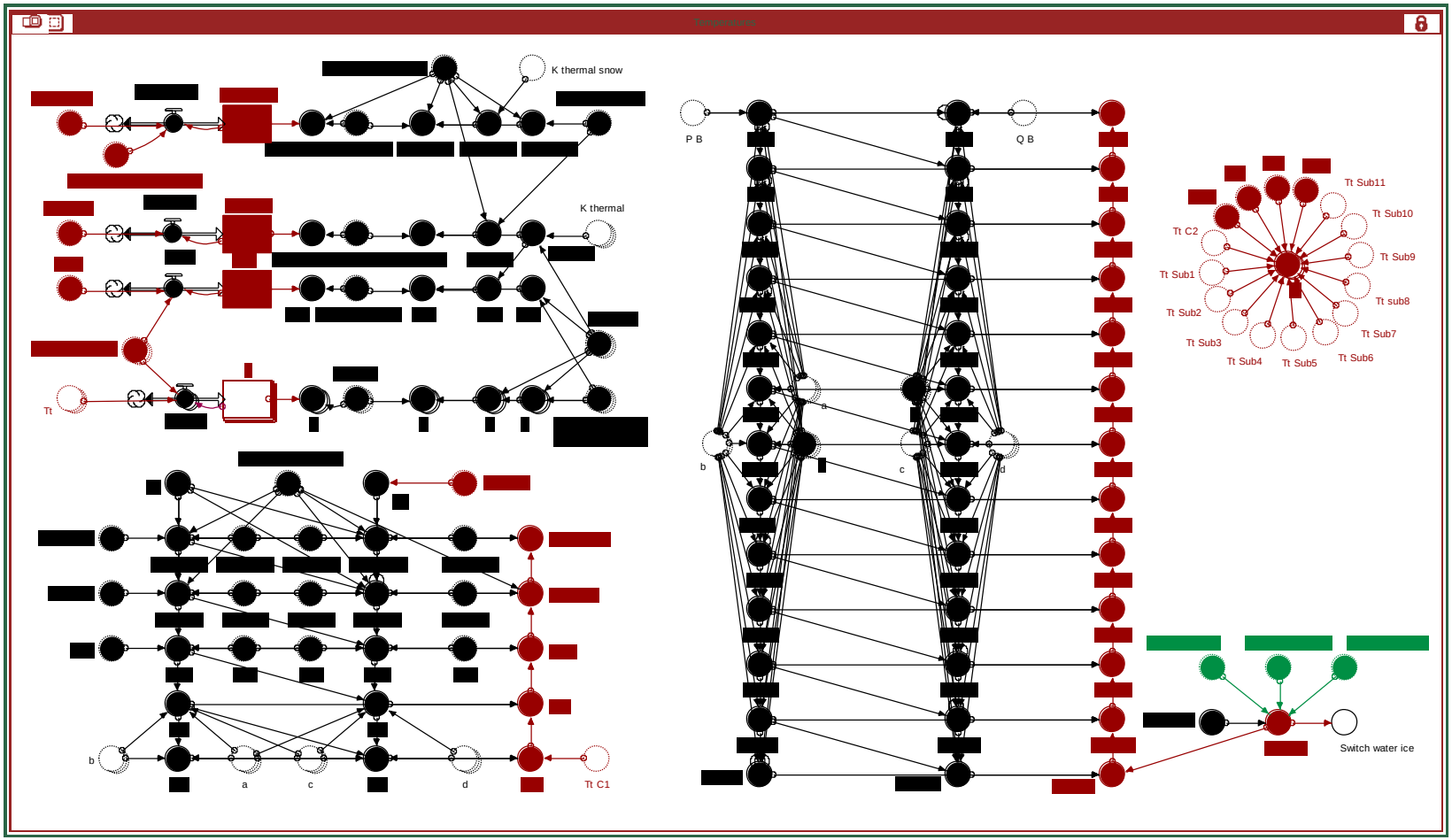


Figure 19. Temperature module showing thermal conductivity and soil layer temperature.

$$C = C_{H20} * V_{H20} + C_{ice} * V_{ice} + C_{air} * V_{air} + C_{OM} * V_{OM} + C_{min} * (V_{min} + V_{CF}) \quad (22)$$

where,

C_x = volumetric heat capacity in cal cm^{-3} $°C^{-1}$ of water, ice, air, organic matter, and mineral soil, respectively

V_x = volumetric content (dimensionless) of water, ice, air, organic matter, mineral soil and coarse fragments, respectively

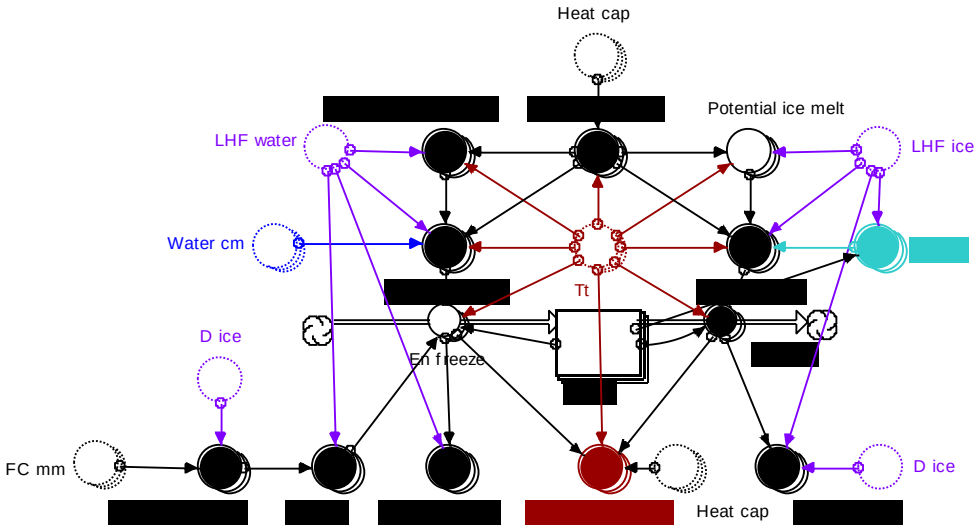


Figure 20. Heat capacity parameters for determining potential water freeze or potential ice melt, found in the snow and ice module.

MODEL LIMITATIONS

With ForHyM, each watershed under consideration is treated as a single point for incoming and outgoing water and heat flow. Doing so assumes that these flows unfold uniformly across the entire watershed area. Therefore, it does not take into account variations in slope, soil type, vegetation type flow accumulation, changes in soil moisture and drainage across the watershed. ForHyM, however, can also be applied to any particular point within a watershed provided provisions can be made to account for incoming seepage. Seepage can be expected to occur along hill slopes with impermeable

subsoils, or along the bottom of seepage zones due to upwelling groundwater, if such points are located within the seepage zone of foot slopes.

While ForHyM2 tracks changes in soil moisture, temperature, and frost over time, it does not track dynamic changes in soil properties pertaining to organic matter content and density. The former would occur gradually over time depending on changes in vegetation cover over time, while the latter would occur as a result of wetting and thawing, freezing and drying, and traffic-induced soil compaction. Such changes, if known, can be included within ForHyM by way of additional data input. Alternatively, ForHyM can be applied to any particular combination of soil density and organic matter content for any particular layer, to learn as to how these changes would affect water and heat retention and flows through each particular soil profile or watershed.

LITERATURE CITED

Arp, P.A., Yin, X. 1992. Predicting water fluxes through forests from monthly precipitation and mean monthly air temperature records. *Canadian Journal of Forest Research*. 22:864-877.

Balland, V., Arp, P.A. 2005. Modeling soil thermal conductivities over a wide range of conditions. *Journal of Environmental Engineering Science.* 4:549-558.

Balland, V., Pollacco, J.A.P., and Arp, P.A. 2008. Modeling soil hydraulic properties for a wide range of soil conditions. *Ecological Modeling*. 219:300-316.

Bhatti, J.S., Fleming, R.L., Foster, N.W., Meng, F.-R., Bourque, C.P.A., Arp, P.A. 2000. Simulations of pre- and post-harvest soil temperature, soil moisture, and snowpack for jack pine: comparison with field observations. *Forest Ecology and Management*. 138:413-426.

Brady, N.C., Weil, R.R. 2001. *The Nature and Poperties of Soils*. 13th ed. Upper Saddle River, New Jersey: Prentice Hall.

Jutras, M.-F., Nasr, M., Castonguay, M., Pit, C., Pomeroy, J., Smith, T. P., Zhang, C.-F., Ritchie, C.D., Meng, F.-R., Clair, T.A., Arp, P.A. 2011. Dissolved organic cardon concentrations and fluxes in forest catchments and streams: DOC-3 model. *Ecological Modeling*. doi:10.1016/j.ecolmodel.2001.03.035.

Meng, F.-R., Bourque, P.A., Jewett, K., Daugharty, D., Arp, P.A. 1995. The Nashwaak experimental watershed project: analysing effects of clearcutting on soil temperature, soil moisture, snowpack, snowmelt and streamflow. *Water, Air and Soil Pollution*. 82:363-374.

Yin, X., Arp, P.A. 1994. Fog contributions to the water budget of forested watershed in the Canadian Maritime provinces: a generalized algorithm for low elevations. *Atmosphere-Ocean*. 32:553-565.

CHAPTER 5 – MODELING K_{SAT}

INTRODUCTION

This chapter describes the methods used to model K_{sat} for each representative soil layer of the six watersheds studies. This was done (i) by assembling all the required data inputs across each watershed; (ii) by comparing the actual with modeled stream discharge and snowpack accumulation; and (iii) by generating hydrothermal results from the PTFs integrated in ForHyM2.

OUTLINE OF METHODS

Data Collection

In order to run ForHyM2 for each watershed in the study, all of the input data required to run both the STELLA and Excel user interfaces was acquired. Local weather data (daily average temperature and precipitation, both rain and snow in cm) was obtained from Environment Canada's National Climate Data and Information Archive (Table 5). The resulting weather data was inspected to ensure day-to-day continuity, because ForHyM2 relies on a gap-free equidistant data set to ensure complete alignment between model output and recorded weather. Missing data was estimated by way of regression analysis and using data from nearby weather stations for missing data prediction.

Table 5. List of weather stations and hydrometric stations used to collect primary input data to run ForHyM for each watershed.

Watershed	Weather Station	Hydrometric Station	Model Run Years
Moosepit Brook, NS	Kejimkujik National Park (ID: 71599)	Moosepit Brook at Tupper Lake (ID: 01EE005)	1999-2004
Pockwock, NS	Pockwock Lake & Halifax Int'l Airport (ID: 71395)	Peggy Brook[1]	1999-2003
Hayward Brook, NB	Parkindale	Watershed 1[2]	1993-1997
Lac Laflamme, QC	Foret Montmorency	Lac Laflamme (ID: 02PD018)	1990-1996
Turkey Lakes, ON	Wawa Airport (ID:71738)	Turkey Lakes stream 31[3]	1996-2005
Rithet Creek, BC	Sooke Lake Dam[4]	Rithet Creek[4]	1994-2003

[1] From the Pockwock-Bowater Watershed Management Project
[2] From the Hayward Brook Watershed Study
[3] From Great Lakes Forestry Center, CFS
[4] From Capital Regional District

The stream discharge for both Moosepit Brook and Lac Laflamme were obtained from the Water Survey of Canada's Hydrometric Data Archive (Environment Canada 2012). Stream discharge for Peggy Brook basin was obtained from records of the Pockwock-Bowater Watershed Management Project (Chi 2008; personal communication). Stream discharge for the Hayward Brook watershed was acquired from records of the Hayward Brook Watershed Study (Pomeroy 2003; Chi 2008; Basin 1; personal communication). The stream discharge data for Turkey Lakes was obtained from the Great Lakes Forestry Center data records via personal communication with Fred Beall (Arp and Yin 1992, Basin 31; also see Arp and Yin 1992; Yin and Arp 1998; Jutras and Arp 2011). The stream discharge from Rithet Creek was acquired from the Capital Regional District (Zhu and Mazumder 2008; personal communication).

Catchment characteristics and soil properties by layer (horizon thickness, texture, OM, coarse fragments, and quartz fraction) were obtained from various sources, notably

the Canadian Soil Information Services (CANSIS) provincial soil reports and previous studies using ForHyM2 (CANSIS 2000; Arp and Yin 1992) (Appendix I). The soil at each location was represented by the forest floor (or LFH layer), the A and B layers, and the C layer. The substrate below the C layer was represented by 1 m intervals to a depth of 12 m, i.e., the depth to isothermal conditions year-round was filled in as best as possible for each of the sites using the CANSIS reports.

Data Quality Control

Matters regarding data quality control were examined by following these leads:

- Individual data entries may be incorrect due to human error, pertaining to typographical errors (mistype digits, misplaced decimals, misalignment of data records).
- Confusion pertaining to data units (i.e., stream discharge units often vary from one reported study to another, for example using L/hr instead of m^3/sec).
- Missing data, either blank, shown as not recorded, below detection, or consider trace, and sometimes labeled zero (i.e., temperature inputs need to be continuous with no missing data or ForHyM2 assumes missing data to be 0°).

Model Calibration

Calibration is the process of adjusting model parameters so that the output variables correspond with actual data for several years, notably stream discharge (peak

highs and lows, timing, and cumulative discharge) and snowpack accumulation. The best calibrations are then analyzed in terms of the goodness-of-fit between the actual and modelled values, at the daily, weekly, monthly, and annual summation levels. Failure to achieve reasonable correspondence leads to further examinations

Water balance at watershed scale	
PETadjustor	1
Snow density and snowmelt	
Air temperature adjustor	0.06
Density of fresh snow	0.15
Water flows	
Surface runoff adjustor	1
Infiltration in FF adjustor	1
Interflow in FF adjusor	2
Infiltration in A & B adjustor	0.5
Interflow in A & B adjustor	2
Infiltration in C1& C2 adjustor	0.5
Interflow (base flow) in C1& C2 adjustor	2
Stream to ground flow adjustor	1

Figure 21. Calibration panel for ForHyM in the Excel interface, used to calibrate catchment specific evopotranspiration, snow parameters and water flow.

The calibration tab in the Excel interface was used to adjust the water balance, snow density and snowmelt, as well as the water flow (Figure 21). Each of the adjustors is connected through dynamic links to the STELLA interface (Figure 22). The water balance calibration consists of a potential evapotranspiration multiplier (PET, mm/yr) adjustor (1 is default, meaning the built-in PET calculations are used as originally formulated). Water balance is also accounted for by calibrating the stream to ground flow adjustor, which controls the new deep water percolation function.

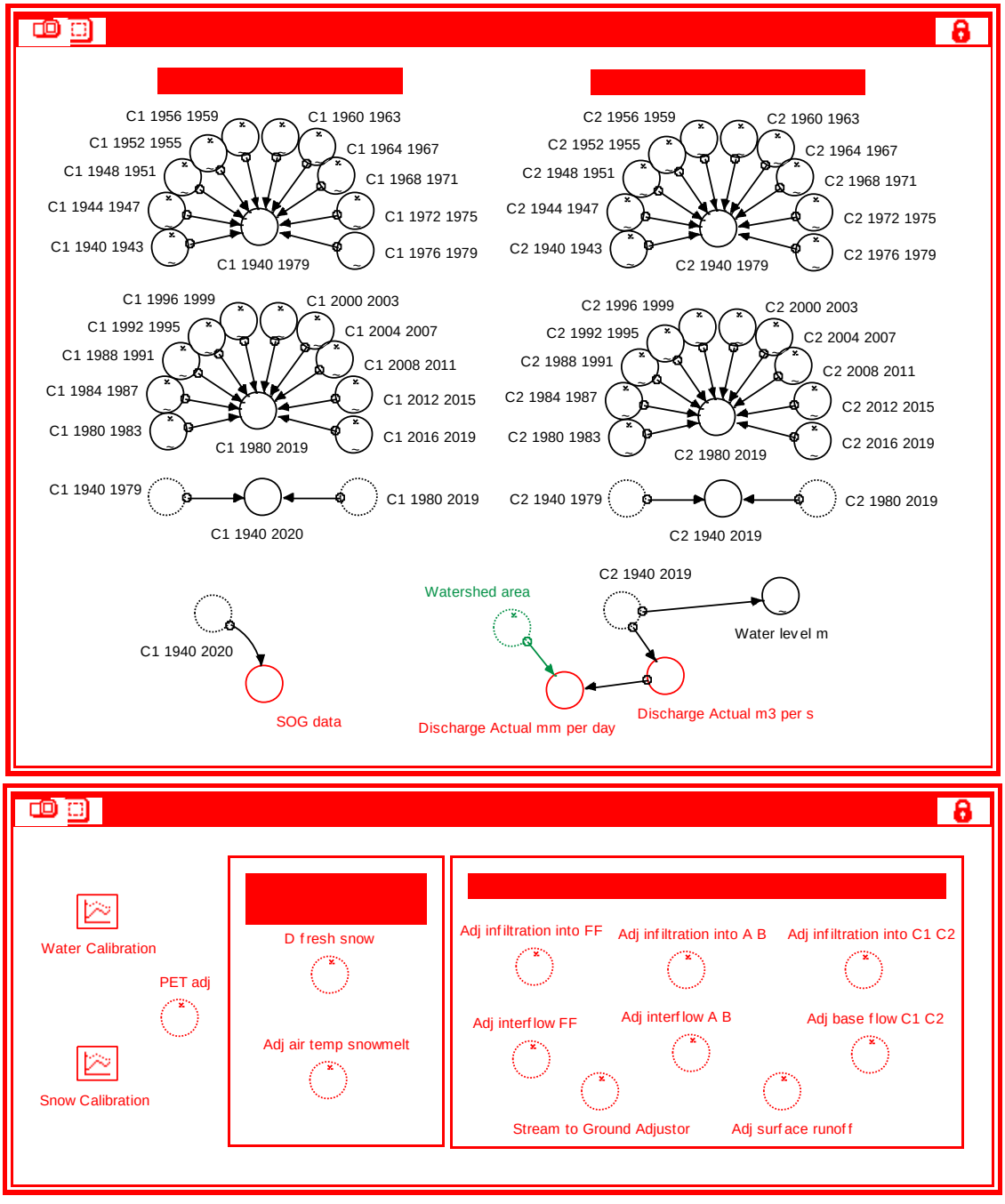


Figure 22. Calibration parameters and connections for ForHyM in STELLA

The snow density and snowmelt calibration parameters are an air temperature gradient multiplier and a density of fresh snow adjustor. Increasing this gradient makes the snowpack melts faster, whereas increasing the density of fresh snow makes the snowpack accumulations deeper and there more insulative. The water flows calibration consists of K_{sat} multipliers to estimate surface runoff, infiltration and percolation of the forest floor, soil (combined A and B horizons), and subsoil (combined C horizons). The A and B horizons is combined in the calibration process because of minimal variation between the two. With each horizon broken down into infiltration and percolation, the overall stream discharge can be meticulously calibrated to match up with actual stream discharge data. Appendix II has an overview of the methodology for proper stream discharge and snowpack calibration as a part of the ForHyM2 User's Manual.

The overall water balance was observed at both Moosepit Brook (1999-2005) and Hayward Brook (1992-1999) in order to see the difference that the deep water percolation function made on the model runs.

Calculating Results

With the water flows properly calibrated, ForHyM2 was run and the hydrothermal outputs were collected including: D_b and D_p (g cm^{-3}), FC (%), PWP (%) and K_{sat} (cm hr^{-1}) (Eq. 15-19; Balland et al. 2008), as well thermal conductivity (W m^{-1} $^{\circ}C^{-1}$) and volumetric heat capacity (cal cm^{-3} $^{\circ}C^{-1}$) (Eq. 20-21; Balland and Arp 2005). Also included in the output analysis was the general breakdown of OM (%), coarse fragments (%), and porosity, as well as sand and clay (%). Since the calibration process is applied

further down in the model after K_{sat} has been produced, in order to have correct K_{sat} outputs, they must be multiplied by the calibration adjustors. The final tabulated K_{sat} outputs were then compared to previously published results from similar sites in order to validate the model outputs.

A statistical analysis was conducted on the calibrated hydraulic parameters. StatView®, a computer statistics application, was used to perform a simple linear regression analysis for each of the sites at daily, weekly, monthly, and yearly time intervals. The different time intervals were used to check the overall correlation between actual and modelled discharge at intervals, which would be useful for time interval analysis and comparison. The statistical analysis consisted of the corresponding coefficient of determination (R^2), the best-fitted regression coefficient (β), root mean square error (RMSE), as well as the standard error (SE) and T- and P-values for each of the basins examined.

RESULTS

Table 6 provides an overview of the stream discharge and snowpack calibrations for each watershed location. The graphs in Figures 23-28 show how the calibrated results compare with the actual values at each location. In calibrating snowpack, the snow-to-air temperature adjustors ranged from 0.06-0.1 and the density of fresh snow ranged from 0.12-0.16 (Table 6). With Lac Laflamme, the temperature adjustor of 0.15 and a snowpack density adjustor of 0.35 were exceptionally high. Due to proximity, the Atlantic sites (Moosepit Brook, Peggy Brook, and Hayward Brook) shared very similar values for the snowpack adjustors. Peggy Brook had a larger temperature adjustor (0.1),

which means the snowpack is prone to earlier melting, likely due to low vegetation cover within the upper portions of the Peggy Brook watershed (Figure 24). In calibrating stream discharge, the lateral flow adjustors the FF, A&B, and C layers at Hayward Brook were particularly low, being 0.05, 0.02, and 0.05 respectively. At Lac Laflamme these adjustments were also low (Table 6). In addition, both watersheds needed a deep percolation adjustment of 0.68 and 0.1, respectively. This implies that 68% or 10% of the water that would reach the subsoil at Hayward Brook and Lac Laflamme would flow deeper into the ground, and would not come up again into the stream channel above the discharge gauges. Figures 29-31 show the comparison of the cumulative water balance for Moosepit Brook, Hayward Brook, and Lac Laflamme.

Tables 7 and 8 show the results of hydrothermal initialization, parameterization and calibration process across all six basins. For the forest floor, the K_{sat} estimates predicted using Eq. 19 and the corresponding ForHyM calibrated values are low, ranging from 0.30-0.60 cm hr^{-1}, but coincide with values related to organic soils (Verry et al. 2011). Within the A&B layers, the calibrated K_{sat} values range from about 3 to 83 cm hr^{-1}, being lowest for Hayward Brook. Within the C layers and subsoil, the estimated and calibrated K_{sat} values were generally much lower than for the A&B layers by one to two orders of magnitude, especially for watersheds with compacted tills, namely Turkey Lakes (~0.05 to 13.30 cm h^{-1}).

Table 6. Hydraulic conductivity and snowpack adjustments by site.

	Moosepit Brook (NS)	Peggy Brook (NS)	Hayward Brook (NB)	Turkey Lakes (ON)	Lac Laflamme (QC)	Rithet Creek (BC)
Snowpack adjustments						
Snow-to-air temperature gradient multiplier	0.06	0.1	0.08	0.08	0.15	0.1
Density of fresh snow	0.15	0.15	0.12	0.16	0.35	0.12
K_{sat} multipliers (factors)						
Surface runoff adjustor	1	1	1	1	1	1
Forest floor infiltration	1	1	2	1	1	1
Forest floor interflow	2	2	0.05	1	0.5	2
A&B horizon infiltration	0.5	1	2	1	1	1
A&B horizon interflow	2	1.75	0.02	0.14	0.05	0.14
C horizon infiltration	0.5	1	2	1	1	1
Baseflow	2	2	0.05	0.5	0.1	2
Baseflow not entering stream	0	0	0.1	0	0.68	0

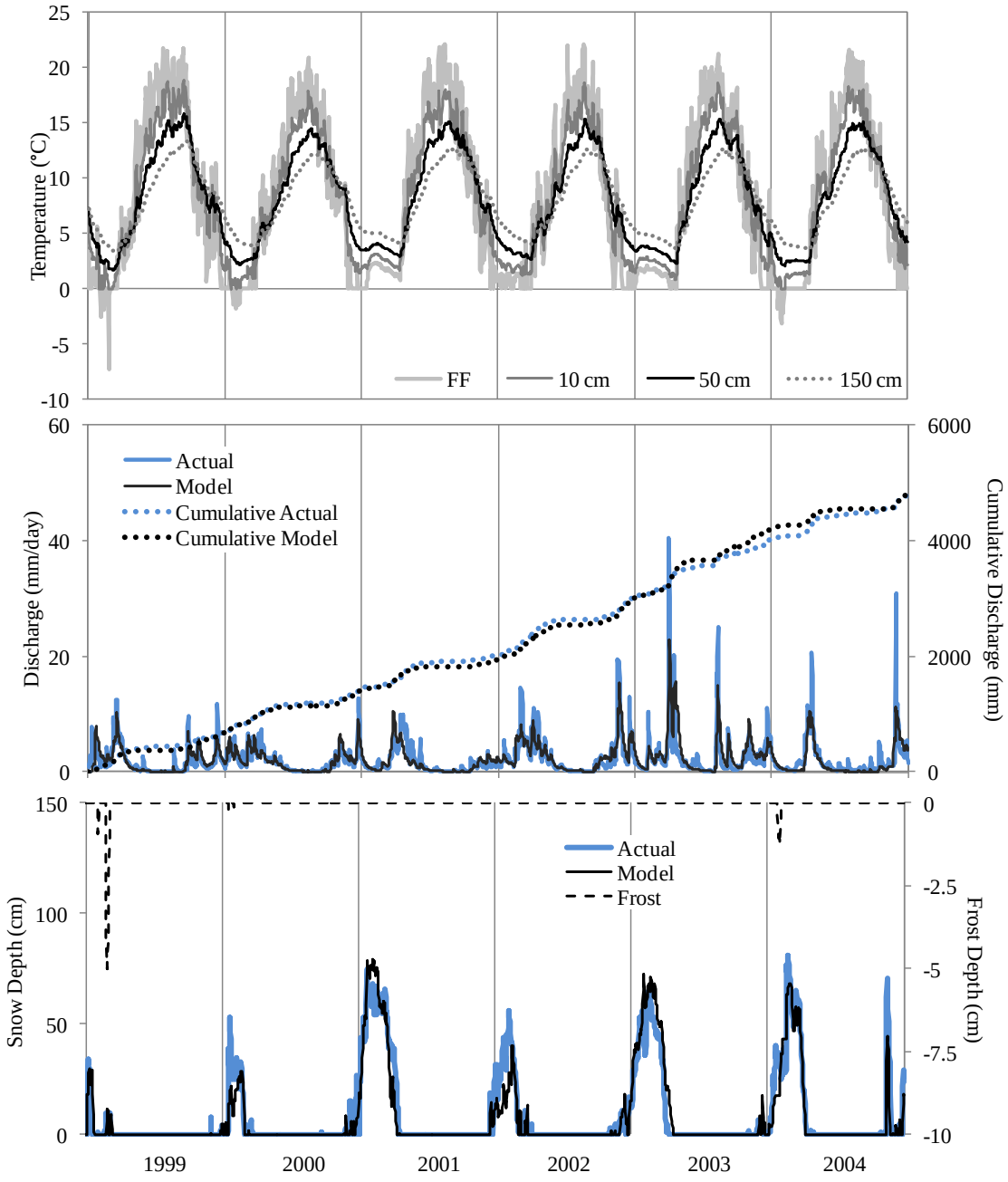


Figure 23. ForHyM2 generated output for snowpack, frost depth, soil temperature, and stream discharge for Moosepit Brook, NS from 1999-2004.

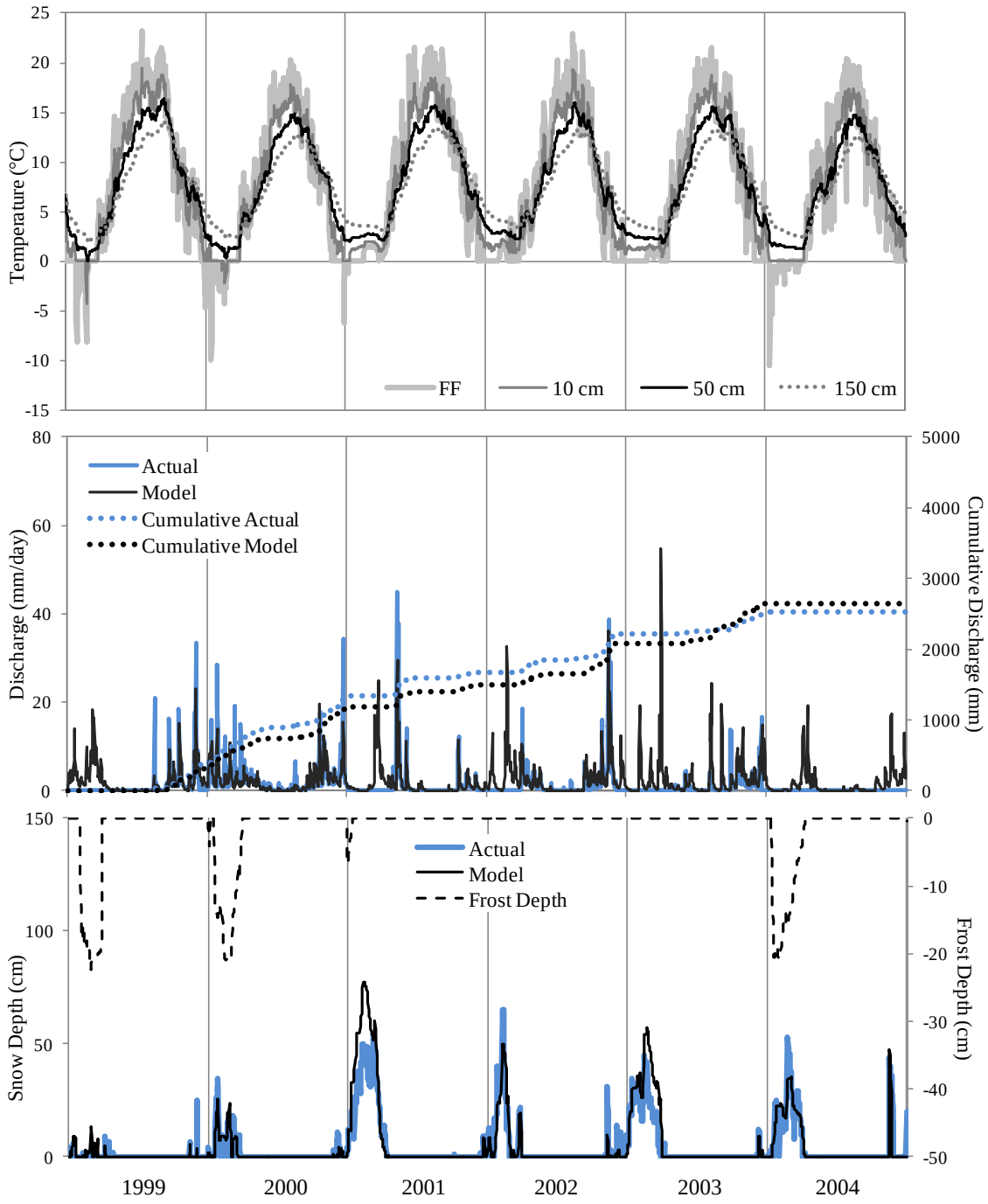


Figure 24. ForHyM2 generated output for snowpack, frost depth, soil temperature, and stream discharge for Peggy Brook, NS from 1999-2004.

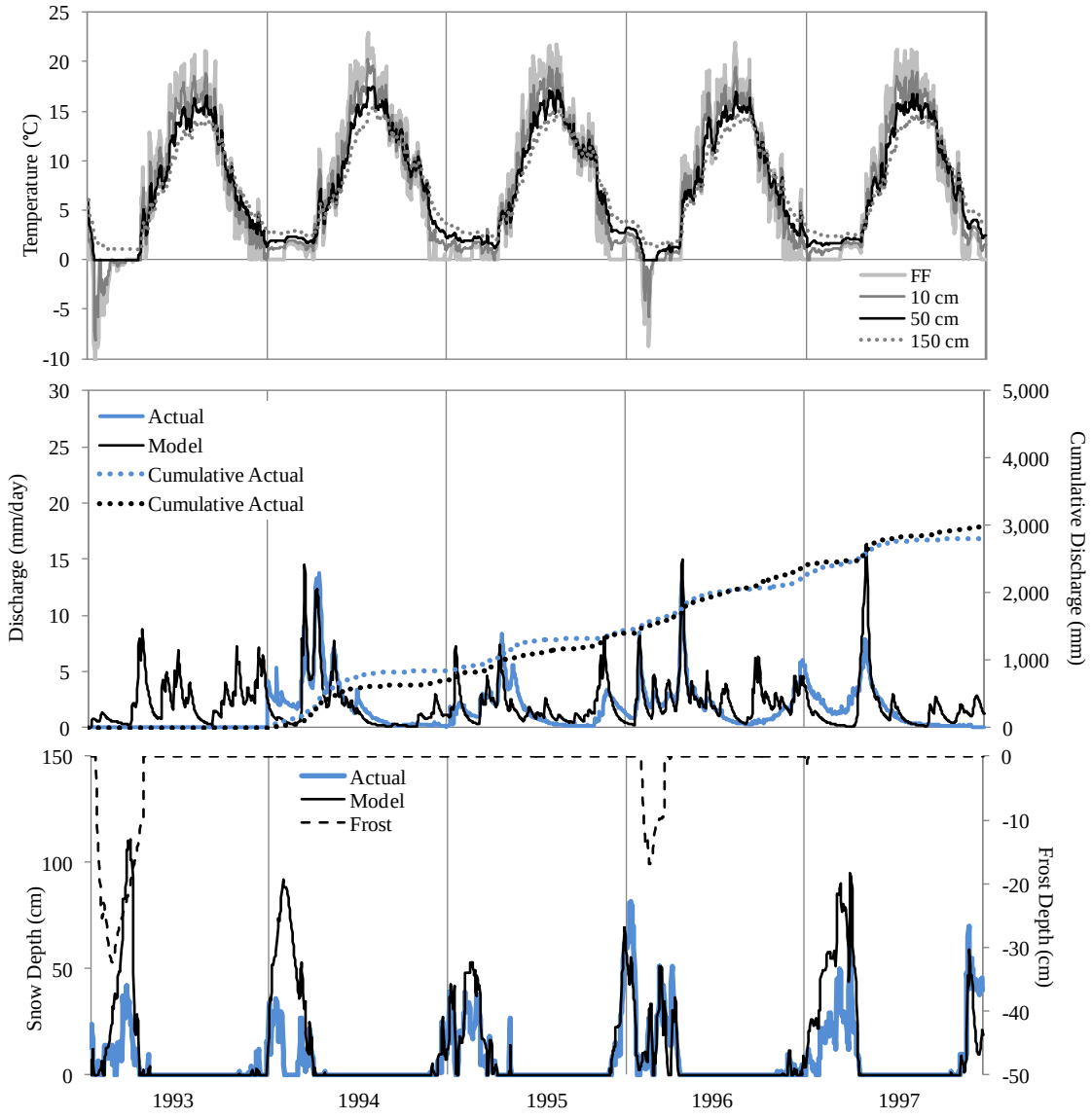


Figure 25. ForHyM2 generated output for snowpack, frost depth, soil temperature, and stream discharge for Hayward Brook, NB from 1993-1997.

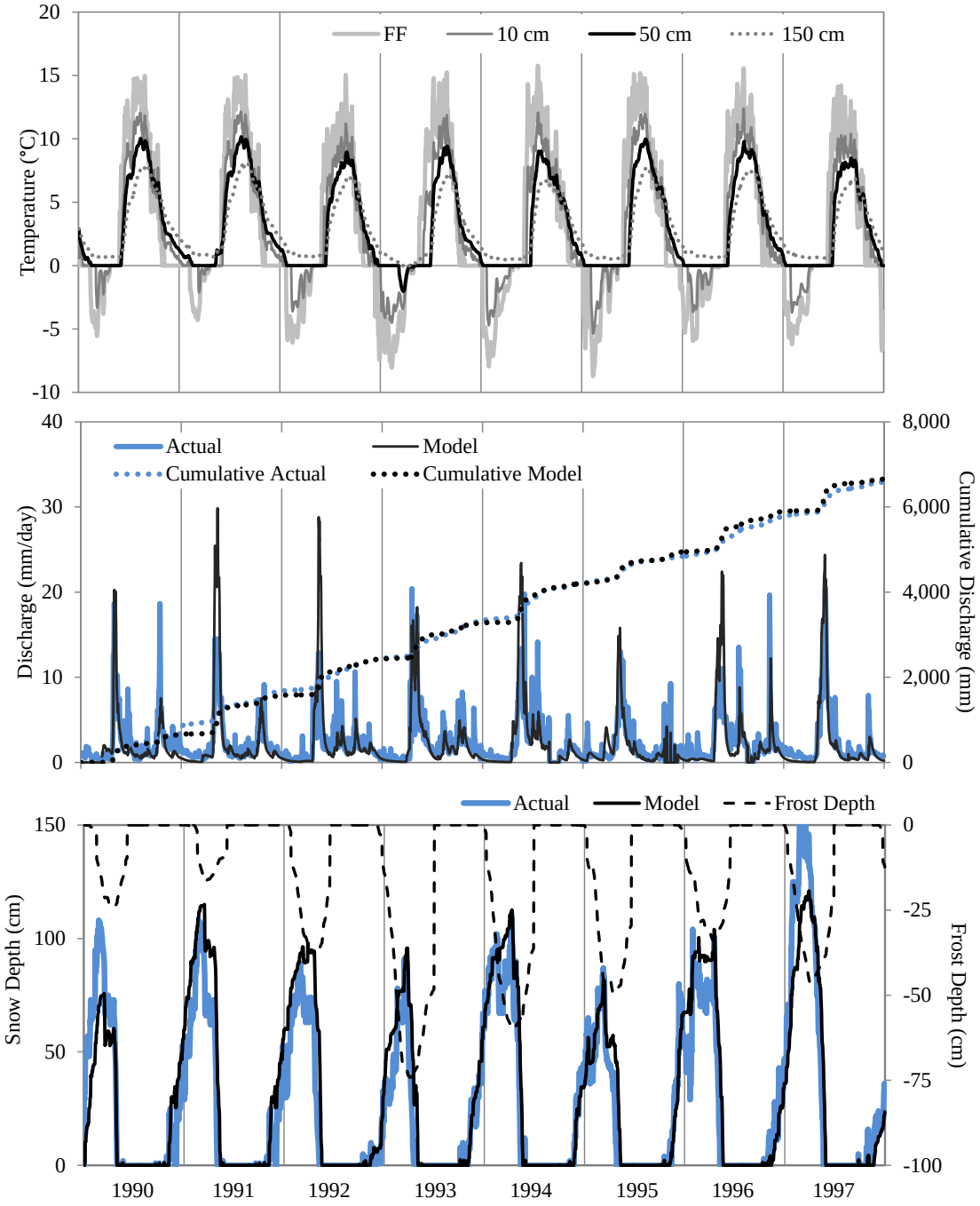


Figure 26. ForHyM2 generated output for snowpack, frost depth, soil temperature, and stream discharge for Lac Laflamme, QC from 1990-1997.

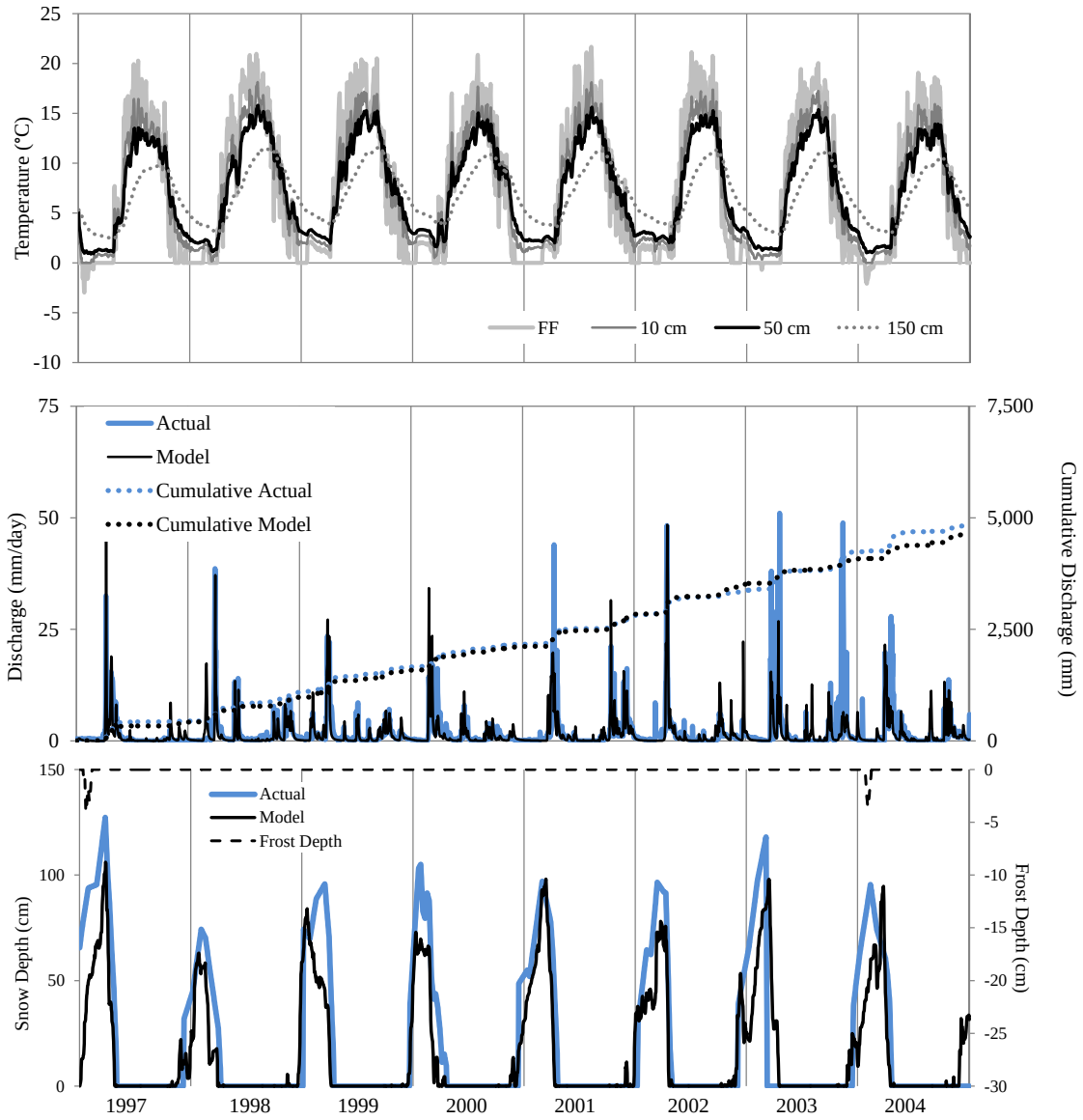


Figure 27. ForHyM2 generated output for snowpack, frost depth, soil temperature, and stream discharge for Turkey Lakes, ONT from 1997-2004.

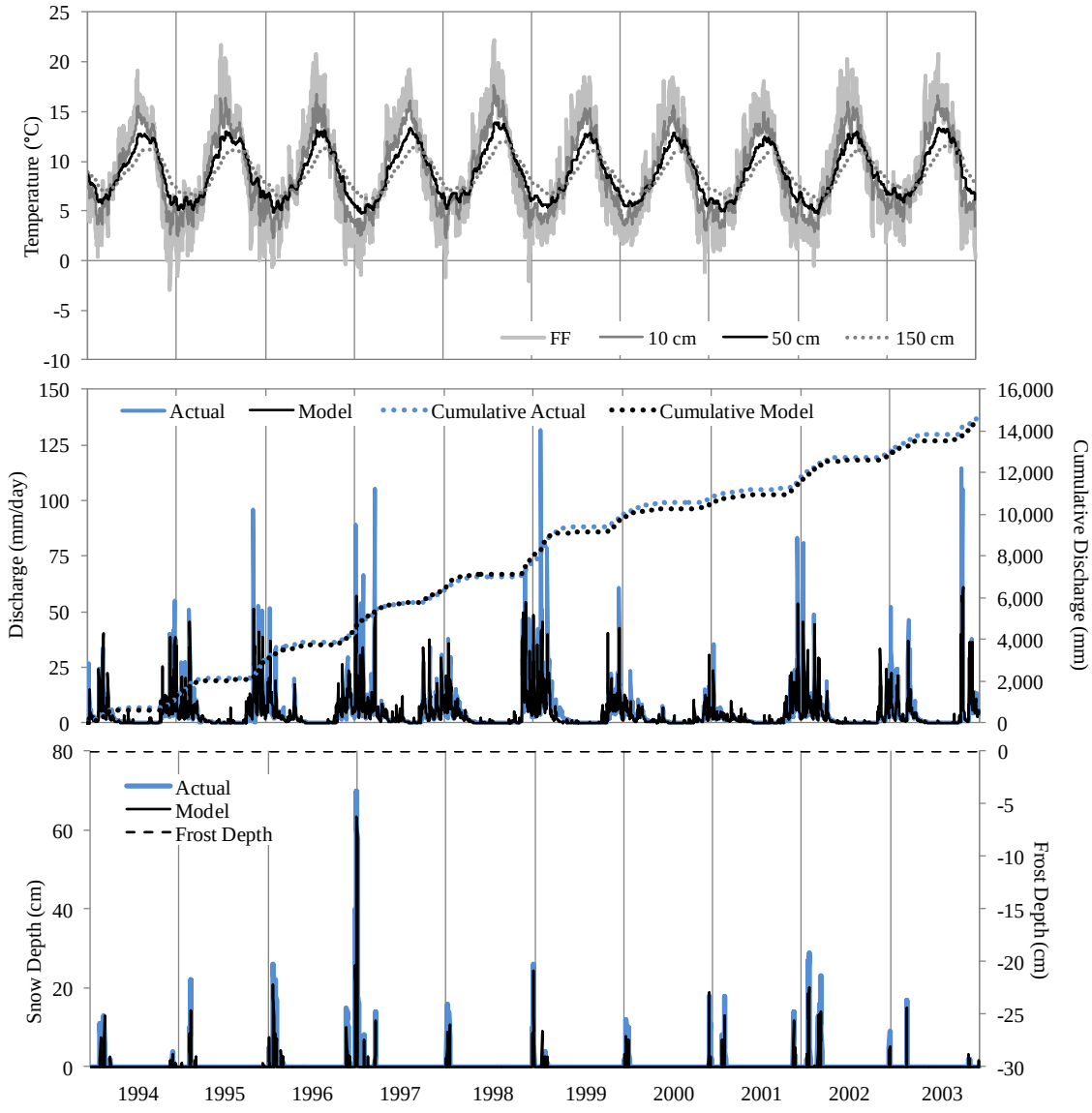


Figure 28. ForHyM2 generated output for snowpack, frost depth, soil temperature, and stream discharge for Rithet Creek, BC from 1994-2003.

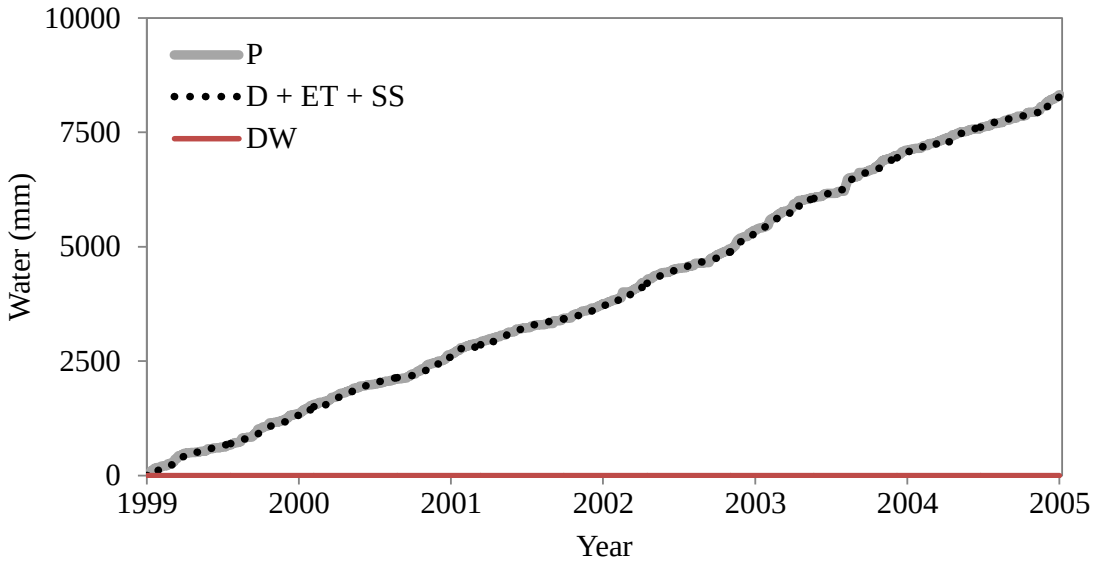


Figure 29. Overall cumulative water balance, including precipitation (P), discharge (D), evapotranspiration (ET), soil storage (SS), and deep water (DW) for Moosepit Brook, NS.

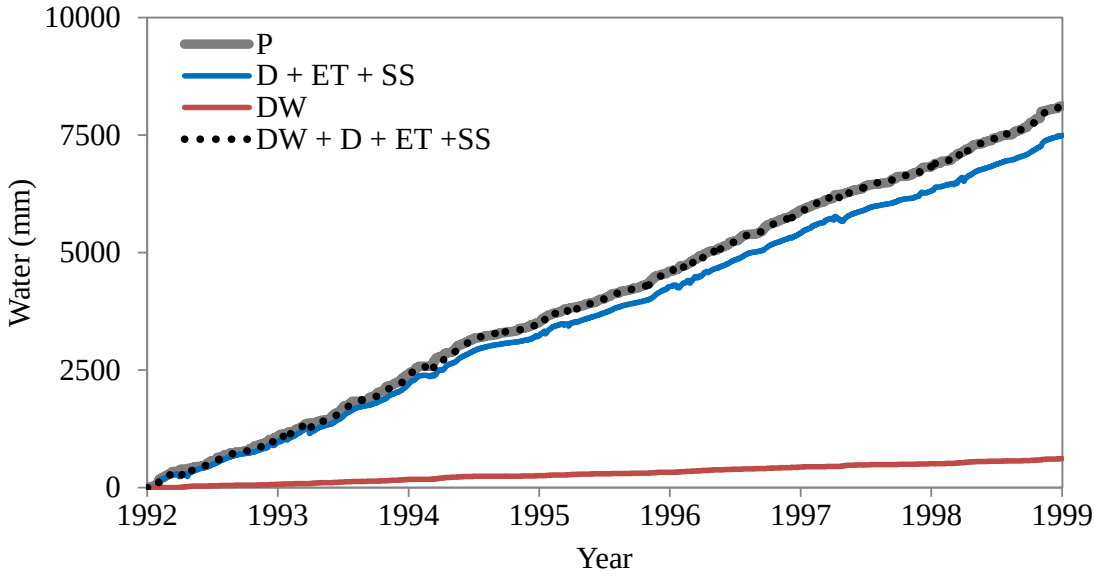


Figure 30. Overall cumulative water balance, including precipitation (P), discharge (D), evapotranspiration (ET), soil storage (SS), and deep water (DW) for Hayward Brook, NB.

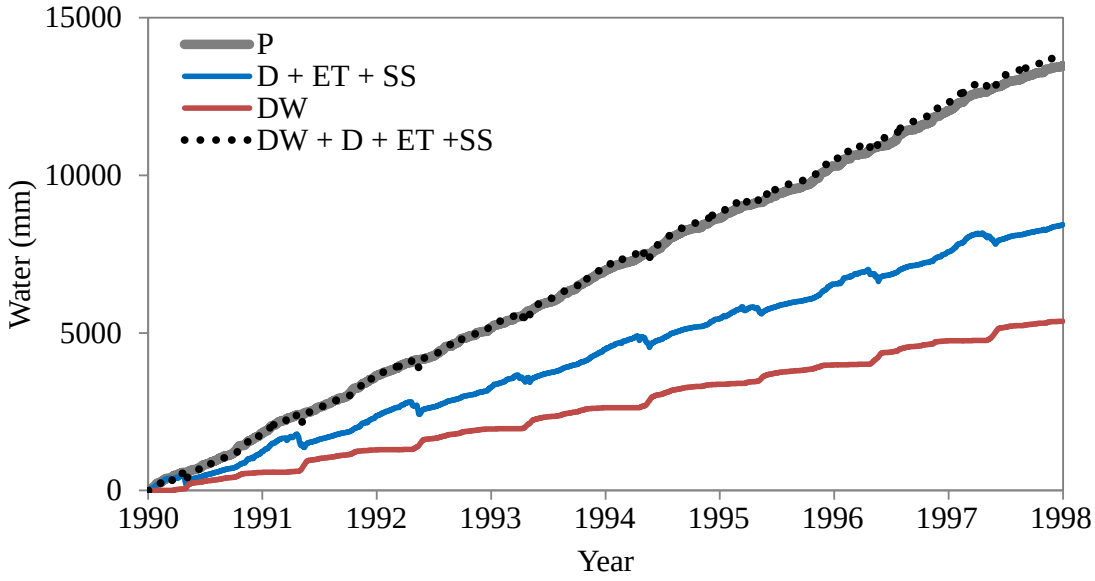


Figure 31. Overall cumulative water balance, including precipitation (P), discharge (D), evapotranspiration (ET), soil storage (SS), and deep water (DW) for Lac Laflamme, QC.

Table 9 displays of the cumulative discharge results for each basin, and breaks these down by basin-calibrated percentage of runoff, interflow, and baseflow. The corresponding goodness-of-fit is compiled in Table 10, and the related scatter plots of actual versus modeled values are shown in Figures 32 to 37. Note that there is generally good agreement between the actual and basin-calibrated stream discharge at the daily to annual time scales (Table 8). The R^2 ranged from 0.55-0.99 across all time intervals.

Table 7. Hydrothermal soil profile, needed for the daily soil moisture, temperature and stream discharge calculations.

Parameters	Moosepit Brook			Pockwock			Hayward Brook			Lac Laflamme			Turkey Lakes			Rithet Creek		
	FF	A& B	C	FF	A& B	C	FF	A& B	C	FF	A& B	C	FF	A& B	C	FF	A& B	C
D_b, g cm^{-3}	0.32	1.32	1.70	0.32	1.32	1.70	0.06	0.90	1.30	0.16	1.15	1.52	0.16	1.09	1.85	0.16	0.74	1.87
D_p, g cm^{-3}	1.33	2.48	2.60	1.33	2.48	2.60	1.33	2.48	2.58	1.33	2.58	2.48	1.33	2.48	2.58	1.33	2.27	2.55
FC, %	0.28	0.21	0.15	0.28	0.21	0.15	0.27	0.10	0.12	0.13	0.20	0.05	0.27	0.18	0.16	0.30	0.26	0.17
PWP, %	0.10	0.07	0.06	0.10	0.07	0.06	0.10	0.05	0.04	0.03	0.10	0.04	0.10	0.06	0.08	0.11	0.09	0.06
Thermal conductivity, W m^{-1} °C^{-1}	0.59	1.34	2.01	0.59	1.34	2.01	0.60	1.31	1.87	0.52	1.05	2.00	0.60	1.45	2.01	0.52	0.99	2.44
Heat Capacity, cal cm^{-3} °C^{-1}	0.42	0.46	0.57	0.42	0.46	0.57	0.35	0.36	0.48	0.46	0.35	0.43	0.49	0.47	0.56	0.41	0.44	0.54
Organic matter content, %	100	5	0.1	100	5	0.1	100	5	1	100	1	5	100	5	1	100	15	2
Coarse Fragments %	-	10	20	-	10	20	-	20	25	-	4	14	-	10	10	-	10	20
Sand, %	-	40	45	-	40	45	-	90	60	-	82	80	-	30	60	-	60	60
Clay, %	-	20	15	-	20	15	-	10	20	-	6	10	-	20	10	-	20	20
K_{sat}, cm hr^{-1} (Eq. 8)	0.30	41.50	6.65	0.30	41.50	6.65	0.30	150.00	21.70	0.30	45.05	20.53	0.30	39.80	0.10	0.30	45.67	0.58
K_{sat}, cm hr^{-1} (Eq. 8 x Table 5 multiplier)	0.60	83.00	13.30	0.60	72.63	13.30	0.60	3.00	1.09	0.15	2.25	2.05	0.30	5.57	0.05	0.60	6.39	1.16
K_{sat}, cm hr^{-1} (References)	-	0.01-54[d]	0.05-4.66[d]	-	0.01-54[d]	0.05-4.66[d]	-	-	-	-	2.88-26.76[a]	14.4[a]	-	3.36[b]	0.036[b]	-	3.64[c]	-
Porosity	0.76	0.47	0.35	0.76	0.47	0.35	0.95	0.64	0.50	0.88	0.56	0.39	0.88	0.56	0.28	0.88	0.67	0.27
Porosity (References)	-	-	-	-	-	-	-	-	-	-	0.65[a]	0.40[a]	-	0.6[b]	0.44[b]	-	-	-

[a] Barry et al. (1988), Barry et al. (1990) and Prévost et al. (1990); [b] Murray and Buttle (2005); [c] Bryant (2007); [d] Murray (1991)

Table 8. Max, min, and mean values for hydrothermal parameters across all six basins.

Parameters	FF			A&B			C		
	Max	Min	Mean	Max	Min	Mean	Max	Min	Mean
D_b, g cm^{-3}	0.32	0.06	0.20	1.32	0.74	1.09	1.87	1.30	1.66
D_p, g cm^{-3}	1.33	1.33	1.33	2.48	2.27	2.46	2.60	2.48	2.57
FC, %	0.30	0.13	0.26	0.26	0.10	0.19	0.17	0.05	0.13
PWP, %	0.11	0.03	0.09	0.10	0.05	0.07	0.08	0.04	0.06
Thermal conductivity, W m^{-1} °C^{-1}	0.60	0.52	0.57	1.45	0.99	1.25	2.44	1.87	2.06
Heat Capacity, cal cm^{-3} °C^{-1}	0.49	0.35	0.43	0.47	0.35	0.42	0.57	0.43	0.53

Table 9. Stream discharge broken down by runoff, interflow, and baseflow for all six basins.

Site	Runoff (mm)	%	Interflow FF (mm)	%	Interflow A&B (mm)	%	Baseflow (mm)	%	Total Discharge (mm)	Years Run
Moosepit Brook	2.7	0.1	202.3	4.8	682.8	16.1	3341.2	79.0	4229.0	1999-2004
Pockwock	0.0	0.0	623.1	14.5	2085.7	48.6	1578.5	36.8	4287.2	1999-2004
Hayward Brook	0.0	0.0	11.2	0.2	27.7	0.6	4697.4	99.2	4736.2	1993-1998
Lac Laflamme	136.4	2.7	415.8	8.2	34.6	0.7	4491.3	88.4	5078.1	1990-1997
Turkey Lakes	10.4	0.2	406.5	8.2	3561.9	72.1	952.7	19.3	4941.4	1997-2004
Rithet Creek	175.1	1.3	2484.0	19.1	6075.5	46.6	4304.3	33.0	13038.9	1994-2003

Table 10. Comparing ForHyM-modeled with measured daily, weekly, monthly and annual cumulative discharge: actual mean discharge (Q, mm/time interval), coefficient of determination (R^2), linear regression coefficient (β; intercept = 0), root mean square error (RMSE, %), Standard Error (SE), T-Value, and P-Value

	Location	Q	R^2	β	RMSE	St. Error	T-Value	P-Value
Yearly	MB	819.55	0.98	1.04	0.16	0.072	14.41	0.001
	PB	495.52	0.95	1.00	0.30	0.121	8.29	0.0012
	HB	697.94	0.99	1.14	0.06	0.030	37.68	<0.001
	LL	826.36	0.99	1.01	0.14	0.052	19.53	<0.001
	TL	637.84	0.97	0.96	0.20	0.066	14.59	<0.001
	RC	1429.68	0.99	1.01	0.10	0.032	31.83	<0.001
Monthly	MB	68.30	0.90	1.03	0.45	0.044	23.38	<0.001
	PB	56.31	0.87	0.96	0.53	0.056	17.21	<0.001
	HB	62.04	0.78	0.87	0.62	0.070	12.36	<0.001
	LL	68.43	0.82	1.25	0.79	0.067	18.68	<0.001
	TL	53.15	0.85	0.82	0.61	0.035	23.05	<0.001
	RC	119.14	0.95	0.99	0.35	0.021	48.31	<0.001
Weekly	MB	15.76	0.84	0.98	0.65	0.027	36.79	<0.001
	PB	15.20	0.79	0.88	0.77	0.035	24.84	<0.001
	HB	14.47	0.66	0.85	0.85	0.044	19.39	<0.001
	LL	15.83	0.75	1.20	1.01	0.034	35.07	<0.001
	TL	12.27	0.67	0.77	1.10	0.026	29.07	<0.001
	RC	27.22	0.89	1.00	0.62	0.015	65.71	<0.001
Daily	MB	2.25	0.74	0.87	0.87	0.012	71.27	<0.001
	PB	1.36	0.62	0.72	1.58	0.013	54.08	<0.001
	HB	2.07	0.63	0.85	0.92	0.018	48.12	<0.001
	LL	2.27	0.65	1.09	1.20	0.016	68.21	<0.001
	TL	1.75	0.60	0.66	1.49	0.020	32.91	<0.001
	RC	3.92	0.59	0.89	1.00	0.012	72.07	<0.001

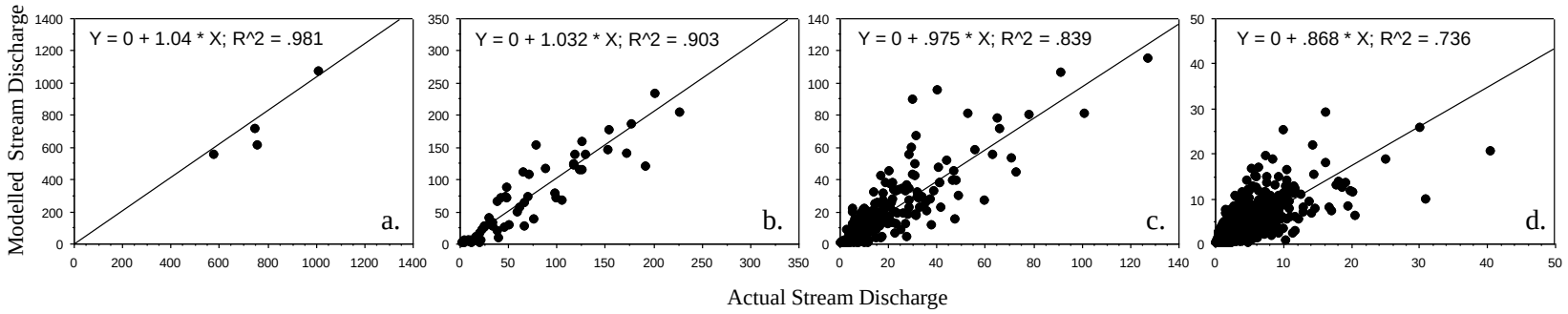


Figure 32. Actual and modelled correlation regression plots with R^2 values for (a) yearly (mm/year), (b) monthly (mm/month), (c) weekly (mm/week), and (d) daily (mm/day) cumulative stream discharge for Moosepit Brook, NS.

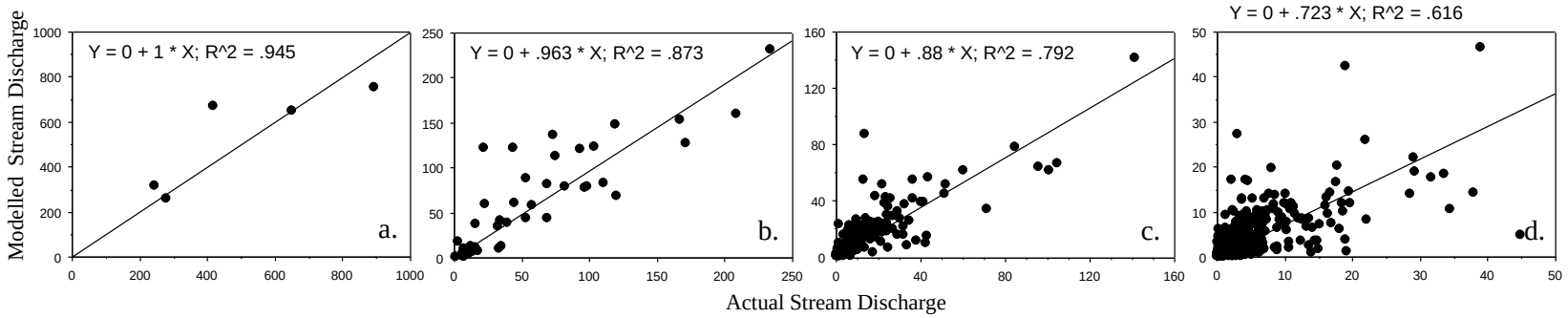


Figure 33. Actual and modelled correlation regression plots with R^2 values for (a) yearly (mm/year), (b) monthly (mm/month), (c) weekly (mm/week), and (d) daily (mm/day) cumulative stream discharge for Peggy Brook, NS.

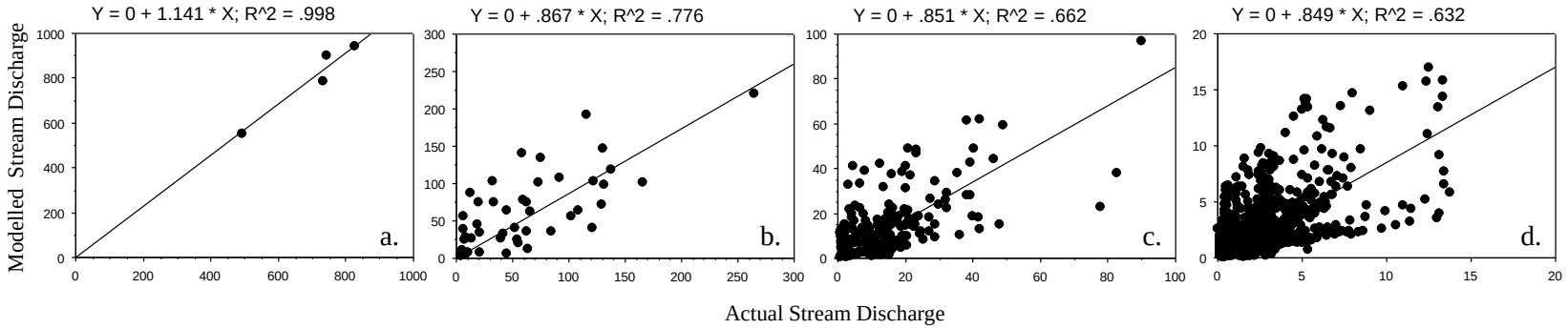


Figure 34. Actual and modelled correlation regression plots with R^2 values for (a) yearly (mm/year), (b) monthly (mm/month), (c) weekly (mm/week), and (d) daily (mm/day) cumulative stream discharge for Hayward Brook, NB.

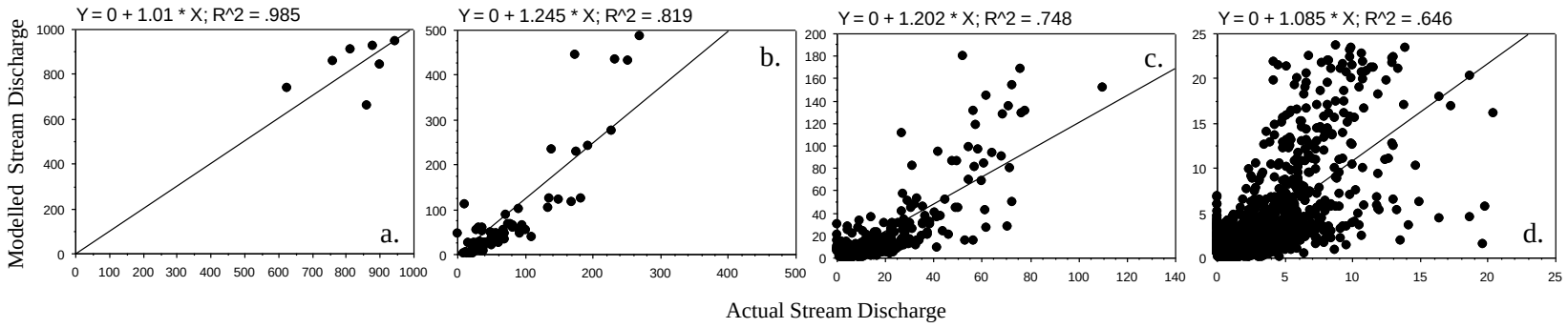


Figure 35. Actual and modelled correlation regression plots with R^2 values for (a) yearly (mm/year), (b) monthly (mm/month), (c) weekly (mm/week), and (d) daily (mm/day) cumulative stream discharge for Lac Laflamme, QC.

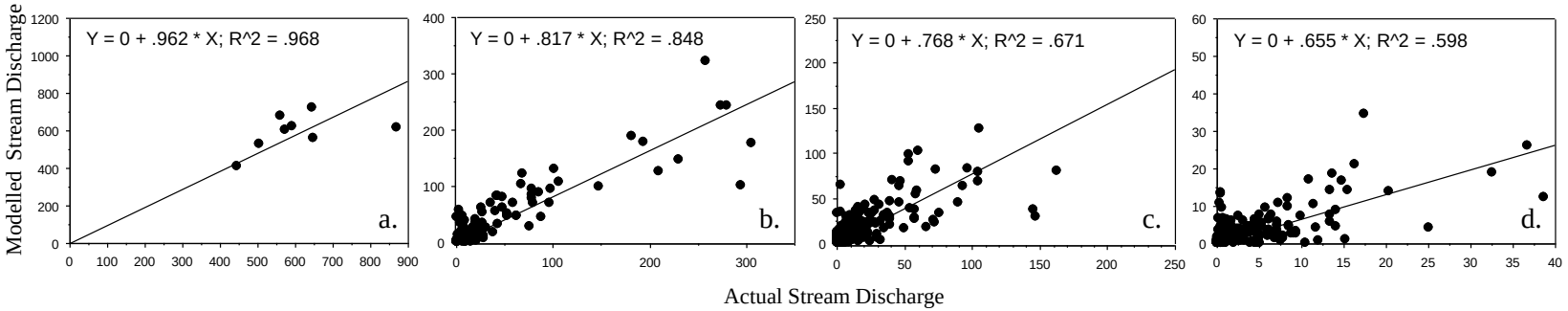


Figure 36. Actual and modelled correlation regression plots with R^2 values for (a) yearly (mm/year), (b) monthly (mm/month), (c) weekly (mm/week), and (d) daily (mm/day) cumulative stream discharge for Turkey Lakes, ON.

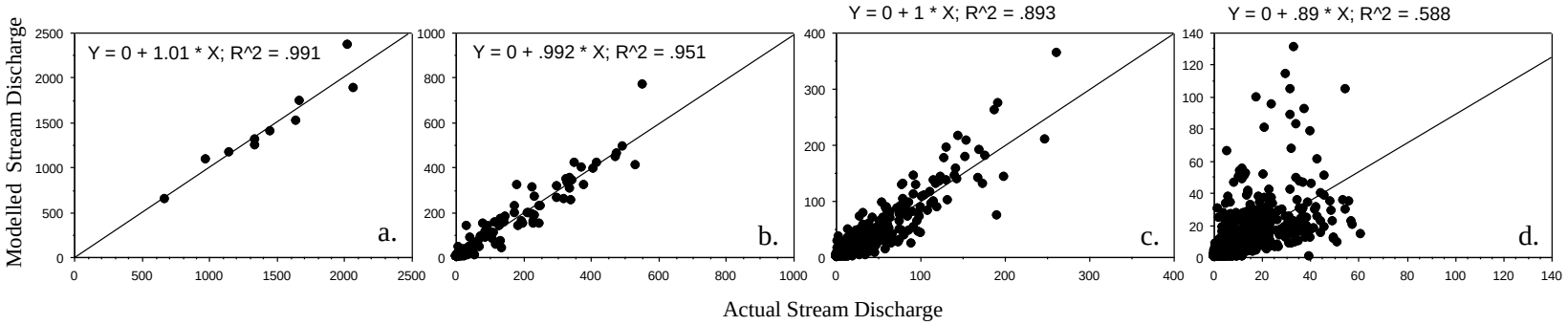


Figure 37. Actual and modelled correlation regression plots with R^2 values for (a) yearly (mm/year), (b) monthly (mm/month), (c) weekly (mm/week), and (d) daily (mm/day) cumulative stream discharge for Rithet Creek, BC.

DISCUSSION

For the snowpack calibrations at Lac Laflamme, it is hypothesized that the snow is heavier because of the softwood rich tree species composition. Snow drip from melting snow on branches causes the snow to compact and turns into ice. Having a temperature adjustor of 0.15 (as appose to 0.06-0.1 at the other watersheds) means that denser snow will melt earlier due to increased air temperature. Both parameters work together because denser snow has a higher thermal conductivity due to larger ice crystals compacted together with smaller air pockets (Fukusako 1990). Rithet Creek, like Lac Laflamme, is also rich in softwood species, but has a much higher average annual forest floor temperature due to being on the Pacific coast (~8.5° vs. ~3.3° in Lac Laflamme). As such, there are very little, if any, snowpack effects on stream discharge, and the snowpack calibration parameters are therefore negligible.

The K_{sat} value for the forest floor is rather low, but corresponds to K_{sat} values normally associated with organic soils. Due to the high porosity of this layer, infiltration occurs quickly. The water so received is, however, released rather slowly to the underlying forest soil and only so once the field capacity of the forest floor is exceeded. As a result, soil layers underneath the forest floor often remain quite dry during the later portion of the summer and during early fall. At this time, soils may also become hydrophobic. As a result, surface water would then flow laterally over short distances towards nearby pits and depressions, where the soil would be moister and permit gradual infiltration and downward percolation.

The K_{sat} adjustments for downward flow varied from 0.5 to 2 (Table 6), and were therefore within the generically determined precision for K_{sat} based on Eq. 19 and the layer specification for soil texture, organic matter, soil depth and soil density. The K_{sat} adjustments for lateral flow were more variable, thereby indicating that lateral flows through the basins were more complex and generally low thereby requiring downward K_{sat} adjustments for interflow, especially for the hummocky basins (Table 6). This was likely due to flow obstructions, such as mounds and pits, empty or partially filled water pools above and below the regolith, erratic changes in soil depth, density, texture, organic matter, coarse fragment, and variations in the surface exposure of partially fractured bedrock especially along ridges, steep slopes and within crevices. For Hayward Brook, the mineral soil K_{sat} was low because (i) the high flow variability of the calcareous subsoil (Schulze-Makuch et al. 1999), and (ii) the topography, which is flat to rolling, encourages water to pool and infiltrate downwards, taking advantage of the high-flow subsoil. In addition, basins underlain by calcareous formations tend to be "leaky" so that the monitored stream discharge does not account for the expected discharge because some of the baseflow enters deep aquifers, and therefore exits the basin below the channel-based stream monitoring station. The deep waterflow percolation adjustor that was added to the hydrology module is used for such instances.

Unlike Hayward brook in which the flow is driven by the baseflow and calcareous bedrock, Lac Laflamme is rich in sandy till and coarse fragments, with a till that can reach up to 5m deep in areas. This deep sandy till deposit would force water to infiltrate deeper, faster as opposed to moving laterally. Even with a large average slope of ~11%,

the tendency for water to flow easily down through the sandy soil forces the water's directional path. The large slope probably explains the lack of restrictions on the forest floor interflow (FF adjustor = 1). Due to the forest floor being at the surface, it is more susceptible to lateral flow due to slope than the deep sandy A&B horizons.

It is estimated that the undulating to hummocky terrain, paired with the ~7% slope at Peggy Brook helps to direct the flow water laterally instead of pooling and infiltrating downwards. Both Moosepit Brook and Peggy Brook have large coarse fragments all throughout the subsoil which could help inhibit the movement of water downwards, acting as a barrier with the deeper loamy soil.

The calibrated K_{sat} values for lateral and downward flow generally fall within the K_{sat} uncertainty range associated with Eq. 19, with the best-fitted RSME values for K_{sat} varying from about ±0.4 to ±0.6 (Balland et al. 2006). This range is similar to that obtained with (i) testing water recharge in wells receiving water from small depressions (about 50 m^2) to catchments up to about 1200 ha or more, and after taking care of the scaling-up effect that is associated with these measurements ($log10K_{sat}$ RMSE = ±0.61; Schulze-Makuch et al. 1999), and (ii) using tension infiltrometer and Guelph permeameter to determine K_{sat} by soil depth at Turkey Lakes ($log10K_{sat}$, RMSE = ± 0.45; Murray and Buttle 2006) and at Lac Laflamme.

For most soils, D_b generally increases with soil depth (Eq. 16). The general decrease in sand content and OM with increasing depth enables the increase in D_b.

Equation 19 shows that K_{sat} decreases logarithmically with decreasing pore space, or increasing bulk density (Balland et al. 2008).

Two different relationships arose between snowpack and frost. As would be expected, frost depth at the Atlantic sites increased in years with little snow cover to insulate the ground (Hardy et al. 2001). In Lac Laflamme and Turkey Lakes, however, the frost reached great depths even in years with large snowpack. This may be due to the texture and hydrology of the soil (low lateral flow allowing water to crystallize), as well as the overall temperature (mean annual temperature in Lac Laflamme is 0.5°C, whereas it is 7.0°C in Moosepit Brook).

The graphs in Figures 28-33 show the variability in correlation between model and actual data. For the most part, the results showed good correlation, with the exception of outliers caused by abnormal peaks in discharge. Theses peaks are usually caused by either (i) a lag in the data from weather stations to stream gauge, or (ii) abnormal seasonal differences (i.e., atypical weather). In some cases, the model calibration doesn't account for abnormal peaks in discharge. Overall, the correlation between modelled and actual stream discharge across all six sites was good, but could be improved by calibrating over more years to try and account for abnormal discharge peaks.

Moosepit Brook and Rithet Creek showed the highest overall discharge correlation across all of the time scales. Hayward Brook had the lowest discharge correlation, presumably due to the difficulty in calibrating caused by its heterogeneous

mixture in bedrock formations. The R^2 of stream discharge correlation by year was much better than the other time intervals. This could be due to the limited amount of year runs, which could be skewing the results. In some instances, the R^2 by year was based on results from less than 6 samples (MB, PB, and HB). In order to account for variation due to seasonal differences, future statistical analysis should be based on more year runs.

Since the study locations represent a range of catchment size from about 70 to 1700 ha, there are no obvious trends in K_{sat} calibrations with catchment size. Hence, the model-derived K_{sat} adjustments for the LFH, A&B and C layers are essentially independent of scale across this range. This is also in general agreement with Schulze-Makuch et al. (1999) who found that the up-scaling requirement for K_{sat} generally stops once the K_{sat} determining flow fields offer no additional heterogeneity. However, Laudon et al. (2007) concluded that stream discharge is less dependent on scale than on wetland coverage per catchment, with discharge contributions of "event" water (or new water) amounting to 50% in wetland-dominated catchment, while limited to 10% to 30% in forest dominated catchments. Considering also (i) that forest catchments are generally permeated by many converging flow channels with varying and weather-dependent thresholds for flow initiation; (ii) that forest catchments in glaciated landscapes, such as the ones of this study are generally underlain by a layer of surface-fractured bedrock; and (iii) that this layer provides additional space for water pooling and hydraulically activated flows towards the streams; it is reasonable to suggest that the K_{sat} estimates and their multipliers in Tables 6 reflect similar flow heterogeneities within each of the many subcatchments for the catchments of this study.

In general, there is a close correspondence between the basin-calibrated and reported K_{sat} values in the literature. For example, Bryant (2007) measured K_{sat} to be 3.64 cm h^{-1} for colluvium, 0.0044 cm h^{-1} for clayey sands, and 5.11 cm h^{-1} for well sorted sands in the Sooke Lake reservoir near Rithet Creek. The ForHyM2-calibrated value for Rithet Creek is 6.39 cm h^{-1}.

Murray and Buttle (2005) looked at the difference in infiltration and soil water content on forested and harvested slopes in Turkey Lakes. They tested 4 sites within Turkey Lakes using a Guelph permeameter. They found that in the upper ablation till K_{sat} averaged 3.6 cm h^{-1}, whereas in the deeper dense basal till K_{sat} slowed down with depth to roughly 0.036 cm h^{-1}. The ForHyM2- calibrated K_{sat} values amounted to 5.57 cm h^{-1} and 0.05 cm h^{-1} for the ablation and basal till layers, respectively.

Barry et al. (1990) modelled snowmelt runoff in Lac Laflamme. Using the hydrological model HYFOR, they calculated an average K_{sat} for a depth of 0-60cm to be 26.76 cm h^{-1} and for 14.4 cm h^{-1} for subsoils. A similar study by Prévost et al. (1990) used the VSAS2 (a variable source area model) and produced K_{sat} values of 57.7 cm h^{-1} near the surface A horizon to 21.9 cm h^{-1}, for the deeper B horizon. Another study by Barry et al. (1988) measured *in situ* K_{sat} with two methods (i) fiberglass resistance blocks, to measure water potential twice daily, and (ii) time domain reflectometry (TDR), to measure soil moisture content weekly. The resulting estimates for K_{sat} using the resistance blocks varied from 2 to 18 cm h^{-1} for a depth of 10-110cm. The TDR method produced K_{sat} levels from ~4 to 10 cm h^{-1} between 20-80 cm deep, and >75 cm h-1 in

soils deeper than 90cm. In this case, the authors located a fine-textured, low density, loamy sand horizon which would, presumably: (i) reduce lateral stream flow through the A&B layers due to high water retention capacity, but (ii) encourage deep percolation and deep subsoil flow in the sandier subsoil. The ForHyM2-calibrated K_{sat} values fall within the range of these studies reporting a K_{sat} average of 18 cm h^{-1} for the A&B layers and 7.18 cm h^{-1} for the C layers and subsoil.

A study by Murray (1991) developed a method for estimating K_{sat} for select soils in Nova Scotia using 142 different horizons in various soils. For glacial tills, average K_{sat} values for compacted to well sorted and ploughed A&B horizons ranged from 0.01 to 54 cm h^{-1}. For the subsoils, the K_{sat} ranged from 0.05 to 4.66 cm h^{-1}. The parameters that were used in ForHyM2 correspond with the upper end of Murray's (1991) K_{sat} class distribution. His S11, class which is described as having large drainage tiles, with granular, friable texture, has a range of > 40 cm/h^{-1}. The ForKyM2-calibrated K_{sat} values for the Moosepit Brook and Pockwock A&B layers amounted 83 and 72 cm/h^{-1}, respectively. These numbers are at the upper range of the Marray (1991) study, but do reflect the generally more permeable conditions of forest soils in comparison with the soils of fields used for cropping and grazing.

CONCLUSIONS

Optimally, in order to perfectly replicate any natural functions, all parameters would have to be known. Given that gathering all known parameters would be costly, let alone determining the variability of each parameter at any given time (i.e. seasonal

variations) and at different locations, there is always a level of uncertainty associated with hydrological modeling. Nevertheless, in the context of each watershed study and in comparison with results from similar studies, ForHyM2 produced reasonable results with and without basin-specific calibrations regarding the extent of water retention and flow rates for run-off, infiltration, interflow, percolation, baseflow stream discharge and K_{sat}. Special calibration adjustments were needed on sites with high slope, landform and substrate heterogeneity.

LITERATURE CITED

Arp, P.A., Yin, X. 1992. Predicting water fluxes through forests from monthly precipitation and mean monthly air temperature records. *Canadian Journal of Forest Research*. 22:864-877.

Balland, V., Arp, P.A. 2005. Modeling soil thermal conductivities over a wide range of conditions. *Journal of Environmental Engineering Science.* 4:549-558.

Balland, V., Pollacco, J.A.P., Arp, P.A. 2008. Modeling soil hydraulic properties for a wide range of soil conditions. *Ecological Modeling*. 219:300-316.

Barry, R., Plamondon, A.P., Stein, J. 1988. Hydrologic soil properties and application of a soil moisture model in a balsam fir forest. *Canadian Journal of Forest Research*. 18:427-234.

Barry, R., Prevost, M., Stein, J., Plamondon, A.P. 1990. Simulation of snowmelt runoff pathways on the Lac Laflamme watershed. *Journal of Hydrology*. 113:103-121.

Bryant, D. 2007. "Geomorphic and hydrologic effects on nutrient distribution in riparian areas surrounding the Sooke Lake Reservoir." MSc Thesis, Department of Biology, University of Victoria, Victoria, BC.

Burch, G.J., Moore, I.D., Burns, J. 2006. Soil hydrophic effects on infiltration and catchment runoff. *Hydrological Processes*. 3(3):211-222.

CANSIS. 2000. "Canadian Soil Information System." (http://sis.agr.gc.ca/cansis/).

Chi, X. 2008. Hydrogeological assessment of stream water in forested watershed: temperature, dissolved oxygen, pH, and electrical conductivity. Unpublished. MSc. Thesis., University of New Brunswick, Fredericton, NB.

Environment Canada. 2012. Water Survey of Canada. *Hydrometric Data.* From http://www.wsc.ec.gc.ca/applications/H2O/index-eng.cfm

Ferreira, A.J.D., Coelho, C.O.A., Walsh, R.P.D., Shakesby, R.A., Cabellos, A., Doerr, S.H. 2000. Hydrological implications of soil water-repellency in Eucalyptus globulus forests, north-central Portugal. *Journal of Hydrology*. 231:165-177.

Fukusako, S. 1990. Thermophysical properties of ice, snow, and sea ice. *International Journal of Thermophysics.* 112:353-373.

Hardy, J., Groffman, P., Fitzhugh, R., Henry, K., Welman, A., Demers, J., Fahey, T., Driscoll, C., Tierney, G., Nolan, D. 2001. Snow depth manipulation and its influence on soil frost and water dynamics in a northern hardwood forest. *Biogeochemistry*. 56:151-174.

Jutras, M.-F., Arp, P.A. 2011. "Determination of hydraulic conductivity from soil characteristics and its application for modeling stream discharge in forest catchments." Pp. 189-202 in *Hydraulic Conductivity - Issues, Determination and Applications*, edited by Lakshmanan Elango (Ed.). InTech.

Laudon, H., Demidov, V.N., Seibert, J., Morth, M. 2007. The role of catchment scale and landscape characteristics for runoff generation of boreal streams. *Journal of Hydrology*. 198-209:198.

Murray, C.D., Buttle, J.M. 2005. Infiltration and soil water mixing on forested and harvested slopes during spring snowmelt, Turkey Lakes Watershed, central Ontario. *Journal of Hydrology*. 306:1-20.

Murray, G. 1991. The Development of an estimation method for the saturated hydraulic conductivity of selected Nova Scotia Soils. MSc. Thesis. McGill University, Montreal.

Pomeroy, J.H. 2003. Stream turbidity signatures within the Hayward Brook watershed study. Unpublished. MSc. Thesis, University of New Brunswick, Fredericton, NB.

Prévost, M., Barry, R., Stein, J., Plamondon, A.P. 1990. Snowmelt runoff modeling in a balsam fir forest with a variable source area simulator (VSAS2). *Water Resource Research*. 26(5):1067-1077.

Schulze-Makuch D. Carlson D., Cherkauer D., Malik P. 1999. Scale dependency of hydraulic conductivity in heterogenous media. Ground Water. 37:904-919.

Verry, E.S., Boelter, D.H., Paivanen, J., Nichols, D.S., Malterer, T., Gafni, A. 2011. "Physical Properties of Organic Soils." in *Peatland Biogeochemistry and Watershed Hydrology at the Marcell Experimental Forest*, edited by Randall Kolka, Stephen Sebestyen, Elon S. Verry, and Kenneth N. Brooks. Pp. 135-176

Wang, T., Zlotnik, V.A., Wedin, D., Wally, K. D. 2008. Spatial trends in saturated hydraulic conductivity of vegetation dunes in the Nebraska Sand Hills: Effects of depth and topography. *Journal of Hydrology*. 349:88-97.

Zhu, J. Z., Mazumder, A. 2008. Estimating nitrogen exports in response to forest vegetation, age and soil types in two coastal-forested watershed in British Columbia. *Forest Ecology and Management*. 255:1945-1959.

CHAPTER 6 – SENSITIVITY ANALYSIS

INTRODUCTION

Soil hydraulic conductivities at saturation (K_{sat}) are highly variable in space and time. For example, K_{sat} varies spatially along and perpendicular to dominant flow paths depending on directional changes in soil texture and structure. Temporal changes would mostly be related to changes in soil bulk density either (i) in response to gradual soil formation processes, or (ii) quick to periodic compaction or de-compaction impacts of land-use operations from horticulture, agriculture, and forestry to industrial and residential developments. Changes in weather and climate also affect K_{sat} through freezing and thawing, swelling and shrinking, and the extent of rooting (or the lack thereof) and the related soil-structure forming effects of soil organic matter build-up or loss.

This chapter explores how changes in hydraulic conductivity may affect modelled rates of water flow through forested watersheds, with flows referring to infiltration, percolation, run-off, interflow, baseflow, and stream flow. This is done by way of sensitivity analyses to ascertain changes in flow rates on account of changing K_{sat} values. All of this is done for two well-studied watershed studies, referring to Moosepit Brook, Nova Scotia and Turkey Lakes, Ontario. The equation used for estimating K_{sat} on account of changes in soil texture, structure, density, and organic matter content is given by (Balland et al. 2006).

$$\log_{10} K_{sat} = -0.98 + 7.94 \log_{10}\left(\mathrm{D_p} - \mathrm{D_b}\right) + 1.96\ \mathrm{SAND} \tag{19}$$

This chapter documents how changes in texture and organic matter affect $\log_{10}K_{sat}$ for the forest floor above the rooted and non-rooted soil layers of mineral soils at the two study locations, and addresses the effects of the state of soil organic matter decomposition on D_b, D_p and $\log_{10}K_{sat}$ in organic soils as well. This Chapter also addresses the extent that scenario-based changes in K_{sat} affect stream flow and the rate of evapotranspiration from organic soils from fully forested to boggy. Conversely, evapotranspiration dependent on the extent of leaf canopies and soil permeability plays a role on soil water retention and water transmittance towards the streams (Dube et al. 1995).

METHODS

The analysis is centered on two of the watershed studies, namely Moosepit Brook, east of Kejimkujik National Park, Nova Scotia and Turkey Lakes, in Ontario, near Sault St. Marie north of Lake Superior. These two sites were chosen to represent the variation in range of slope, vegetation and soil. Eight scenarios were run for one year (2003 for Moosepit Brook and 2000 for Turkey Lakes), including a status quo scenario, which utilized the watershed's original texture and organic matter parameters for a base comparison. The eight scenarios represented the actual soil conditions in terms of soil texture and organic matter (Scenario 1), varying the soil texture sand, silt, or clay (Scenarios 2, 3, and 4), and varying the soil organic matter content (Scenarios, 5, 6, 7, and 8), as follows:

A) Normal Scenario

1. Status Quo

Table 11. Status quo scenario soil input parameters for Moosepit Brook and Turkey Lakes.

Horizons	**Moosepit Brook, NS**					**Turkey Lakes, ONT**				
	Depth (cm)	Sand (%)	Silt (%)	Clay (%)	OM (%)	Depth (cm)	Sand (%)	Silt (%)	Clay (%)	OM (%)
A	21	66	24	10	4.5	15	66	24	10	5
B	21	66	24	10	9	30	66	24	10	3
C	50+	82	12	6	4.5	50+	22	65	13	2

B) Changing soil texture

2. Sand = 95% sand, 1% silt, 4% clay
3. Silt = 7% sand, 87% silt, 6% clay
4. Clay = 25% sand, 25% silt, 50% clay

C) Changing organic matter content

5. Double status quo OM
6. Half status quo OM
7. No OM throughout entire mineral soil profile
8. 100% OM throughout entire mineral soil profile

The sand texture percentages for scenarios 2-4 were chosen to demonstrate the effects of varying texture on K_{sat} from sandy and sandy loam soils to silty and clayey soils (Figure 38). The organic matter levels for scenarios 5-8 were chosen to demonstrate the effects of changing the organic matter on content from very small in mineral soils to fully organic soils. For the organic soil condition, three sub-scenarios were chosen to account for variations in forest cover from 100 % (fully forested), 50% (varying from forested to boggy) and 0% (open moss and shrub-covered bogs with no trees). This is to demonstrate changing K_{sat} levels from high to low increases the amount of water available for evapotranspiration according to the climate and weather affected conditions at Moosepit Brook and Turkey Lakes.

Finally, ForHyM2 was run with the new soil parameters and the outputs generated for these scenarios (K_{sat}, D_b, and D_p) were broken into topsoil (average value from the A and B horizons) and subsoil (average value from the upper C+ horizons). The stream discharge by horizon from each scenario was also analyzed for trends.

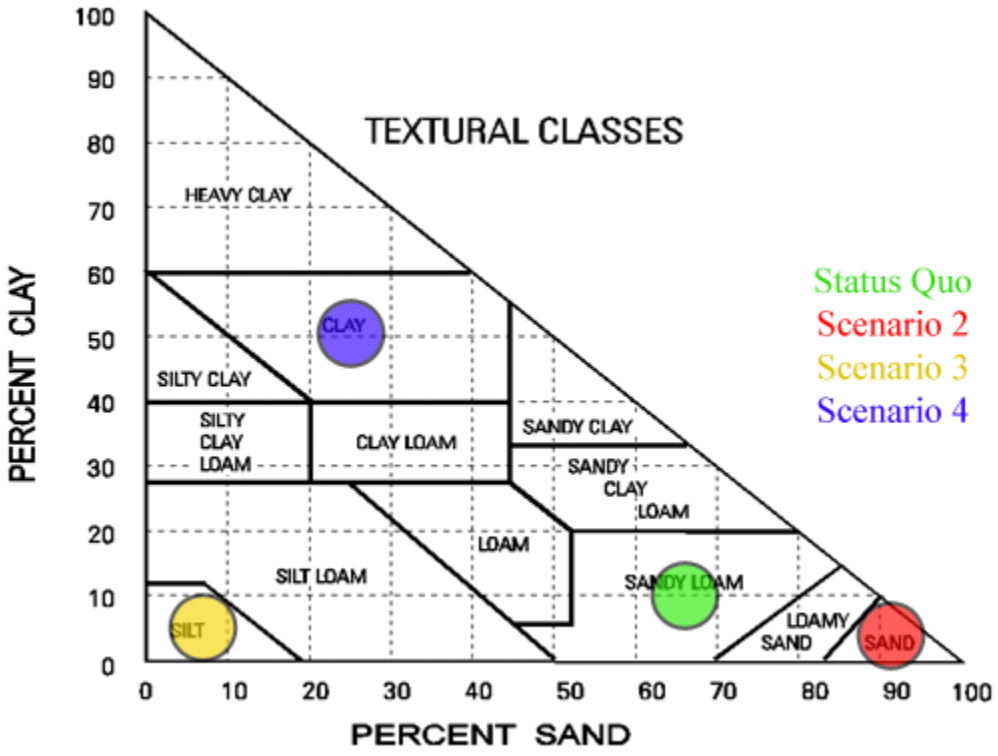


Figure 38. Mineral texture class triangle for fine soil (CANSIS 2000), with textures from scenarios 1-4 highlighted.

RESULTS

The results of this analysis are shown in Table 12 and in Figures 39 to 41 for Moosepit Brook and Figures 42-44 for Turkey Lakes. As shown, increasing the sand content (Scenario 2) leads to deeper water infiltration into the soil, which in turn increases the baseflow contribution towards the stream. With low sand content (Scenario

3), water accumulates in the A&B horizons with very little water infiltrating deeper. The extent of water infiltration in Scenario 4 is midway between Scenarios 2 and 3. The results obtained by varying OM to lower and higher values were complex. For example, Scenario 7 (OM = 0) would increase D_b, thus lowering K_{sat} and thereby increasing the lateral flow components through the soil. In contrast, Scenario 5 with its increased OM content would enhance the baseflow. However, increasing the OM content towards 100% would reverse this trend, because the difference between D_p and D_b is generally smaller for fully humified organic soils than for mineral soils. Note that soil compaction would also render the K_{sat} determining D_p - D_b difference quite small.

Table 13 shows the total discharge broken down by runoff, interflow in the forest floor, interflow in the mineral soil (A&B), and baseflow for both watersheds over all 8 scenarios. It also shows the Scenario-based shifts in percent discharge. For example, Scenario 3 and 8 had the highest shift in discharge from baseflow to interflow for the Moosepit Brook watershed. For Turkey Lakes, Scenario 2 produced the largest change from the Scenario 1 results. Figure 45 illustrates the relationship between increasing K_{sat} in the A&B horizon and the proportional distribution of the stream flow contributions in terms of surface run-off, forest flow and A&B layer interflow, and baseflow including subsoil flow. At Moosepit Brook, the relatively flat terrain (1% slope on average and uncompacted subsoil) favours baseflow over interflow from low K_{sat} values upwards. In contrast, the hummocky terrain at Turkey Lakes (8% slope on average, with compacted subsoil) favours interflow over baseflow except where the ground would be very sandy.

Table 12. Sensitivity results for various levels of sand and OM against K_{sat}, D_b and D_p for Moosepit Brook and Turkey Lakes.

Scenarios	**Moosepit Brook, NS**						**Turkey Lakes, ON**					
	K_{sat}, cm h^{-1}		D_b, g cm^{-1}		D_p, g cm^{-1}		K_{sat}, cm h^{-1}		D_b, g cm^{-1}		D_p, g cm^{-1}	
	Topsoil	Subsoil	Topsoil	Subsoil	Topsoil	Subsoil	Topsoil	Subsoil	Topsoil	Subsoil	Topsoil	Subsoil
1: Status quo	48.40	5.95	0.95	1.61	2.48	2.59	39.80	0.10	1.09	1.85	2.55	2.61
2: Sand	162.90	29.15	0.93	1.50	2.48	2.59	136.25	14.70	1.06	1.54	2.55	2.61
3: Silt	3.05	0.15	1.00	1.86	2.48	2.59	2.50	0.05	1.15	1.92	2.55	2.61
4: Clay	7.15	0.50	0.99	1.80	2.48	2.59	5.80	0.10	1.15	1.84	2.55	2.61
5: Double OM	60.60	13.30	0.72	1.48	2.33	2.54	56.05	0.30	0.90	1.68	2.45	2.57
6: Half OM	31.35	2.70	1.14	1.70	2.56	2.62	30.55	0.05	1.19	1.85	2.59	2.61
7: No OM	12.60	0.75	1.41	1.83	2.65	2.65	14.50	0.00	1.39	2.06	2.65	2.65
8: 100% OM	0.39	0.39	0.16	0.16	1.34	1.34	0.39	0.39	0.16	0.16	1.34	1.34

Table 13. Lateral flows and stream discharge for Scenarios 1-8 for Moosepit Brook and Turkey Lakes.

Site	Scenario	Runoff (mm)	%[2]	Interflow FF (mm)	%[2]	Interflow A&B (mm)	%[2]	Baseflow (mm)	%[2]	Total Discharge (mm)	Years Run
Moosepit Brook	1	2.7	0.1	202.3	4.8	682.8	16.1	3341.2	79.0	4229.0	1999-2004
	2	2.6	0.1	202.4	4.7	512.0	11.9	3580.4	83.3	4297.0	
	3	7.0	0.2	209.5	5.1	2653.0	64.4	1251.5	30.4	4121.0	
	4	2.7	0.1	202.4	4.8	1609.7	38.3	2391.4	56.9	4206.0	
	5	2.6	0.1	202.3	4.8	450.0	10.6	3578.0	84.5	4233.0	
	6	2.7	0.1	202.4	4.8	964.0	22.8	3054.8	72.3	4224.0	
	7	2.7	0.1	202.3	4.8	1675.8	39.8	2329.9	55.3	4210.7	
	8	250.6	7.7	472.8	14.5	918.0	28.2	1619.0	49.6	3261.0	
	8[1]	503.0	11.7	738.1	17.2	1340.6	31.2	1720.5	40.0	4302.2	
	8[2]	925.6	16.4	1108.7	19.6	1853.1	32.8	1763.5	31.2	5650.9	
Turkey Lakes	1	1.1	0.0	375.9	9.1	2990.0	72.2	772.9	18.7	4139.0	1997-2004
	2	3.3	0.1	376.1	8.8	301.0	7.1	3588.5	84.1	4269.0	
	3	114.9	2.8	521.2	12.8	2635.0	64.8	796.5	19.6	4068.0	
	4	19.4	0.5	389.1	9.4	1965.0	47.3	1782.1	42.9	4156.0	
	5	2.2	0.1	376.1	9.1	2314.0	55.8	1454.4	35.1	4146.0	
	6	0.5	0.0	375.8	9.1	3273.0	79.2	485.6	11.7	4135.0	
	7	0.0	0.0	374.8	9.1	3457.0	83.9	290.7	7.1	4122.0	
	8	21.3	0.6	412.2	11.6	42.4	1.2	3088.1	86.6	3564.0	
	8[1]	21.6	0.6	419.9	10.7	48.3	1.2	3428.4	87.5	3918.0	
	8[2]	20.8	0.5	427.2	10.0	54.7	1.3	3779.1	88.3	4282.0	

[1] 50% vegetation [2] 10% vegetation

[2] % values refer to the calculated percent contributions of run-off, FF interflow A&B interflow and baseflow to stream discharge.

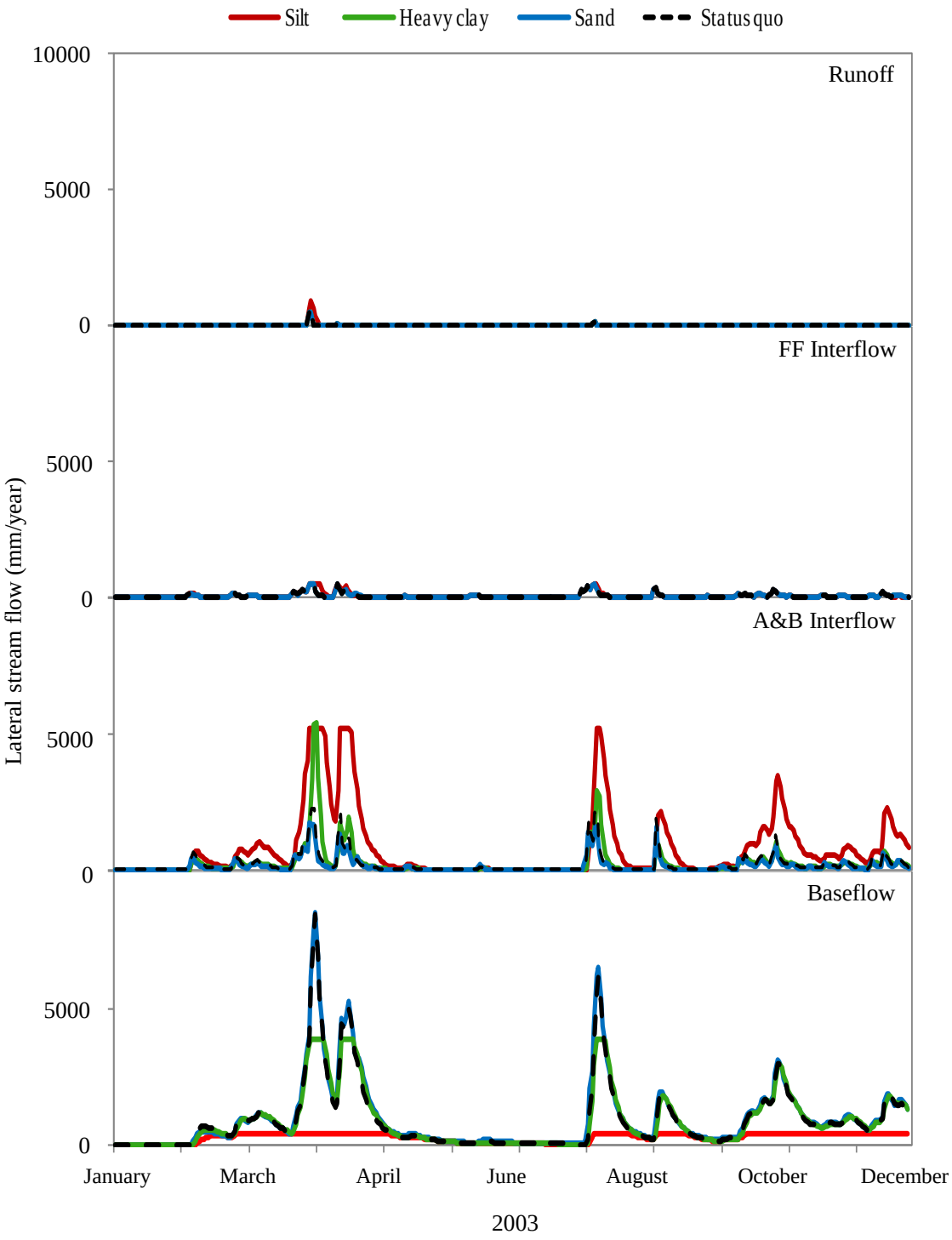


Figure 39. Lateral stream flow broken down by horizon for texture sensitivity scenarios (Sand, Silt, Heavy clay) versus status quo, for Moosepit Brook, NS in 2003.

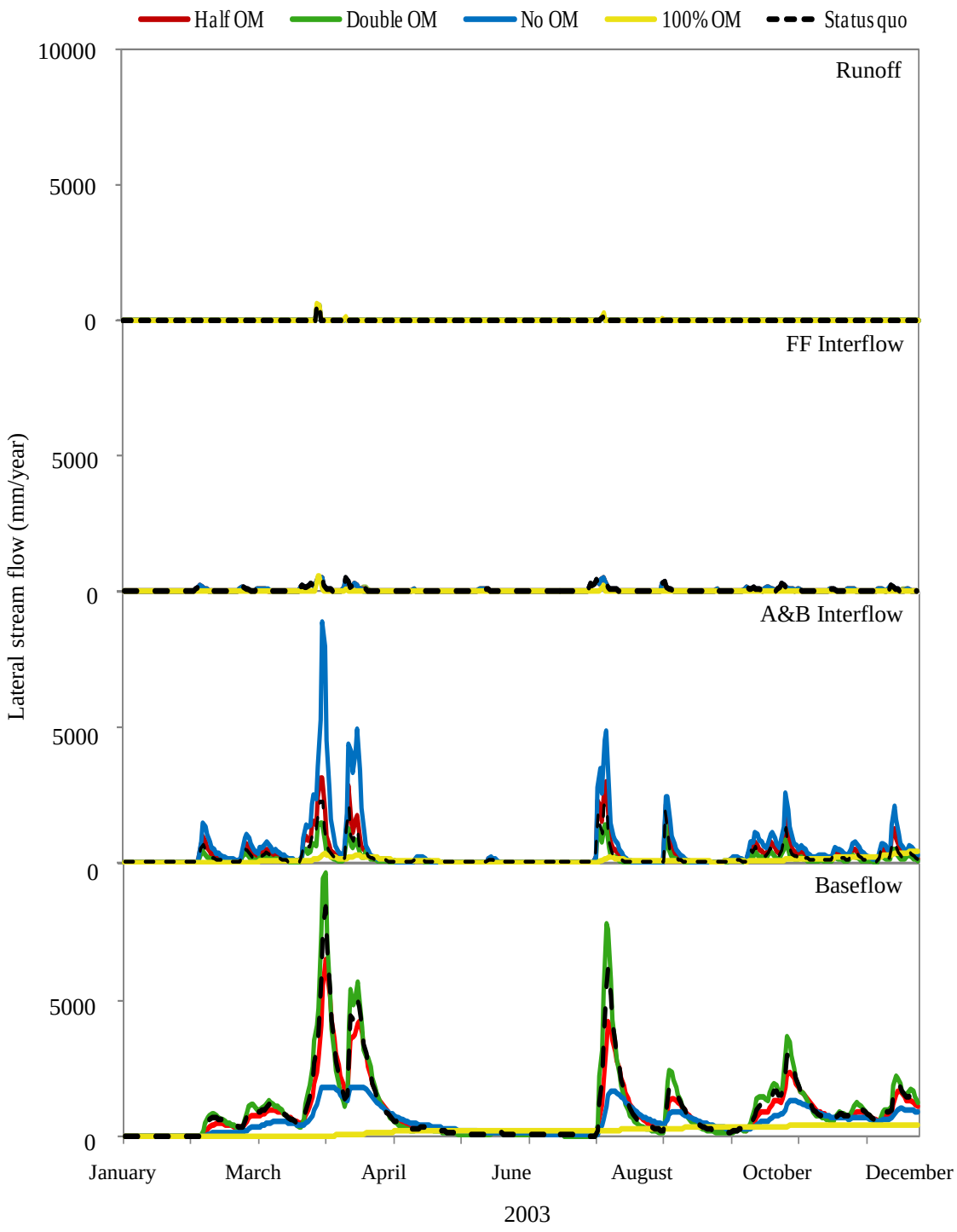


Figure 40. Lateral stream flow broken down by horizon for OM sensitivity scenarios (Double OM, Half OM, no OM, 100% OM) versus status quo, for Moosepit Brook, NS in 2003.

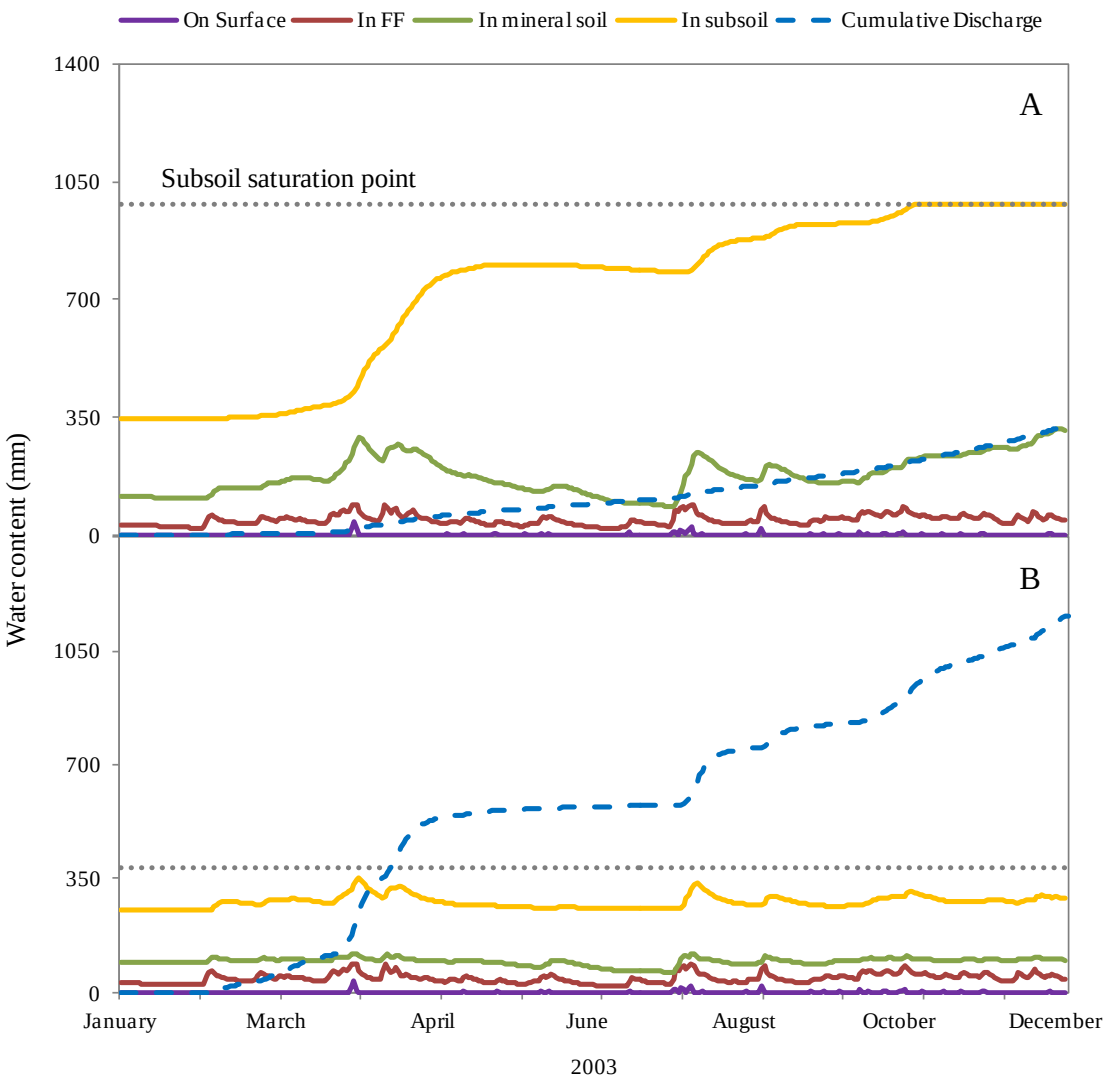


Figure 41. Soil water content on the surface, in the forest floor, in the mineral soil, and in the subsoil, as well as the cumulative discharge for, a) scenario with 100% OM, and b) status quo, for Moosepit Brook, NS in 2003.

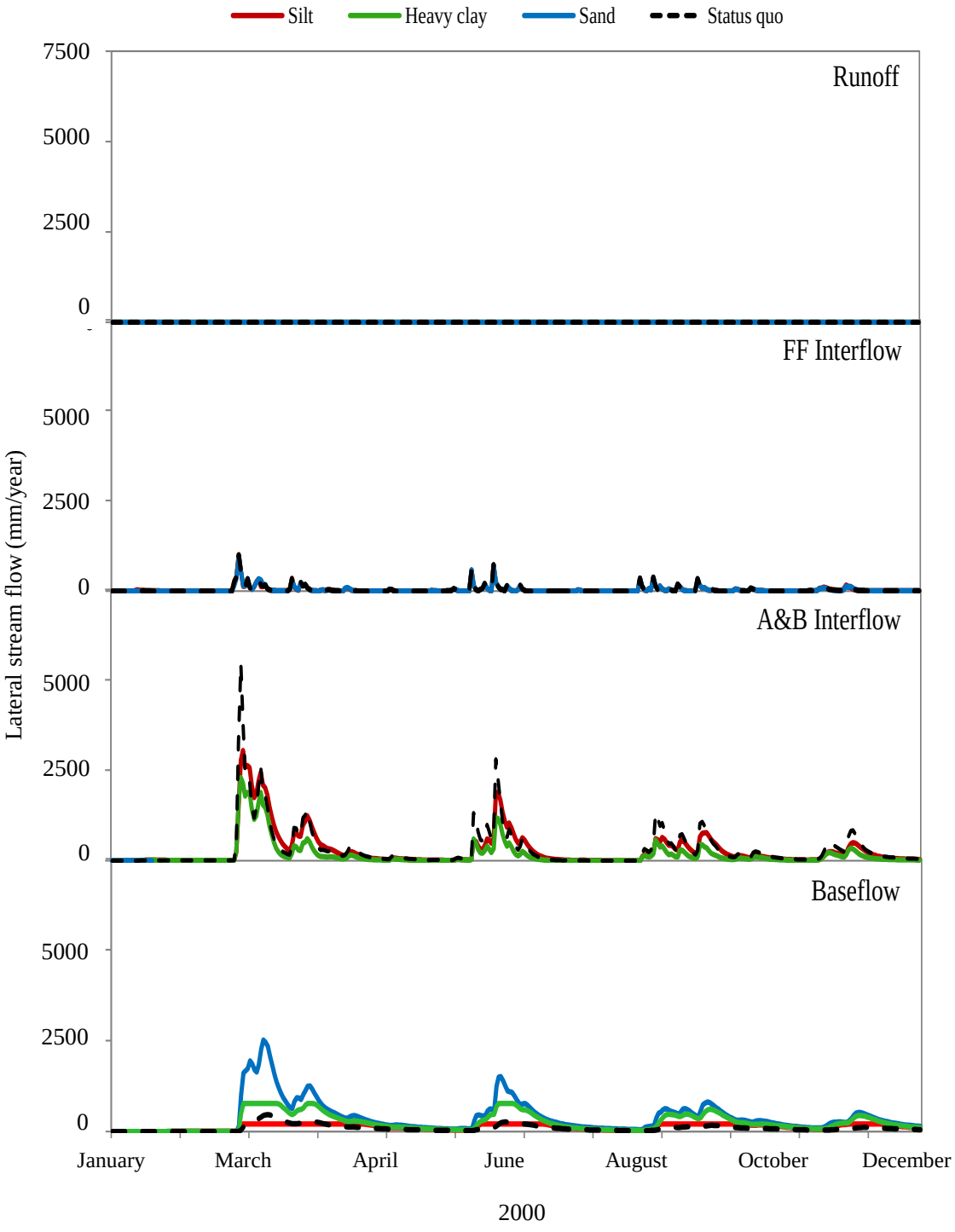


Figure 42. Lateral stream flow broken down by horizon for texture sensitivity scenarios (Sand, Silt, Heavy clay) versus status quo, for Turkey Lakes, ON in 2000.

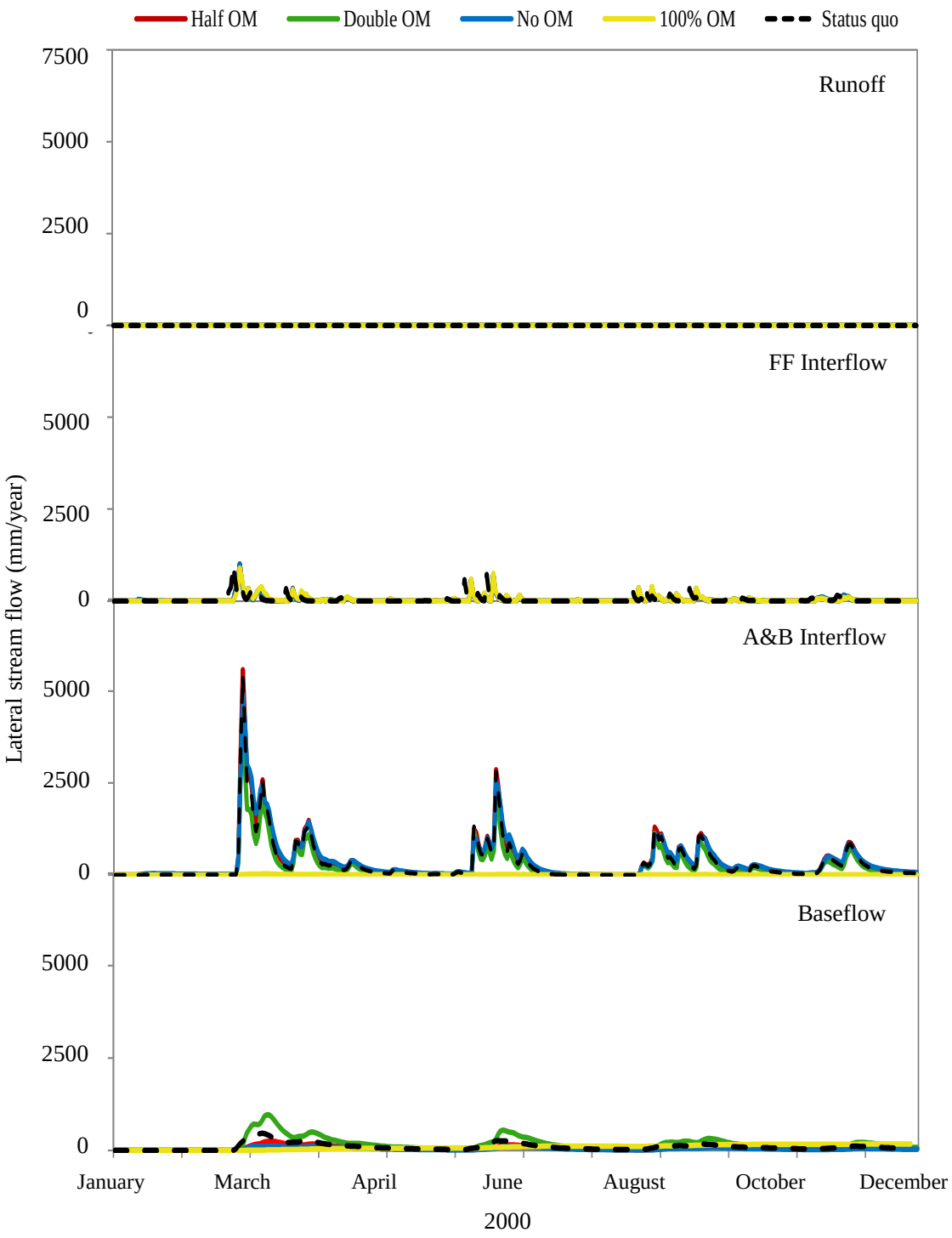


Figure 43. Lateral stream flow broken down by horizon for OM sensitivity scenarios (Double OM, Half OM, no OM, 100% OM) versus status quo, for Turkey Lakes, ON in 2000.

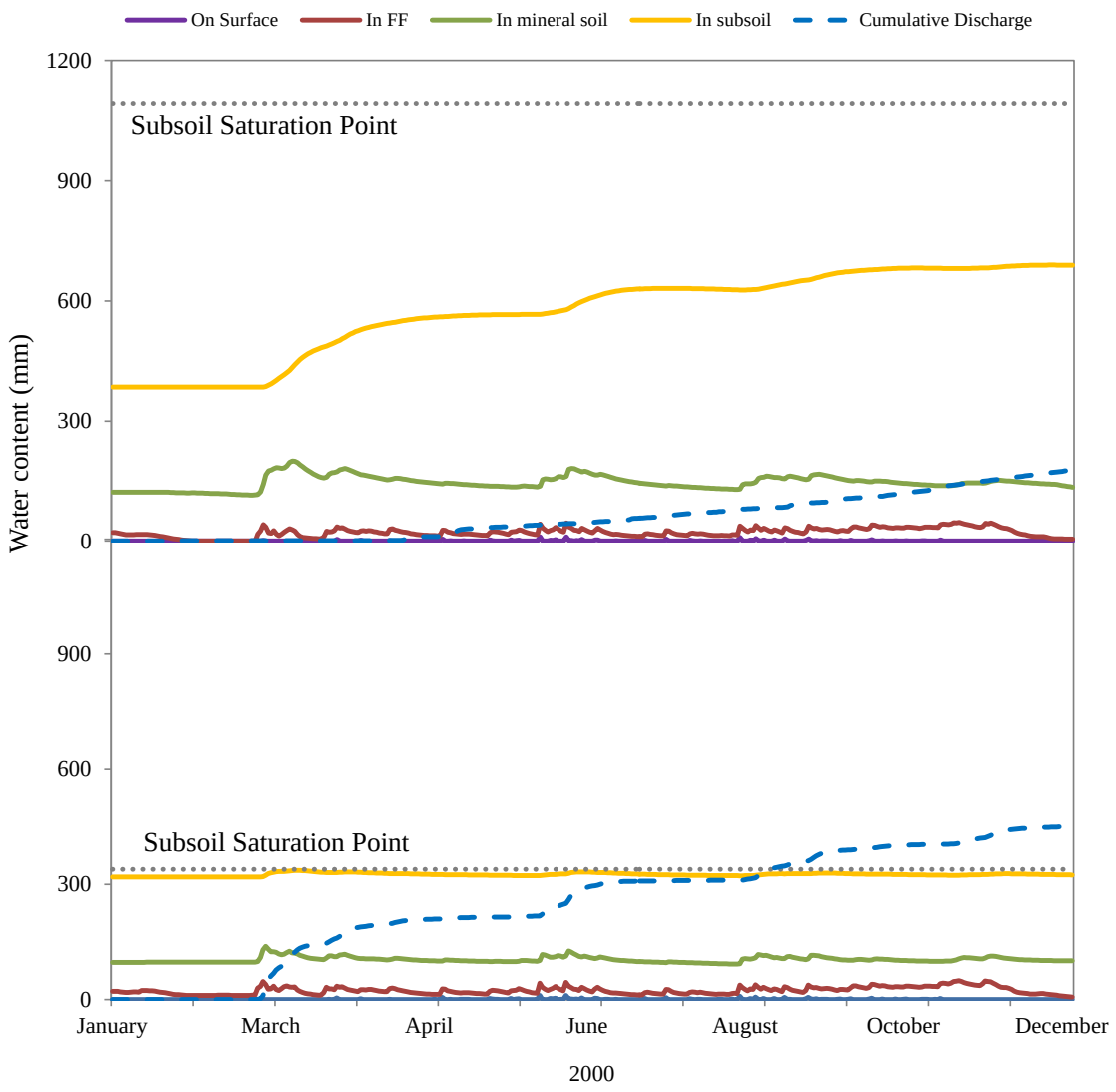


Figure 44. Soil water content on the surface, in the forest floor, in the mineral soil, and in the subsoil, as well as the cumulative discharge for, a) scenario with 100% OM, and b) status quo, for Turkey Lakes, ON in 2000.

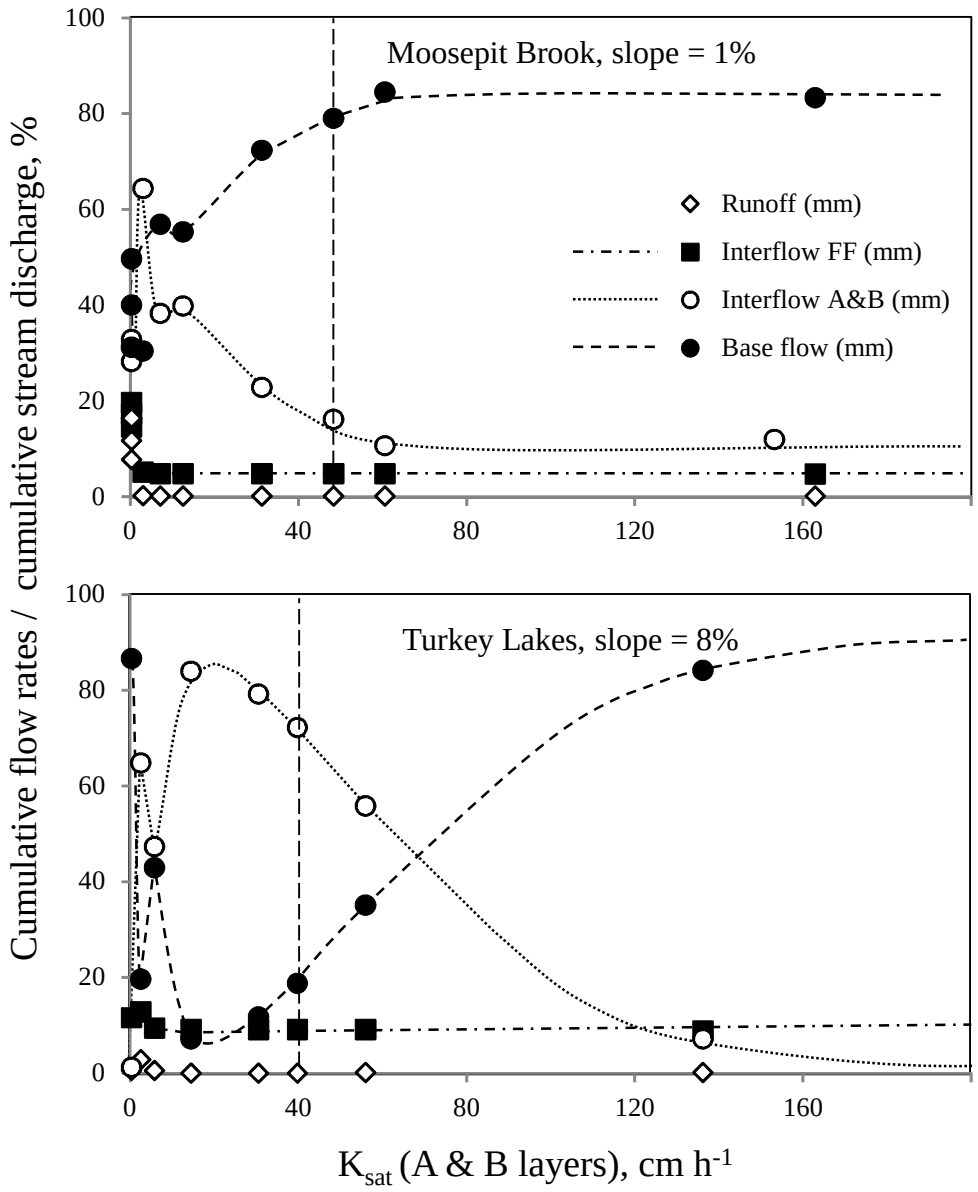


Figure 45. K_{sat} of the A&B layers by cumulative stream discharge % for Moosepit Brook (top), and Turkey Lakes (bottom) across all 8 scenarios (vertical dashed line represents the status quo scenario).

As shown in Figure 46, reducing the % of vegetation cover would lead to water pooling within and on the soil at Moosepit Brook, but not at Turkey Lakes, mainly due to the differences in watershed slopes (flatter for the former at about 1%, and higher for the latter at about 8%), as well as the reduction in evapotranspiration, which affects water retention in the soil.

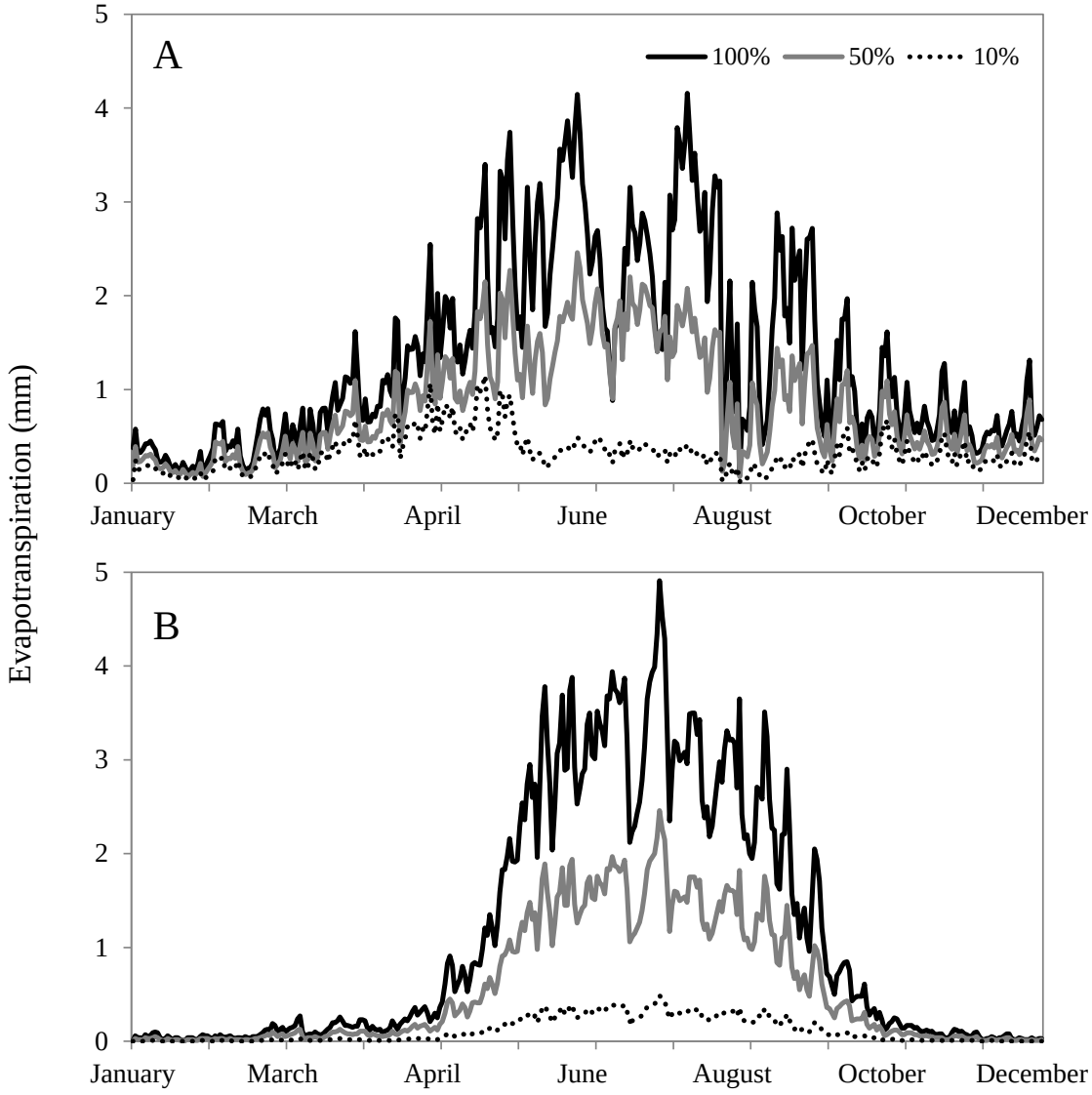


Figure 46. Evapotranspiration (FF + A&B) at Moosepit Brook (A) during 2003 and Turkey Lakes (B) during 2000, for scenario 8 (100% OM), with status quo (100% vegetation), scenario 8^1 (50% vegetation), and scenario 8^2 (10% vegetation).

DISCUSSION

The difference for both sites in terms of the interflow versus baseflow contributions through the mineral soil layers towards the streams (Figure 45) is, as calculated, mainly related to differences in slope and soil permeability. With increasing

soil permeability, water would, as to be expected, percolate downward rather than sideways. The low subsoil permeability at Turkey Lakes would, however, force the water to follow the path of least resistance laterally through the upper soil layers horizons. Low soil and subsoil flow rates during the snowmelt season and frozen soil conditions would further accentuate lateral flow leading towards surface run-off and forest floor interflow. At low overall soil permeability, however, lateral versus downward flow would be strongly influenced by layer-specific variations in soil organic matter: typically, soil organic matter increases K_{sat} in mineral soils. Within organic soils, decreases with increasing state of organic matter decomposition (Boelter 1965; Boelter 1968; Boelter and Verry 1977; Letts et al. 2000;), thereby enable more lateral flow at the surface, but low water flow through organic subsoils. For example, well decomposed "sapric" organic matter has a hydraulic conductivity of 1.03 to 0.38 cm/h and a bulk density range of 0.2 to 0.16 g/cm^3 (Boelter 1968; Boelter and Verry 1977). Therefore, setting K_{sat} = 0.30 cm/h and D_b = 0.20 g/cm^3, as done for Scenario 8, represents partial to well decomposed "hemic-sapric" organic profile as suggested by Silc and Stanek (1977) and Boelter (1968). In detail, the plots in Figure 40 and 43 shows that Scenario 8 implies low flow rates through the lower peat layers, and Figure 45 illustrates how variable the mix of lateral versus downward flow becomes at low K_{sat} values at the transition from organically enriched mineral soils to fully organic soils.

Change in % vegetation cover also affects the movement and retention of water through soils and watersheds. For example, Moosepit Brook has a flat terrain (1% slope), allowing water to pool at the surface, especially in flat areas with low vegetation cover.

With less vegetation on site, there is less overall evapotranspiration (Figure 46). Dubé et al. (1995) studied eight forested wetlands along the St. Lawrence River. They observed that the water table would rise into the upper soil layers after clear cutting. In contrast to Moosepit Brook, Turkey Lakes has a greater slope (8%) which, thereby, promotes interflow and baseflow without pooling at the surface especially at locations with intermediate to high soil permeability (Figure 46).

CONCLUDING REMARKS

Watershed-based K_{sat} calibrations have shown that the calibrated values for K_{sat} pertaining to downward and lateral flow generally vary by a factor of 2 to 3 in comparison to corresponding values generated via Eqs. 16 to 19. As shown, this variation leads to uncertainties in quantifying exactly how much of the water that percolates through each watershed is subject to run-off, interflow, and baseflow. These uncertainties, however, do not affect the time of the flow responses apart from small delays and extended flow periods. In general, flows across watersheds tend to be well synchronized, regardless of major differences in texture, density, and organic matter content (Figures 39, 40 and 42, 43). However, watersheds with the more compacted soils will be more peaked and therefore will be flashier than watersheds that allow deep percolation (Lull 1959; Kramer and Boyer 1995; Kozlowski 1999; Brady and Weil 2001). The strongest impact of varying the flow from shallow to deep deals with the water quality signature of these flows from forest watersheds: deep water percolation during summer leads to cooler and purer water with elevated pH than shallow water percolation (Steeves 2004). During winter, deep percolation and persistent baseflow tends

to be warm compared to cold and non-persistent flow at the surface due to soil freezing (Steeves 2004; Chi 2008). Flow along the surface will be colored towards brown and acidic (Jutras et al. 2011).

While texture, organic matter and soil density will not change drastically throughout undisturbed watersheds, such changes can be expected to occur during and after times of intense surface operations, especially under poor weather conditions. For example, forest operations during times of poor soil trafficability lead to ruts and increased soil compaction (McNabb et al. 2001; Froehlich and McNabb 1984). Consequently, soil compaction leads to lower K_{sat} values and therefore lower infiltration, but higher surface run-off, which – in turn - will result in greater soil erosion and subsequent stream sedimentation (Harr et al. 1979). Trails across the slopes of watersheds will also compact the soil underneath the trails, which means more water retention upslope along the trails, therefore leading to weather-effected trail destabilization or ditches and cross drains to divert the water away from the trail bed (Jamshidi et al. 2008). The main advantage of the above formulation is that it allows for daily weather-related projections concerning downward and lateral water flow rates in forested watersheds at times when soils are at saturation, or near saturation, i.e., at those times when the quantification of these flows is the most critical in terms of estimating the overall effects of water flow on soil stability, water quality, and hydrological infrastructures downstream.

LITERATURE CITED

Balland, V., Pollacco, J.A.P., Arp, P.A. 2008. Modeling soil hydraulic properties for a wide range of soil conditions. *Ecological Modelling*. 219:300-316.

Boelter, D. H. 1965. Hydraulic Conductivity of Peats. *Soil Science*. 1004:227-231.

Boelter, D.H. 1968. "Important physical properties of peat materials." in Proceedings, third international peat congress; 1968 August 18-23. Quebec, Canada: Department of Energy, Minds and Resources and National Research Council of Canada. Pp. 150-154

Boelter, D.H., Verry, E. 1977. "Peatland and water in the northern lake states." General Technical Report NC-31, U.S. Dept. of Agriculture, Forest Service, North Central Forest Experiment Station, St. Paul, MN.

Brady, N.C., Weil, R.R. 2001. The Nature and Properties of Soils. 13th ed. Upper Saddle River, New Jersey: Prentice Hall.

Chi, X. 2008. Hydrogeological assessment of stream water in forested watershed: temperature, dissolved oxygen, pH, and electrical conductivity. Unpublished. MSc. Thesis. University of New Brunswick, Fredericton, NB.

Dubé, S., Plamondon, A., and Rothwell, R. 1995. Watering up after clear-cutting on forested wetlands of the St. Lawrence lowland. Water Resource Research. 315:1740-1750.

Froehlich, H.A., McNabb, D.H. 1984. "Minimizing soil compaction in Pacific Northwest forests." Proceedings Forest Soils and Treatment Impacts Conference, Knoxville, TN.

Harr, R.D., Fredriksen, R.L., Rothacher, J. 1979. "Changes in streamflow following timber harvest in southwestern Oregon." Forest Service Resoure Paper PNW-249, USDA, Pacific Northwest Research Station, Portland, Oregon.

Jamshidi, R., Jaeger, D., Raafatnia, N., Tabari, M. 2008. Influence of two ground-based skidding systems on soil compaction under different slope and gradient conditions. *International Journal of Forest Engineering*. 19:9-16.

Jutras, M.-F., Arp, P.A. 2011. "Determination of hydraulic conductivity from soil characteristics and its application for modelling stream discharge in forest catchments." Pp. 189-202 in *Hydraulic Conductivity - Issues, Determination and Applications*, edited by Lakshmanan Elango (Ed.). InTech.

Kozlowski, T.T. 1999. Soil compaction and growth of woody plants. *Scandinavian Journal of Forest Research.* 614:596-619.

Kramer, P.J., Boyer, J.S. 1995. *Water Relations of Plants and Soils*. Sand Diego: Academic Press Inc.

Letts, M.G., Roulet, N.T., Comer, N.T., Skarupa, M.R., Verseghy, D.L. 2000. Parametrization of peatland hydraulic propoerties for the Canadian land surface scheme. *Atmosphere-Ocean*. 138:141-160.

Lull, H.W. 1959. *Soil Compaction on Forest and Range Lands*. Forest Services, U.S. Department of Agriculture. 36p.

McNabb, D.H., Startsev, A.D., Nguyen, H. 2001. Soil wetness and traffic level effects on bulk density and air-filled porosity of compacted boreal forest soils. *Soil Science Society Journal of America*. 65:1238-1247.

Silc, T., Stanek, W. 1977. Bulk density estimation of several peats in northern Ontario using the Von post humification scale. *Canadian Journal of Soil Science*. 57:75.

Steeves, M.T. 2004. Pre- and post-harvest groundwater temperatures and levels, in upland forest catchments in Northern New Brunswick. Unpublished. MSc. Thesis, University of New Brunswick, Fredericton, NB.

CHAPTER 7 - CONCLUSIONS

THESIS SUMMARY

The K_{sat}, SP, FC, PWP values generated from layer-specific values for D_b, D_p, sand, clay, organic matter and soil depth based on the Balland et al. (2008) specifications produced reasonable results regarding the ForHyM2 calculations pertaining to water retention, run-off, infiltration, interflow, percolation, baseflow and stream discharge for each of the six catchment areas of this study. Fine-tuning the results by matching actual with modelled stream discharge calibrations generally kept the best-fitted K_{sat} values for infiltration, percolation and interflow within a factor of two for each soil layer (forest floor, A and B layers combined, and C and subsoil layers combined). For the well-drained watersheds at Turkey Lakes, Lac Laflamme, and Rithet Creek, extra downward adjustments for interflow were needed, likely due to the combined effects of (i) high slope heterogeneities, which would lengthen the average flow path assumption for lateral flow for each catchment, and (ii) substrate non-uniformities, especially when fractured bedrock or porous limestone underneath shallow surface deposits encourage deep percolation instead of lateral flow. For example, the high downward K_{sat} adjustments at Hayward Brook in New Brunswick are likely due to the greater porosity of the calcareous shales, which – in turn – require larger K_{sat} adjustments for soil and subsoil percolation. Similar adjustments would have to be made for agricultural areas where the flow rates would be accelerated by drainage tiles and ditches. Additional K_{sat} adjustments would be needed where soil bulk densities (D_b) change on account of surface and sub-surface

compaction, weather-induced soil shrinking and swelling, and freezing and thawing. In summary, the process of:

1. estimating K_{sat}, FC, PWP and soil porosity from soil survey data for soil depth, texture and organic matter,
2. using these estimates as initial values for modeling the daily changes in the hydrothermal conditions and flows through of forest catchments, and
3. subsequently calibrating K_{sat} to improve the run-off, infiltration, percolation, interflow and baseflow calculations,

generated good agreements between modelled and monitored stream discharge for the six forest catchments of this study at the daily level, year-round. Adjustments were required for the catchments on steep and calcareous terrains.

ORIGINAL CONTRIBUTIONS

This thesis provides a detailed analysis on how stream-discharge calibrated K_{sat} values vary across six well-studied watersheds representing diverse conditions for climate, topography, bedrock geology and vegetation. The detailed examination of how K_{sat} varies by soil layer a led to further improvements of ForHyM2 as used by Steeves (2004) and Chi (2008).

1. Simplifying the flow calculations for each soil layer by going back to the original formulation of Darcy's Law (Eq. 1).
2. Adding a deep flow component, to divert some of the ForHyM2 estimated baseflow away from the cumulative stream discharge calculations, to account for the fact that not all of the water that percolates through the watershed will

always reach the stream above or at the stream gauging location. This would particularly noticeable where some or all of the surface water percolates into (i) deep-seated aquifers, (ii) highly and deeply fractured bedrock, and (iii) channel-permeated limestone formations.

3. Improving the ForHyM2 User Manual, with a brief introduction and focusing on calibration (Appendix II).
4. Submitting two chapters in books dealing specifically with assessing hydraulic conductivities in soils and other geological substrates; one chapter has already been published, while the other one is in development (Jutras and Arp 2011).
5. Placing the K_{sat} calculations and subsequent ForHyM2 calculations into the context of estimating water-transferred dissolved organic carbon (DOC) from uplands to wetlands and streams (Jutras et al. 2011).
6. Adding a ForHyM2 section to the web-site of the Forest Watershed Research Centre at UNB at http://watershed.for.unb.ca/.

SUGGESTIONS FOR FUTURE WORK

Organic Matter Integration

A framework for integrating sites with purely organic soil (such as bogs or fens) would increase the soil range applicability of ForHyM2. As it currently stands, ForHyM2 views all organic soils (OM=100%) the same, as deep sapric peats. In order to model the hydrological discharge more accurately in peatlands, a gradient should be created to take into consideration the change in peat porosity, water content yield, and bulk density with depth (Boelter and Verry 1977). Even given the change in OM parameters with depth, peatlands shouldn't be viewed as sites of singular composition. One site could contain

only sphagnum moss for 5 meters, with a large K_{sat} and small D_b, whereas another site could have very shallow profile with old, highly decomposed peat with a fraction of K_{sat} and D_b. In ForHyM2, current water content and porosity controls the amount of (i) water that can move freely through the site, (ii) the volumetric fraction of ice that can form, and (iii) water can percolate through the horizons based on empty pore spaces. Within the fine-earth fraction of mineral soils with varying organic matter content (coarse fragments excluded), porosity depends on bulk density and particle density via Eq. 16. For fully organic soils, porosity and bulk density also depend on the von Post index, which is used to specify the state of organic matter decomposition. To account for this, Balland et al. (2008) set the aK_{sat} parameter equal to $(2.5 \pm 0.2) - (0.046 \pm 0.004)$ $vanPost_index^2$. Account for decomposition effects on bulk as well as particle density, and reviewing literature estimates for K_{sat} from non-decomposed to well humified peat should broaden the application of ForHyM2 to quantify water retention and vertical as well as lateral flow through peatland bogs.

Calibration Automation

Thus far, the systematic ForHyM2 calibrations for lateral and downward flow are done manually, by soil layer. These calibrations can be time consuming step, and require considerable familiarity with the model formulation and the modeling process as well. To some extent, this calibration was greatly facilitated by using Balland et al. (2008) formulation for initializing the K_{sat} values for each soil layer according to already existing watershed information, and is further facilitated by way of the results of this Thesis. Ideally, more could be done to apply least-squares optimization routines for generating

layer-specific K_{sat} values that match model generated with actual stream-discharge. Doing so, however, requires re-programming ForHyM2 using another modeling platform such as Model Maker, to take advantage of its built-in least-squares routines for parameter fitting.

Spatial Application of ForHyM2

ForHyM2 produces aspatial outputs for each watershed. Each watershed, however, can be further divided into (i) its subcatchments, and/or (ii) its hydrographic response units (HRU), each representing fairly uniform conditions for slope, soil, bedrock, climate and vegetation conditions. ForHyM2 can then be run for each subcatchment, or each HRU. A programming script could then be developed that would track the ForHyM2 output from each unit or catchment over time, and the results so acquired can then be entire into a geospatial database for analysis and geospatial visualization purposes.

Web-site realization

Work continues on making ForHyM2 as is currently formulated for general use via web-site service. To protect the overall integrity the Intellectual properties of this program, it was decided (i) to re-script the model, and (ii) to enable model used through license arrangements.

LITERATURE CITED

Balland, V., Pollacco, J.A.P., Arp, P.A. 2008. Modeling soil hydraulic properties for a wide range of soil conditions. *Ecological Modelling*. 219:300-316.

Boelter, D.H., Verry, E. 1977. "Peatland and water in the northern lake states." General Technical Report NC-31, U.S. Dept. of Agriculture, Forest Service, North Central Forest Experiment Station, St. Paul, MN.

Chi, X. 2008. Hydrogeological assessment of stream water in forested watershed: temperature, dissolved oxygen, pH, and electrical conductivity. Unpublished. MSc. Thesis. University of New Brunswick, Fredericton, NB.

Jutras, M.-F., Arp, P.A. 2011. "Determination of hydraulic conductivity from soil characteristics and its application for modelling stream discharge in forest catchments." Pp. 189-202 in *Hydraulic Conductivity - Issues, Determination and Applications*, edited by Lakshmanan Elango (Ed.). InTech.

Jutras, M.-F., Nasr, M., Castonguay, M., Pit, C., Pomeroy, J., Smith, T. P., Zhang, C.-F., Ritchie, C. D., Meng, F.-R., Clair, T. A., Arp, P.A. 2011. Dissolved organic cardon concentrations and fluxes in forest catchments and streams: DOC-3 model. *Ecological Modeling*. doi:10.1016/j.ecolmodel.2001.03.035.

Steeves, M.T. 2004. Pre- and post-harvest groundwater temperatures and levels, in upland forest catchments in Northern New Brunswick. Unpublished. MSc. Thesis. University of New Brunswick, Frederiction, NB.

APPENDIX I – PRIMARY FORHYM2 MODELING INPUTS

The following watershed site characteristics were collected for each of the six sites in the study and used as primary inputs in the Excel interface for ForHyM2.

1.1 INPUTS FOR RITHET CREEK

Watershed Characteristics	
Latitude (°N)	49.5
Altitude (m)	375
Watershed area (ha)	1680
Aspect	0
Slope (°)	10
Coniferous fraction	1
Deciduous fraction	0
Root depth[1]	6
Wetland Ratio	0
LAI Max Deciduous	0
LAI Max Coniferous	0
Temperature code[2]	0
Subsoil moisture code	0
Mean yearly snow depth (cm)	1
Climate factor	0
Fog function	0
Distance to coast (km)	15
Beginning of harvest	2100
End of harvest	2100
Harvest type	0
Growth rate	0.47
Mean growing season (days)	280

Soil layers	Thickness (cm)	Texture[3]	OM (%)	CF (%)	Quartz (%)
Forest floor	10	0	1	0	0
A	30	4	0.2	0.1	0.3
B	50	4	0.1	0.1	0.3
C1	100	4	0.02	0.2	0.3
C2	100	4	0	0.2	0.3
Subsoil 1	100	4	0	0.4	0.3
Subsoil 2	100	4	0	0.6	0.3
Subsoil 3	100	4	0	0.9	0.3
Subsoil 4	100	4	0	0.9	0.3
Subsoil 5	100	4	0	0.9	0.3
Subsoil 6	100	4	0	0.9	0.3
Subsoil 7	100	4	0	0.9	0.3
Subsoil 8	100	4	0	0.9	0.3
Subsoil 9	100	4	0	0.9	0.3
Subsoil 10	100	4	0	0.9	0.3
Subsoil 11	100	4	0	0.9	0.3

References used for inputs:

Jungen, J.R., Ag, P. 1985. Soils of Southern Vancouver Island. British Columbia Soil Survey, Ministry of Environment, Government of British Columbia, Victoria, B.C.

Zhu, J.Z., Mazumder, A. 2008. Estimating nitrogen exports in response to forest vegetation, age and soil types in two coastal-forested watershed in British Columbia. *Forest Ecology and Management*. 255:1945-1959.

1.2 INPUTS FOR TURKEY LAKES

Watershed Characteristics	
Latitude (°N)	47.03
Altitude (m)	485
Watershed area (ha)	4.62
Aspect	-45
Slope (°)	4.53
Coniferous fraction	0
Deciduous fraction	1
Root depth[1]	6
Wetland Ratio	0
LAI Max Deciduous	0
LAI Max Coniferous	0
Temperature code[2]	0
Subsoil moisture code	0
Mean yearly snow depth (cm)	23
Climate factor	0
Fog function	1
Distance to coast (km)	2000
Beginning of harvest	1997.5
End of harvest	1997.7
Harvest type	0
Growth rate	0.47
Mean growing season (days)	155

Soil layers	Thickness (cm)	Texture[3]	OM (%)	CF (%)	Quartz (%)
Forest floor	7	0	1.00	0	0
A	15	4	0.05	0.1	0
B	30	4	0.03	0.1	0
C1	50	5	0.02	0.1	0
C2	100	5	0.01	0.2	0
Subsoil 1	100	4	0	0.4	0
Subsoil 2	100	4	0	1	0
Subsoil 3	100	4	0	1	0
Subsoil 4	100	4	0	1	0
Subsoil 5	100	4	0	1	0
Subsoil 6	100	4	0	1	0
Subsoil 7	100	4	0	1	0
Subsoil 8	100	4	0	1	0
Subsoil 9	100	4	0	1	0
Subsoil 10	100	4	0	1	0
Subsoil 11	100	4	0	1	0

References used for inputs:

Arp, P.A., Yin, X. 1992. Predicting water fluxes through forests from monthly precipitation and mean monthly air temperature records. *Canadian Journal of Forest Research*. 22:864-877.

Hazlett, P.W., Semkin, R.G., Beall, F.D. 2001. Hydrologic pathways during snowmelt in first-order stream basins at the Turkey Lakes Watershed. *Ecosystems*. 4:527-535.

Murray, C.D., Buttle, J. M. 2005. Infiltration and soil water mixing on forested and harvested slopes during spring snowmelt, Turkey Lakes Watershed, central Ontario. *Journal of Hydrology*. 306:1-20.

1.3 INPUTS FOR LAC LAFLAMME

Watershed Characteristics	
Latitude (°N)	47.19
Altitude (m)	800
Watershed area (ha)	69
Aspect	-70
Slope (°)	6
Coniferous fraction	1
Deciduous fraction	0
Root depth[1]	6
Wetland Ratio	0
LAI Max Deciduous	0
LAI Max Coniferous	0
Temperature code[2]	0
Subsoil moisture code	0
Mean yearly snow depth (cm)	50
Climate factor	0
Fog function	0
Distance to coast (km)	400
Beginning of harvest	2100
End of harvest	2100
Harvest type	0
Growth rate	0.47
Mean growing season (days)	146.6

Soil layers	Thickness (cm)	Texture[3]	OM (%)	CF (%)	Quartz (%)
Forest floor	18	0	1.00	0	0
A	10	1	0.01	0.04	0.53
B	60	1	0.05	0.134	0.402
C1	40	2	0.04	0.05	0.273
C2	100	2	0.00	0.12	0.316
Subsoil 1	100	1	0	0.9	0
Subsoil 2	100	1	0	0.9	0
Subsoil 3	100	1	0	0.9	0
Subsoil 4	100	1	0	0.9	0
Subsoil 5	100	1	0	0.9	0
Subsoil 6	100	1	0	0.9	0
Subsoil 7	100	1	0	0.9	0
Subsoil 8	100	1	0	0.9	0
Subsoil 9	100	1	0	0.9	0
Subsoil 10	100	1	0	0.9	0
Subsoil 11	100	1	0	0.9	0

References used for inputs:

Arp, P.A., Yin, X. 1992. Predicting water fluxes through forests from monthly precipitation and mean monthly air temperature records. *Canadian Journal of Forest Research*. 22:864-877.

Barry, R., Prevost, M., Stein, J., Plamondon, A.P. 1990. Simulation of snowmelt runoff pathways on the Lac Laflamme watershed. *Journal of Hydrology*. 113:103-121.

1.4 INPUTS FOR HAYWARD BROOK

Watershed Characteristics	
Latitude (°N)	45.52
Altitude (m)	162
Watershed area (ha)	508
Aspect	2
Slope (°)	4.6
Coniferous fraction	0.5
Deciduous fraction	0.5
Root depth[1]	3
Wetland Ratio	0
LAI Max Deciduous	0
LAI Max Coniferous	0
Temperature code[2]	0
Subsoil moisture code	0
Mean yearly snow depth (cm)	16.1
Climate factor	0
Fog function	0
Distance to coast (km)	35
Beginning of harvest	1995.4
End of harvest	1995.8
Harvest type	0
Growth rate	0.47
Mean growing season (days)	155

Soil layers	Thickness (cm)	Texture[3]	OM (%)	CF (%)	Quartz (%)
Forest floor	10	0	1.00	0.1	0
A	10	1	0.05	0.2	0
B	30	3	0.09	0.25	0
C1	30	3	0.05	0.5	0
C2	100	4	0.05	0.5	0
Subsoil 1	100	4	0	0.9	0
Subsoil 2	100	4	0	0.9	0
Subsoil 3	100	4	0	0.9	0
Subsoil 4	100	4	0	0.9	0
Subsoil 5	100	4	0	0.9	0
Subsoil 6	100	4	0	0.9	0
Subsoil 7	100	4	0	0.9	0
Subsoil 8	100	4	0	0.9	0
Subsoil 9	100	4	0	0.9	0
Subsoil 10	100	4	0	0.9	0
Subsoil 11	100	4	0	0.9	0

References used for inputs:

Chi, X. 2008. Hydrogeological assessment of stream water in forested watershed: temperature, dissolved oxygen, pH, and electrical conductivity. Unpublished. MSc. Thesis. University of New Brunswick, Fredericton, NB.

Fahmy, S.H., Colpitts, M.C. 1995. Soils of the Fundy Model Forest. Agriculture and Agri-Food Canada, Fundy Model Forest, Fredericton.

1.5 INPUTS FOR POCKWOCK

Watershed Characteristics	
Latitude (°N)	44.83
Altitude (m)	195.58
Watershed area (ha)	273.43
Aspect	-31.41
Slope (°)	3.93
Coniferous fraction	0.75
Deciduous fraction	0.25
Root depth[1]	1
Wetland Ratio	0
LAI Max Deciduous	0
LAI Max Coniferous	0
Temperature code[2]	0
Subsoil moisture code	0
Mean yearly snow depth (cm)	7
Climate factor	0
Fog function	1
Distance to coast (km)	35
Beginning of harvest	2100
End of harvest	2100
Harvest type	1
Growth rate	0.47
Mean growing season (days)	172

Soil layers	Thickness (cm)	Texture[3]	OM (%)	CF (%)	Quartz (%)
Forest floor	10	0	1.00	0.1	0.5
A	21	4	0.05	0.25	0.5
B	50	4	0.09	0.25	0.5
C1	50	4	0.05	0.5	0.5
C2	50	4	0.05	0.5	0.5
Subsoil 1	100	4	0	0.9	0.5
Subsoil 2	100	4	0	0.9	0.5
Subsoil 3	100	4	0	0.9	0.5
Subsoil 4	100	4	0	0.9	0.5
Subsoil 5	100	4	0	0.9	0.5
Subsoil 6	100	4	0	0.9	0.5
Subsoil 7	100	4	0	0.9	0.5
Subsoil 8	100	4	0	0.9	0.5
Subsoil 9	100	4	0	0.9	0.5
Subsoil 10	100	4	0	0.9	0.5
Subsoil 11	100	4	0	0.9	0.5

References used for inputs:

Cann, D.B., Hilchey, J.D., Smith, G.R. 1954. "Soil Survey of Hants County Nova Scotia." Nova Scotia Soil Survey No. 5, Department of Agriculture, Agriculture Canada, Truro.

Chi, X. 2008. Hydrogeological assessment of stream water in forested watershed: temperature, dissolved oxygen, pH, and electrical conductivity. Unpublished. MSc. Thesis. University of New Brunswick, Fredericton, NB.

Vaidya, O.C., Smith, T.P., Fernand, H. 2008. Forestry best management practices: evaluation of alternate streamside management zones on stream water quality in Pockwock Lake and Five Mile Lake watersheds in central Nova Scotia, Canada. *Environmental Monitoring and Assessment*. 137:1-14.

1.6 INPUTS FOR MOOSEPIT BROOK

Watershed Characteristics	
Latitude (°N)	44.43
Altitude (m)	127
Watershed area (ha)	1770
Aspect	0
Slope (°)	0.57
Coniferous fraction	0.5
Deciduous fraction	0.5
Root depth[1]	4
Wetland Ratio	0
LAI Max Deciduous	0
LAI Max Coniferous	0
Temperature code[2]	0
Subsoil moisture code	0
Mean yearly snow depth (cm)	5
Climate factor	0
Fog function	1
Distance to coast (km)	50
Beginning of harvest	2100
End of harvest	2100
Harvest type	0
Growth rate	0.47
Mean growing season (days)	185

Soil layers	Thickness (cm)	Texture[3]	OM (%)	CF (%)	Quartz (%)
Forest floor	10	0	1.00	0	0
A	21	4	0.05	0.1	0
B	21	4	0.09	0.1	0
C1	50	4	0.05	0.25	0
C2	100	4	0.00	0.25	0
Subsoil 1	100	4	0	0.9	0
Subsoil 2	100	4	0	0.9	0
Subsoil 3	100	4	0	0.9	0
Subsoil 4	100	4	0	0.9	0
Subsoil 5	100	4	0	0.9	0
Subsoil 6	100	4	0	0.9	0
Subsoil 7	100	4	0	0.9	0
Subsoil 8	100	4	0	0.9	0
Subsoil 9	100	4	0	0.9	0
Subsoil 10	100	4	0	0.9	0
Subsoil 11	100	4	0	0.9	0

References used for inputs:

Lam, D.C.L., Bobba, A.G., Bourbonniere, R.A., Howell, G.D., Thompson, M.E. 1989. Modeling Organic and Inorganic Acidity in Two Nova Scotia Rivers. *Water, Air, and Soil Pollution*. 46:277-287.

MacDougall, J.L., Nowland, J.L., Hilchey, J.D. 1969. "Soil Survey of Annapolis County Nova Scotia." Nova Scotia Soil Report No. 16, Nova Scotia Department of Agriculture, Canada Department of Agriculture, Truro, Canada.

Yanni, S., Keys, K., Clair, T., Arp, P.A. 2000. Fog and acidification impacts on ion budgets of basins in Nova Scotia, Canada. *Journal of the American Water Resource Association*. 336:619-631.

[1]Root depth code describes the depth reached by the roots of dominant species (for mixed stands, use the medium of major species): Shallow = 1 (e.g., spruces), Medium shallow = 2, Medium = 3, Medium deep = 4, Deep = 5 (e.g., sugar maple), Very deep = 6

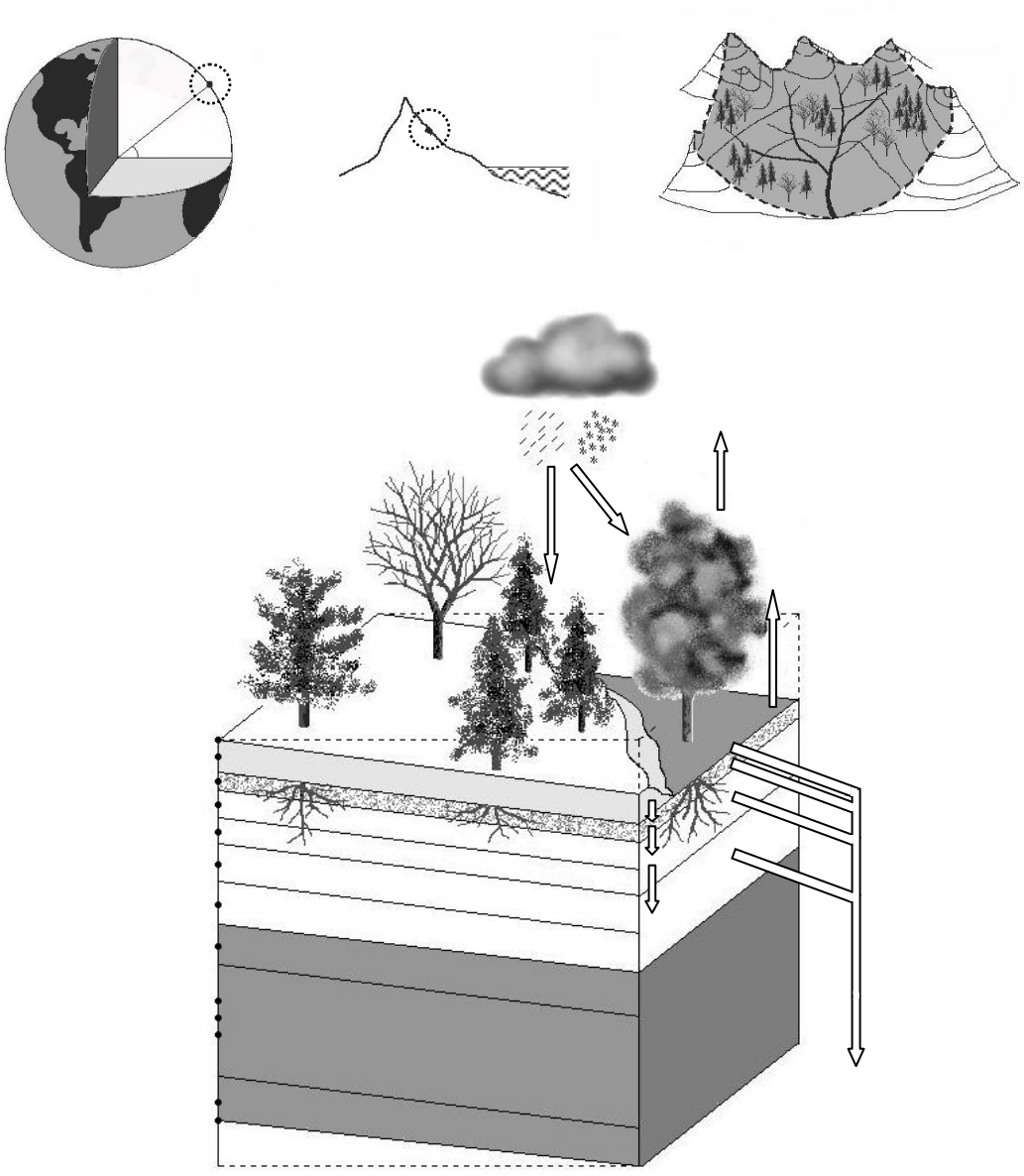
[2]Temperature code: 1 if air temperature data were recorded under the forest canopy; 0 otherwise.

[3]Texture code describes the texture of the mineral part of the fine soil: 100% organic = 0, Sand = 1, Silt = 2, Loamy sand = 3, Sandy loam = 4, Silt loam = 5, Loam = 6, Sandy clay loam = 7, Silt clay loam = 8, Clay loam = 9, Sandy clay = 10, Silt clay = 1, Clay = 12

APPENDIX II – FORHYM2 USER'S GUIDE

Forest Hydrology Model (ForHyM2)

User's guide



INTRODUCTION

The Forest Hydrology Model (ForHyM2) is a STELLA based software that uses daily rain, snow, and mean air temperature as well as basic catchment characteristics as inputs to determines changes in soil moisture and temperature, snowpack (depth, water equivalents, density) and flow rates (run-off, percolation, interflow, baseflow) at the daily level, summer through winter, with and without forest canopies. This manual was created to help users with initializing the model as well as calibrate and run it for their desired outputs.

INSTALLATION

1. Steps to follow

- Install *Microsoft Excel* 2002 or higher
- Install *STELLA Research* 5.1.1 or higher (please note that ForHyM2 does not work well in *STELLA Research* 9.0)
- Copy the "Forhym" folder on the "C" drive of your computer

***Note*:** it is necessary to copy this folder directly on the "C" drive so that the path is "C:/Forhym" for model applications to work properly.

2. Description of model files

The "Forhym" folder contains:

- Model interface: "Interface.xls":
  Importing data (weather and calibration) and defining local characteristics of the watershed studied (slope, aspect, soil texture…) is facilitated by this user-friendly interface using *Excel*. In this interface file, input data are prepared in a suitable format for use by *STELLA*, thanks to automatic "macros".

- Model, *Stella* version: "Forhym.stm":
  This file contains the *STELLA* version of the model. It is the main body of ForHyM, which can be run over the desired period of time.

- A "Data backup" folder contains input data, calibration data and parameters for various sites across Canada, for which the model has already been run and calibrated.

Note: the interface file needs to be open (before *STELLA*, and as long as *STELLA* is open) for dynamic data exchange to work properly.

HOW TO RUN THE MODEL

1. Files to open

- Open "Interface.xls" first, and click on "enable macros"
- Open "Forhym.stm", and click on "yes" when you are asked if you want to re-establish links. This enables dynamic data exchange between the interface and the model.

Attention: **never change anything in the interface if the Stella model is not open**. If you did, the linkage would "break" and the *STELLA* model would not read automatically certain variables into the interface anymore. Once you are done with the changes, **save both** the *Excel* and the *Stella* files.

2. Information to enter

2.1 Input parameters

In the interface, enter required values on the "Input parameters" page to describe the watershed you are working on. Read the built-in comments describing each input needed to find out information and the proper units to use.

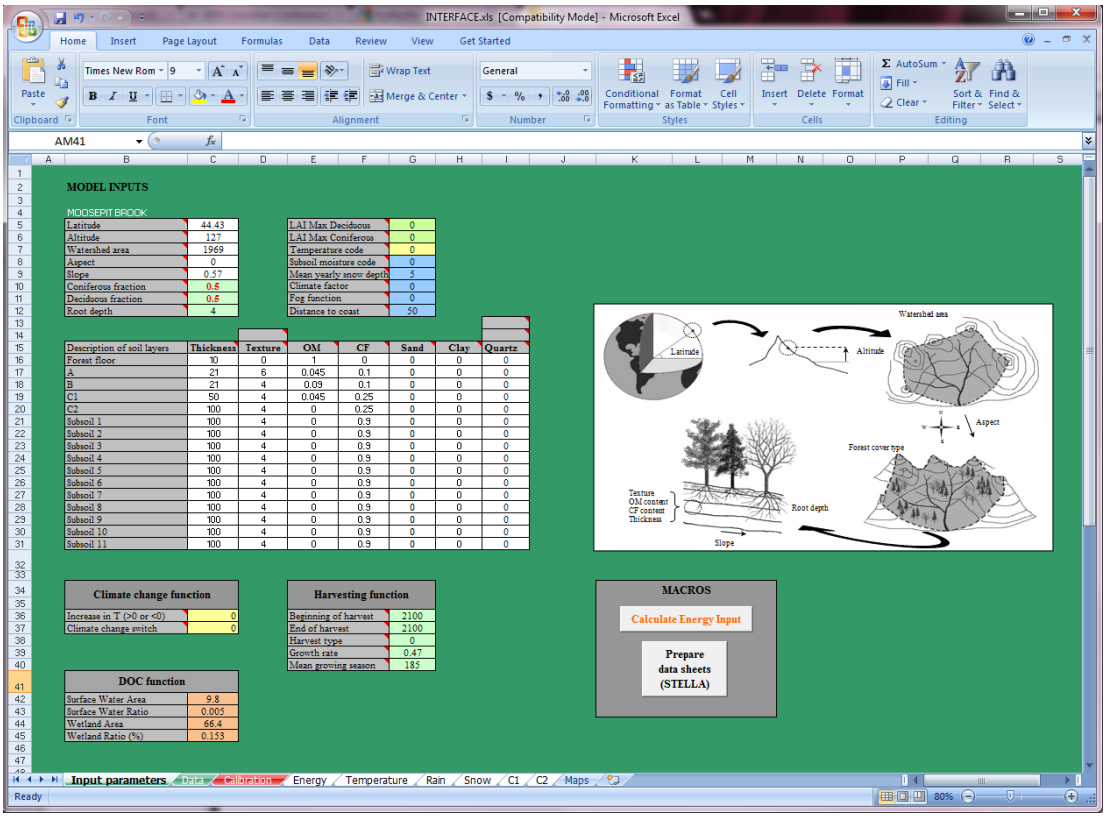


Figure 1. ForHyM2 user interface in Excel showing watershed and soil input parameters.

2.2 Daily data

In the interface, paste daily weather data for the period over which you want to run the model, as well as daily calibration data if you have any, on the "data" worksheet. If there are missing data in the weather records within a period during which you plan to run the model, they will be read as zero (which is a problem for temperatures).

Weather data necessary: (they can be obtained from the closest weather station; for Canada, a lot of records from various stations are available online at http://climate.weatheroffice.gc.ca/climateData/canada_e.html):

- daily mean air temperature (in ºC)
- daily total rain (in mm)
- daily total snow (in mm of water equivalent)

Note: if only daily total precipitation is known, it can be split arbitrarily into rain and snow, above and below 0ºC for example.

2.3 Processing

Once you have entered all the required input parameters and data, press the button to run the macro called **"Calculate energy input"**, and then the macro called **"Prepare data sheets"**.

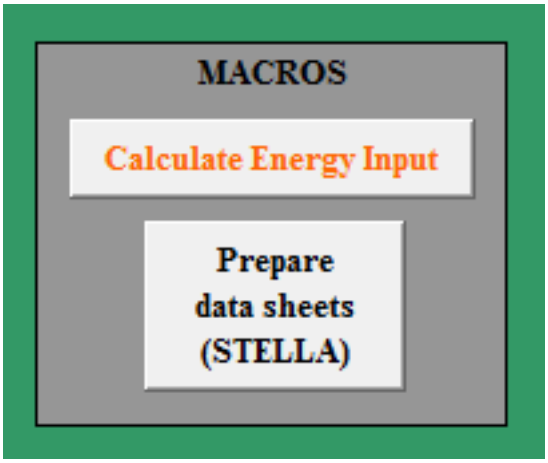


Figure 2. Macro processing buttons in the *Excel* user interface.

2.4 Notes & Fixes

In the *Excel* interface, some worksheets display the results of the calculations done by the above-cited macros (Ex. Energy, Temperature, Rain, Snow, C1 and C2). This is automatic, you don't need to enter anything on these worksheets (*STELLA* imports data from there automatically).

Before running the model double check the links in *STELLA* under "input data" and "calibration data". Sometimes *STELLA* breaks links in the process. An active link is found in the converter with an "x" at the top (Figure 3).

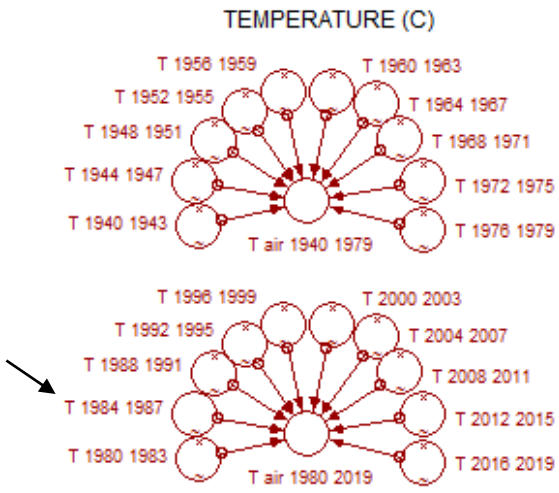


Figure 3. Temperature input parameters in *STELLA* showcasing broken links (black arrow).

In order to fix a broken link copy the column of data from the *Excel* interface (in this case Temperature tab, column 1984-1988). Double click on the broken converter and paste the data in the data column. Click "Paste Link" and then "OK" (Figure 4). This will rebuild the link to the Excel interface.

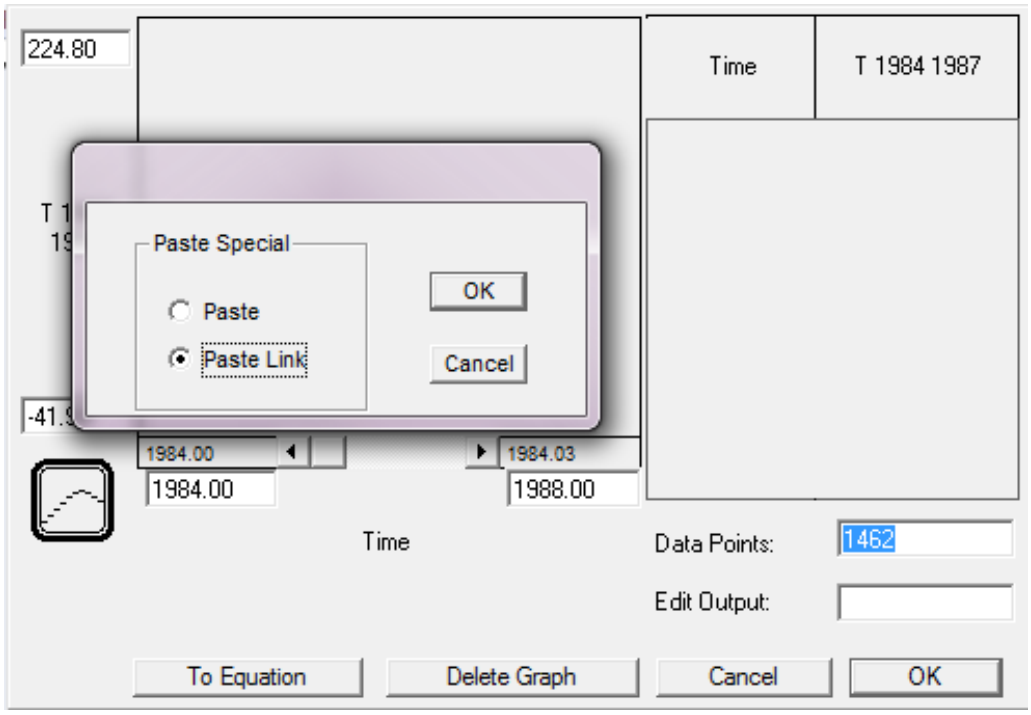


Figure 4. Fixing a broken link in the input parameters.

If an array is accidentally broken, (a converter with multiple layers or horizons, ex. texture), double click on the converter, make sure "Array" is checked in the top left-hand corner, and copy and "paste link" the data from each horizon into the text block in *STELLA*. Use the "row" button to sift through the different horizons (i.e. create a new link for each horizon). It's good to double check the array links by sifting through the rows and making sure the links are still intact.

3. Using STELLA ("Forhym.stm")

3.1 Getting started

In the menus, go into "Run / Time specs" and type a beginning and ending date for your simulation (1995.7 and 1998.2 for example). Enter also the time step of the simulation, called DT. Check "DT as a fraction". DT can be:

- 1/365 (model calculates one value for all variables every day)
- 1/730 (one value for all variables every 12 hours)
- 1/1461 (one value for all variables every 6 hours). (1461=365.25*4 = 3*365+366)

The 1/1461 time step is recommended, as it enables smoother calculations, even though it makes the model run a little slower. It takes into account leap year issues for comparison with actual data. Note that since data input is daily, the model remains a daily model, even if the time step used to run it is smaller than a day.

Choose "Euler's method" as an integration method, and click "Other" as a unit of time.

To start running the model, go into "Run / Run"

3.2 Calibration

Once the model it up and running properly, you will want to calibrate it. Calibrating your output data will help eliminate model errors and provide more realistic output results.

Under the red *Daily Data Calibration* columns in the "Data" tab of the Excel interface you can input:

- thickness of snow on the ground, (in cm)
- stream discharge (in $m^3.s^{-1}$)

If you have other data you want to calibrate with such as soil temperature, water table level and pH, just add new columns in the calibration section and create dynamic links into Stella. Macros are needed to add new columns of data to *STELLA*, therefore you can contact the watershed center for help with this if need be (arp2@unb.ca).

Water balance at watershed scale	
PETadjustor	1
Snow density and snowmelt	
Air temperature adjustor	0.06
Density of fresh snow	0.15
Water flows	
Surface runoff adjustor	1
Infiltration in FF adjustor	1
Interflow in FF adjusor	2
Infiltration in A & B adjustor	0.5
Interflow in A & B adjustor	2
Infiltration in C1& C2 adjustor	0.5
Interflow (base flow) in C1& C2 adjustor	2
Stream to ground flow adjustor	1

Figure 5. Calibration panel for ForHyM in the Excel interface, used to calibrate catchment specific evopotranspiration, snow parameters and water flow.

You can modify various parameters on the "Calibration" worksheet in the *Excel* interface (Figure 5). Increase or decreases these coefficients until a good correlation is found between actual collected data and the model produced data (Figure 6).

The best method for calibrating water flows is by starting with the baseflow and working your way up the soil profile. Baseflow tends to have the most control over general flow trend. Another good method is to open up the interflow graph (found under the green G*raphs and Table* box), as well as the water calibration graph (found under the red *Calibration Parameters* box) and observe the peaks in the modelled stream discharge. In ForHyM, stream discharge is made up of the runoff, interflow in FF, interflow in A&B, and interflow in C1&C2. Therefore, by analyzing the interflow graph you can see which flow is creating a certain peak and change the calibration adjustors to align it.

When calibrating the snow density and snow melt parameters, there are a few things to keep in mind. Increasing air temperature makes the snowpack smaller and melts faster (i.e. shorter and skinnier). Increasing the density of fresh snow makes the snowpacks smaller but melt slower (i.e. shorter but denser, therefore takes longer to melt).

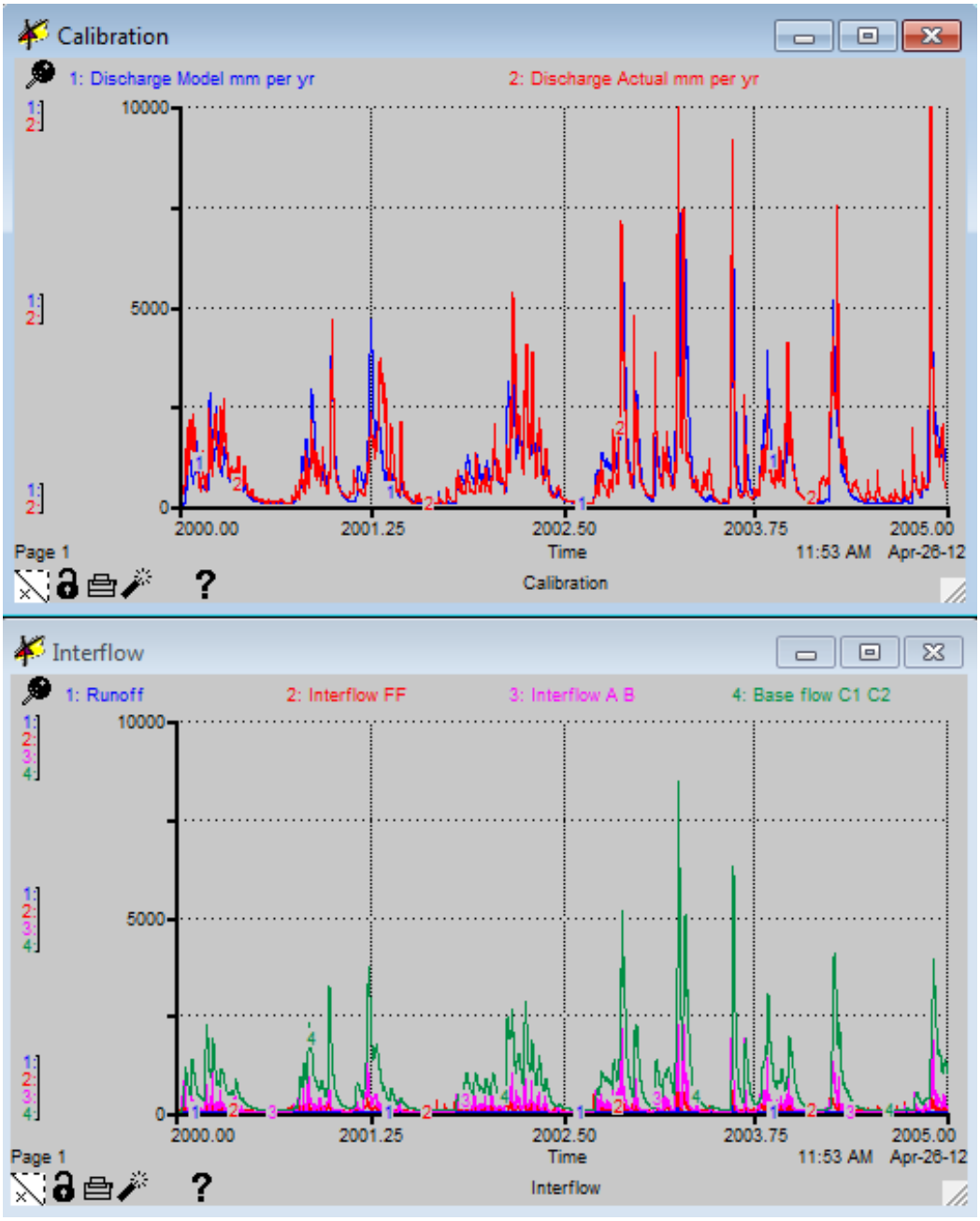


Figure 6. Top graph is an example of correlation between modelled and actual stream discharge calibration data. Bottom graph is a breakdown of interflow to use in calibrating the model discharge. Note that baseflow (green) has a large input into the overall modelled discharge flow.

3.3 Generating and exporting output

You can create both graphs and tables by clicking on the appropriate icons on the toolbar and then clicking anywhere in the model area (Figure 7). If you double-click on an open graph or table, you have access to a list showing all the variables used in the model, sorted by type (box, flow, regular variable, graph variable) and then by alphabetical order. Output is limited to 5 variables per graph, and is unlimited for tables. If you want to avoid creating too many graphs or tables, you can simply add pages to your existing ones (click on the little triangle to create a new page).

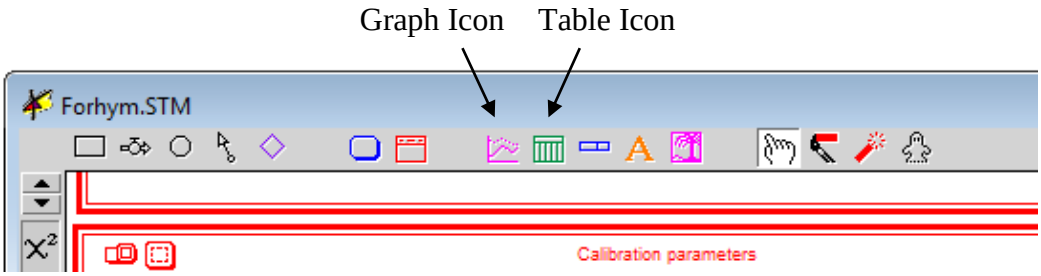


Figure 7. STELLA toolbar for ForHyM.

For tables, you can either choose to display a report interval equal to DT or any other you want. To obtain one value per day independently of the DT used, you can choose a report interval equal to 0.002737851 (= 1/365.25).

The most precision you can get is 6 decimals in *Stella*. To obtain that, double-click on the name of a variable in the table and choose “free float”.

To export a table, open it, then go in the menu and choose “File / Save as text”. The text file created can be opened in *Excel*, where it will have the same appearance as in *Stella*.

CREDITS

This forest hydrology model was first developed by Paul Arp, Fan-Rui Meng, Xiwei Yin (1991 to 1995) and recently upgraded by Paul Arp and Vincent Balland (2001 to 2004) and by Paul Arp and Marie-France Jutras (2009-2012).